Biomarker for the Proteolytic Activity of Neurotrypsin *in vivo*

Dissertation

zur

Erlangung der naturwissenschaftlichen Doktorwürde

(Dr. sc. nat.)

vorgelegt der

Mathematisch-naturwissenschaftlichen Fakultät

der

Universität Zürich

von

Diana Klingler

aus

Deutschland

Promotionskomitee

Prof. Dr. Peter Sonderegger

Dr. Peter Hunziker

Prof. Dr. Heinz Gehring

Zürich 2010

Abbreviations

ACN	acetonitrile
ADAM	a disintegrin and metalloproteinase
AD	Alzheimer's disease
APP	b-amyloid precursor protein
AQUA	Absolute quantification
BACE	b-site APP cleaving enzyme
BLAST	Basic local alignment search tool
Ca^{2+}	calcium-ion
cDNA	complementary DNA
CID	collision-induced dissociation
CSF	cerebrospinal fluid
CNS	central nervous system
2DE	2 dimensional gel electrophoresis
EGFP	enhanced green fluorescent protein
ESI	electrospray ionization
FT ICR	Fourier transform ion cyclotron resonance
FWHM	Ful with half maximum
HEPES	4-(2-hydroxyethyl)-1-piperazineethanesulfonic acid
HPLC	High performance liquid chromatography
ICAT	isotope-coded affinity tag
IgA, (G, M)	immunoglobulin A, (G, M)
iTRAQ	isobaric tags for relative and absolute quantification
K+	potassium-ion
Kb	kilo-base pairs
kDa	kilodalton
KO	knock-out
LC	Liquid chromatography
LC-MS/MS	Liquid chromatography tandem mass spectrometry
LG	laminin-globular domain
LG-3	laminin-globular domain 3 of agrin
LRP-1	low-density lipoprotein receptor-related protein 1
LTD	long-term depression
LTP	long-term potentiation
MALDI	Matrix Assisted Laser Ionization Desorption
Mr	molecular mass
MS	Mass spectrometry
MS/MS	Tandem mass spectrometry
mRNA	messenger RNA
MuSK,	muscle-specific kinase
m/z	mass-to-charge-ratio
Na+	sodium-ion
NMDA	N-methyl-D-aspartate
NMDAR	NMDA-type glutamate receptor
NMJ	neuromuscular junction
PBS	phosphate-buffered saline
PBS-T	PBS with Tween-20
PEI	polyethylenimin
PCR	polymerase chain reaction
PFR	picrotoxin, forskolin, and rolipharm
PTP	Proteotypic peptide

PVDF	polyvinylidene fluoride
ppm	parts per million
RF	radio frequency
RNA	ribonucleic acid
RP	reversed phase
SDS-PAGE	sodium dodecyl sulfate polyacrylamide gel electrophoresis
SILAC	stable isotope labeling by amino acids in cell culture
SRM	selected ion monitoring
TEA	tetraethylammonium chloride
TFA	triflouracetic acid
TIC	total ion chromatogram
TOF	time of flight
tPA	tissue-type plasminogen activator
uPA	urokinase-type plasminogen activator
wt	wild-type

Contents

Summary

The neuronal serine protease neurotrypsin is predominantly expressed in the central nervous system. Its expression level peaks in the first postnatal week followed by a decrease until adulthood. There is evidence that neurotrypsin is involved in neuronal plasticity during development and adulthood. This hypothesis is mainly supported by the finding that a 4 base-pair deletion in the human gene leads to a nonsyndromic form of mental retardation. Recently, the proteoglycan agrin was found to be the unique substrate for neurotrypsin. Neurotrypsin cleaves agrin at two homologous positions which results in the release of the intermediate 90 kDa fragment and the C-terminal 22 kDa fragment (agrin-22) from the N-terminal moiety. To analyze whether agrin is a substrate of neurotrypsin *in vivo* and to quantify the proteolytic activity of neurotrypsin in non-neuronal tissue, a study of serum from neurotrypsin-deficient and neurotrypsin-overexpressing mice was performed. The results confirmed that the catalytic activity of neurotrypsin on agrin was increased in neurotrypsin-overexpressing mice and completely absent in neurotrypsin-deficient mice. Additionally, an age-associated regulation of the neurotrypsin-dependent cleavage product agrin-22 was observed in murine serum. The motoneuron-derived transcripts of the four z splice variants of agrin were characterized as pro-synaptic molecules at the neuromuscular junction. There is strong evidence for a regulatory function of agrin in the central nervous system as well, but until now the differential role of the z-transcripts has not been worked out. In order to identify and quantify the distribution of the four z-transcripts *in vivo*, targeted mass spectrometric analyses were performed. Specific parameter settings were evaluated in order to optimize the elution, fragmentation, and recovery of the specific tryptic peptides of the four agrin-22 z-transcripts. The results showed that synaptic recruitment and externalization of neurotrypsin are regulated by neuronal activity. In addition, the generation of synaptic precursors, namely filopodia, could be rescued in hippocampal slices from neurotrypsin-deficient mice by the application of the neurotrypsin-dependent 22 kDa fragment. Neurotrypsin-dependent cleavage of agrin at the synapse is thought to influence the synaptic function of agrin. Therefore, the processing of agrin by neurotrypsin is suggested as a potential pathway for activity-dependent reorganization and remodeling of synaptic circuits in the brain. To further evaluate the potential functional effects of the neurotrypsin-agrin interaction *in vivo,* human cerebrospinal fluid (CSF) samples were analyzed in relation to age and in the context of neurological disorders such as Alzheimer`s disease and epilepsy. The quantitative analysis of immunoblots confirmed that the proteolytic activity is modulated throughout development and showed a moderate increase in epilepsy patients. In contrast, the amount of agrin-22 was slightly decreased in Alzheimer`s disease.

Furthermore, the proteolytic processing of the transmembrane protein calsyntenin-1 was identified and quantified. Calsyntenin-1 and APP undergo a similar coordinated proteolytic processing. After proteolysis, the transmembrane stump of calsyntenin-1 is internalized and accumulated in an endosomal compartment of the synapse. Thus, proteolysis-dependent translocation is suggested to illustrate an independent downstream event in protease-mediated

synaptic plasticity. To shed light on the processing of calsyntenin-1, the presence of proteolytic fragments was analyzed in human CSF by mass spectrometry. Exclusively calsyntenin-1 ectodomain was found to be accumulated in human CSF. Additionally, it has been recently shown that calsyntenin-1 ectodomain-shedding is increased by induction of synaptic activity. In order to define the functional aspects of calsyntenin-1 processing, human CSF samples were analyzed in association to age and in the relation to neurological disorders such as Alzheimer`s disease and epilepsy. Quantitative immunoblot analysis showed that the proteolytic processing of calsyntenin-1 is consistent throughout aging. In addition, ectodomain shedding is unaltered in Alzheimer`s disease and epilepsy patients.

Zusammenfassung

Die neuronale Serinprotease Neurotrypsin wird vorwiegend im Zentralnervensystem exprimiert. Seine Expression erreicht ihren Höhepunkt in der ersten postnatalen Woche, woraufhin eine Abnahme bis zum Erwachsenenalter folgt. Es gibt Hinweise darauf, dass Neurotrypsin in die neuronaler Plastizität des sich entwickelnden und auch des adulten Nervensystems involviert ist. Diese Hypothese wird vor allen Dingen durch die Feststellung bekräftigt, dass eine Deletion von vier Basenpaaren im menschlichen Gen zu einer schweren Form von geistiger Behinderung führt. Kürzlich wurde herausgefunden, dass das Proteoglykan Agrin das bisher einzige Substrat für Neurotrypsin ist. Neurotrypsin spaltet Agrin an zwei homologen Stellen, was die Freisetzung des intermediären 90-kDa-Fragments und des C-terminalen 22-kDa-Fragments (Agrin-22) vom N-terminalen Teil bewirkt. Um zu analysieren, ob Agrin *in vivo* ein Substrat von Neurotrypsin ist und um die proteolytische Aktivität Neurotrypsins in nicht neuronalem Gewebe zu quantifizieren, wurde eine Studie des Serums von Neurotrypsin knock-out und Neurotrypsin überexprimierenden Mäusen durchgeführt. Die Resultate bestätigen, dass die katalytische Aktivität von Neurotrypsin auf Agrin in Neurotrypsin überexprimierenden Mäusen erhöht ist und in Neurotrypsin knock-out Mäusen durchweg abwesend ist. Zusätzlich konnte in Mausserum eine altersabhängige Regulation des von Neurotrypsin abhängigen Spaltproduktes Agrin-22 festgestellt werden. Die aus den Motoneuronen stammenden Transkripte der vier z-Splice-Varianten von Agrin wurden als ein pro-synaptische Moleküle an der neuromuskulären Kontaktstelle charakterisiert. Es gibt überzeugende Hinweise dafür, dass Agrin auch im Zentralen Nervensystem eine solche regulatorische Funktion zugesprochen werden kann, jedoch ist die differentielle Rolle der z-Transkripte bisher nicht ausgearbeitet worden. Um die *in vivo*-Verteilung der vier z-Transkripte zu identifizieren und quantifizieren, wurden gezielte massenspektrometrische Analysen durchgeführt. Es wurden spezielle Einstellungen der Parameter zur optimierten Elution, Fragmentierung und Rückgewinnung der Agrin-22 z-Transkripten evaluiert. Neueste Ergebnisse zeigten, dass die synaptische Rekrutierung und Ausschüttung von Neurotrypsin durch neuronale Aktivität reguliert werden. Darüber hinaus konnte nachgewiesen werden, dass die Generierung von Vorläufersynapsen, so genannte Filopodien, in Neurotrypsin knock-out Mäusen durch die Zugabe des von Neurotrypsin abhängigen Agrin-22 Fragments wiederhergestellt werden konnte. Es wird vermutet, dass die von Neurotrypsin abhängige Spaltung Agrins an der Synapse seine synaptische Funktion beeinflusst. Folglich wird angenommen, dass die Spaltung von Agrin durch Neurotrypsin einen potenziellen Pfad in der aktivitätsabhängigen Umorganisation und Umgestaltung synaptischer Schaltkreise im Gehirn darstellt. Um den potenziellen funktionalen Effekt der Interaktion von Neurotrypsin und Agrin *in vivo* weiter aufzuklären, wurde humane cerebrospinale Flüssigkeit (CSF) in Bezug auf das Alter und im Kontext neurologischer Störungen wie Alzheimer und Epilepsie analysiert. Die quantitative Analyse der Immunoblots ergab, dass die proteolytische Aktivität während der Entwicklung durchwegs reguliert wird und zeigte zudem einen schwachen Anstieg in Epilepsie Patienten. Im Gegensatz dazu, war die Menge an Agrin-22 in Alzheimer leicht vermindert.

Desweiteren wurde der proteolytische Abbau des transmembranen Proteins Calsyntenin-1 identifiziert und quantifiziert. Calsyntenin-1 und APP werden einem gleichermaßen koordinierten proteolytischen Abbau unterzogen. Nach der Proteolyse wird der transmembrane Stumpf von Calsyntenin-1 internalisiert und in einem endosomalen Kompartiment der Synapse akkumuliert. Die proteolyseabhängige Translokalisierung wird daher als eigenständiger Abbauschritt in der proteasevermittelten synaptischen Plastizität angesehen. Um den Abbau von Calsyntenin-1 weiter aufzuklären, wurde das Vorkommen proteolytischer Fragmente in humanem CSF mit Massenspektrometrie analysiert. Es wurde gezeigt, dass ausschließlich eine Anreicherung der Ectodomäne von Calsyntenin-1 im CSF vorliegt. Es wurde zudem kürzlich gezeigt, dass die Ausschüttung der Ectodomäne von Calsyntenin-1 bei der Induktion synaptischer Aktivität erhöht ist. Um die funktionalen Aspekte des Abbaus von Calsyntenin-1 zu definieren, wurden humane CSF Proben im Zusammenhang mit dem Alter und in Verbindung mit neurologischen Störungen wie Alzheimer und Epilepsie analysiert. Die quantitative Analyse der Immunoblots ergab, dass der Abbau von Calsyntenin-1 beim Altern durchwegs konstant ist. Zusätzlich scheint die Freisetzung der Ectodomäne von Calsytnenin-1 in Alzheimer und Epilepsie unverändert zu sein.

1 Introduction

In this chapter, the conceptual background will be given for the following more detailed approaches in this thesis. I will start with the classification of proteases followed by a detailed introduction about serine proteases in the brain. Then the three proteins of interest in this study will be presented: (1) the neuronal serine protease neurotrypsin, (2) its unique substrate agrin, and (3) the transmembrane protein calsyntenin-1 which is as well a substrate of extracellular proteolysis. Detailed information will be provided about mass spectrometry and possible workflows for quantification will be discussed, followed by a closer look on the discovery of biomarkers.

1.1 Proteases

Proteases (also known as peptidases, proteinases or proteolytic enzymes) catalytically cleave the peptide bonds linking adjacent amino acids in proteins or peptides. They represent approximately 2% of human genes, which makes them the largest enzyme family in man. Due to their ubiquitous presence in virtually any pathophysiological process, proteases are one of the primary targets in drug and biomarker discovery. They are classified into six clans within each clan ranked into families of related proteases based on similarities in their amino acid sequence (Barrett & Rawlings, 2003). The clans show a more distant relation in sequence and are primarily characterized by structural comparison Further criteria for classification are either peptidase specificity or domain architectures. To date, 39 different groups and 183 families are registered:14 aspartic peptidase families (A), 60 cysteine peptidase families (C), 1 glutamic peptidase family (G), 53 families of metallo peptidases (M), 42 serine peptidase families (S), 4 threonine peptidase families (T) and 9 families of unknown catalytic type (U). They are organized in the MEROPS database (http://merops.sanger.ac.uk) which is an integrated source of information about peptidases, substrates and inhibitors (Rawlings et al, 2010). The database covers about 39.000 known cleavage sites in proteins, peptides, and synthetic substrates. Protease specificity and alignments of their substrates offers the information about conserved cleavage sites, and thus the probable physiological relevance. One important class of proetases are the serine proteases which cover about one-third of the protease families.

1.1.1 Serine Proteases

Serine proteases are named according to their nucleophilic serine residue in the active site. They represent about one-third of all peptidases and are divided into four clans: chymotrypsin (S1), subtilisin (S8), carboxypeptidase Y (S10), and Clp protease (S14) (Hedstrom, 2002). The difference among them is based on the structure of their catalytical triad Asp-His-Ser, which forms the catalytic machinery in these molecules (Dodson & Wlodawr, 1998). They are present in eukaryotes, prokaryotes, archae, and virus and are synthesized as inactive precursors ("zymogens") containing N-terminal extensions. Proteolytic processing activates the zymogen, releasing the N-terminus. Protease specificity of chymotrypsin-like serine proteases is based on the P1/S1 interaction (based on the nomenclature of Schechter & Berger, 1967), where P1-P1' denotes peptide residues on the acyl and leaving group side of the scissile bond. The adjacent peptide residues are numbered S1-S1' and denote corresponding enzyme binding sites. Chymotrypsin-like proteases are implemented in many essential physiological functions including digestion, hemostasis, apoptosis, signal transduction, reproduction, and immune response (Neurath, 1984; Johnson, 2000; Joseph et al, 2001; Coughlin, 2000; Barros et al, 1996). In the central nervous system (CNS), they have been as well implicated in physiological and pathophysiological pathways and are involved in a huge number of processes during neuronal development.

In the following section some general information about proteases in the CNS will be provided and their importance will be described by means of the tissue-plasminogen activator (tPA) which is the predominant expressed plasminogen activator (PA) in the brain.

1.1.2 Proteases in the brain

Biosynthesis of active neuropeptides or peptide hormones is usually based on the generation of a precursor protein. Proteolytic processing as well as other molecular modifications increase the number of potential products and lead to a wide range of mature products from the basic transcript. Extracellular serine proteases are expressed in the developing and adult nervous system (Davies et al, 1998). They are implemented in the regulation of neurogenesis, cell migration, axonal growth, and synapse elimination. Extracellular proteolysis leads to structural and functional changes at synapses in the brain. This mechanism allows reorganization and elimination of established synaptic circuits, as well as generation of new synapses. It is described to be important for adaptive changes in signal transmission which are the base of learning and memory. In addition, they contribute to neuronal death, tumor growth and invasion. They are as well suggested to be involved in several forms of neuropathologies, including neurodegenerative diseases (e.g. Alzheimer's disease (AD), Parkinsons's disease), demyelination diseases (e.g. multiple sclerosis), and epileptic seizures.

Tissue-type plasminogen activator

In the central nervous system the well-known extracellular serine protease tPA has received great attention. tPA is localized in the intravascular space between the blood and the brain (i.e. neurovascular unit), as well as in the parenchyma consisting of neurons, astrocytes and microglia (Siao et al, 2003; Nicole et al, 2001). Thus, tPA serves different roles which depend on the compartment. The inactive zymogen plasminogen is the main substrate of tPA in the

intravascular space. It is primarily a thrombolytic enzyme, as plasmin`s main substrate is fibrin. Hence, recombinant tPA is used for treatment in acute stroke due to its thrombolytic activity (The National Institute of Neurological Disorders and Stroke rt-PA Stroke Study group, 2005). It remains the only FDA-approved treatment of ischemic stroke. Nonetheless, there are reports about enhanced excitotoxic neuronal cell death and it is known that tPA also has a deleterious effect on the ischemic brain including cytotoxicity and increased permeability of the neurovascular unit with the development of cerebral edema (Armstead et al, 2010).

In the brain parenchyma, the function of tPA is multifaceted and associated with synaptic plasticity and cell death (Benchenane et al, 2004; Samson & Medcalf, 2006). There is growing evidence, that the tPA function is controlled either by plasminogen-dependent or –independent pathways (Tsirka et al, 1995; Chen & Strikland, 1997; Yepes et al, 2000). A major number of reports demonstrate tPA as a direct modulator of glutamatergic transmission. Currently, there are three models how tPA mediates neuromodulatory effects via the NMDA receptor (NMDAR). (1) tPA cleaves the NR1 subunit of NMDAR which could modify the Ca2+ signaling leading to changes in long term potentiation (LTP) (Liot et al, 2004; Kvajo et al, 2004). The direct function of this process is so far unknown. (2) Non-proteolytic interaction and upregulation of the NR2B subunit of NMDAR induces phosphorylation of extracellular signal-regulated kinase 1/2 (ERK 1/2) mediating LTP and long term depression (LTD) (Pawlak et al, 2005; Medina et al, 2005; Ito-Ishida et al, 2006). (3) Binding of tPA to the low-density lipoprotein receptor-related protein (LRP-1) increases the level of cyclic adenosine monophosphate (cAMP) and protein kinase A (PKA) activity which results in synaptic potentiation (Huang et al, 1996; Wang et al, 2003).

Expression of tPA is relatively low in the central nervous system (CNS) (Sappino et al, 1993). However, it was shown to be increased due to events such as LTP, seizures and motor learning (Carroll et al, 1994; Kian et al, 1993; Seeds et al 1995). tPA is rapidly released into the synaptic cleft in response to stimuli followed by neuronal depolarization (Yepes et al, 2002). In addition, a relation between tPA and dopaminergic transmission was hypothesized for the CA1 and CA3 region of the hippocampus during induction of LTP (Baranes et al, 1998). It could be assessed that overexpression of tPA in the murine CNS enhances LTP in both, hippocampal LTP and special learning and memory performance (Madani et al, 1999). The activity of extracellular tPA is modulated by inhibitors like neuroserpin, a serine protease inhibitor (serpin) and plasminogen activator inhibitor-1 (PAI-1) (Yepes & Lawrence, 2004). Neuroserpin`s inhibitory effect is suggested to play a neuroprotective role (Galliciotti & Sonderegger, 2006).

1.2 Neurotrypsin

Neurotrypsin is a trypsin-like serine protease with a unique domain composition (Gschwend et al, 1997). The presence of a putative signal sequence and the lack of a transmembrane domain characterize neurotrypsin as a secreted protein. Human neurotrypsin has a molecular mass of about 97 kD and consists of a proline-rich basic domain, a kringle domain, four scavenger receptor cysteine-rich (SRCR) domains and the C-terminal protease domain (Figure 1-1 (A); Proba et al, 1998). In contrast, the molecular mass of murine neurotrypsin is of approximately 85 kDa, due to the expression of only three SRCR domains (Figure 1-x1(B); Gschwend et al, 1997).

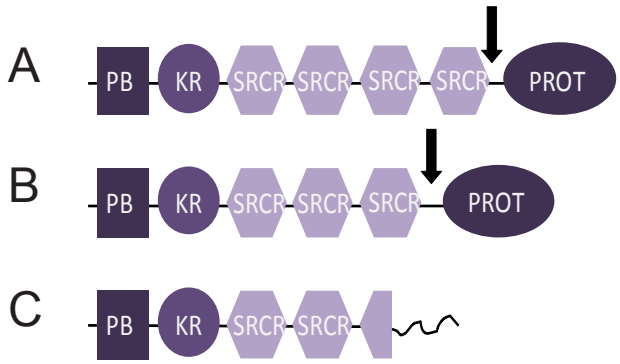

Figure 1-1. Schematic representation of the neurotrypsin domain structure. (A) human neurotrypsin (Proba et al, 1998). (B) mouse neurotrypsin (Gschwend et al, 1997). (C) truncated neurotrypsin (Molinari et al, 2002). SP, putative signal peptide (aa 1 – 20); PB, proline-rich basic segment (aa 21 – 91); KR, kringle domain (aa 92 – 166); SRCR1 through SRCR4, SRCR domains 1 – 4(aa 170 – 271, aa 280 – 381, aa 387 – 487, and aa 500 – 601); ZA, segment with homology to zymogen activation region of tPA (aa 671 – 630); PROT, serine protease domain (aa 631 – 875).

The typical S1 type serine protease domain of human and murine neurotrypsin is located in the C-terminal part of the molecule. The zymogen activation site is located proximal to this domain and includes the conserved catalytic triad of serine peptidases. Neurotrypsin is proteolytically activated by cleavage at the zymogen activation site followed by separation of the protein into two chains which are still connected via a disulfide bond. The cascade of catalytic activation of neurotrypsin is so far not known. The non-catalytic domains are thought to mediate binding of neurotrypsin to cell surfaces or extracellular matrix molecules (ECM), navigating the peptidase to its site of action or to arrange it in the proximity of its substrates.

1.2.1 Neurotrypsin expression in the CNS

Human neurotrypsin was isolated from a human fetal brain cDNA library using a PCR-amplified probe (Proba et al, 1998). In-situ hybridization in adult murine nervous system suggested a highly intriguing expression pattern of neurotrypsin mRNA in a distinct subset of neurons in the cerebral cortex, the hippocampus and the amygdala (Figure 1-2; Gschwend et al, 1997). These brain areas are implicated in processing and storing learned behavior and memories.

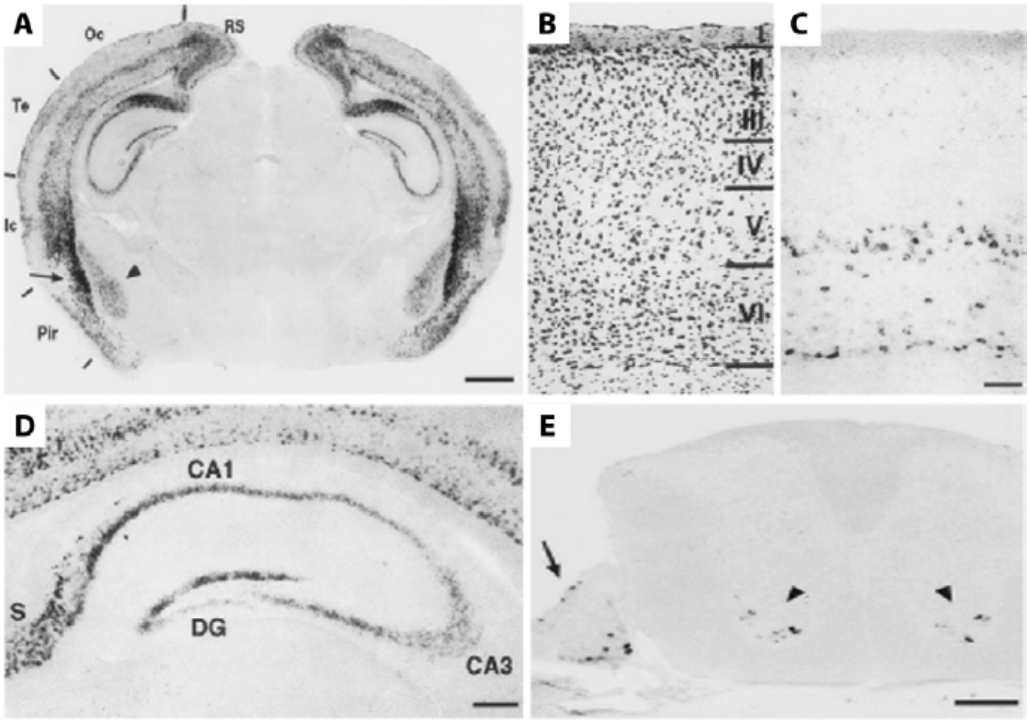

Figure 1-2. In situ hybridisation of sections from different CNS regions of adult mice using DIG-labeled neurotrypsin antisense cRNA. A, Brain section cut in a dorsocaudal-rostroventral plane (angle: approximately 30° to the coronal plane). The section was hybridized with a neurotrypsin antisense riboprobe. Labeling is seen in distinct layers throughout the neocortex (Te, temporal cortex; Oc, occipital cortex) with a more widespread labeling in the transition zones between iso- and allocortex (Ic, insular cortex; RS, retrosplenial cortex). In the allocortex, labeling is detected in the piriform cortex (Pir), with a strong labeling in the endopiriform nucleus (arrow), and in the hippocampal formation (see also D). Neurotrypsin expression is also seen in the lateral amygdala (arrowhead). Scale bar: 1 mm. B, C, Consecutive coronal sections of the parietal cortex, either stained with cresyl violet B, or hybridized with neurotrypsin antisense riboprobe C. Cortical layers are marked in B. C, Large positive neurons are seen in the lower half of layer V. In layer VI, positive cells are found throughout the layer, but concentrated at the border to the white matter. Weak labeling is associated with cells scattered in layers II and III. No labeling is detected in layers I and IV. Scale bar in C represents 100 μm. D, Coronal section of the hippocampus. Labeling is detected in neurons of the subiculum (S), in pyramidal neurons of CA1 and CA3, and in granule neurons of the dentate gyrus (DG). Scale bar: 300 μm. E, Cross section of the cervical spinal cord. Large cells are labeled in the motor columns (arrowheads). Labeling is also detected in the DRG (arrow). Scale bar: 300 μm. Figure and text taken and modified from (Gschwend et al., 1997).

The spatio-temporal mRNA expression of neurotrypsin during pre- and postnatal development in mouse brain suggests a role of neurotrypsin in morphogenesis of non-neuronal tissues, as well as in crucial stages of neuronal development, in particular in axonal target invasion, synaptogenesis and Schwann cell differentiation (Wolfer et al, 2001).

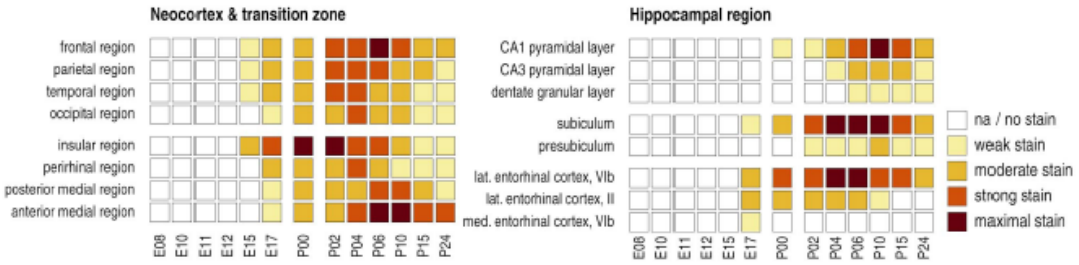

Figure 1-3. Semi-quantitative time course of neurotrypsin mRNA expression in neural tissues during pre- and postnatal development. Columns represent developmental stages. Rows represent regions. The shading pattern of each box indicates the average signal intensity, assigned to one of the four staining levels listed on the right in the figure. E: embryonic, P: postnatal. Figure and text modified from (Wolfer et al, 2001).

The semi-quantitative time course confirms that neurotrypsin mRNA expression lasts until adulthood (Figure 1-3). The mRNA expression peaks at postnatal day 10 (P10), decreases by P16 and continues with low levels in the seven month old murine CNS. Thus, there is evidence that neurotrypsin is involved in neuronal plasticity during development and in the adult. Neurotrypsin was found to be important for cognitive brain functions, as a 4bp deletion in the coding region leads to the generation of a truncated protein lacking the catalytic domain (Figure 1-1 (C); Molinari et al, 2002). This inactive variant of neurotrypsin causes a severe form of nonsyndromic mental retardation in humans. The affected children exhibited severe deficits in cognitive development after normal psychomotor development during the first 18 months. Beside this, neurotrypsin has been localized to presynaptic nerve terminals of excitatory synapses in human brain and in the hippocampus and cerebral cortex of the murine brain based on pre-embedding immunogold labeling (Figure 1-4; Molinari et al, 2002; Stephan et al, 2008). Besides, neurotrypsin seems to be secreted and activated under certain stimuli (Frischknecht et al, 2008). Its synaptic recruitment as well as its externalization is regulated by neuronal activity, and externalized neurotrypsin is accumulated at the synapse for minutes before disappearing due to diffusion or degradation. Taken together, these findings characterize neurotrypsin as regulator of adaptive synaptic functions during later stages of development and suggest an activity-dependent extracellular proteolytic function of neurotrypsin at the synapse.

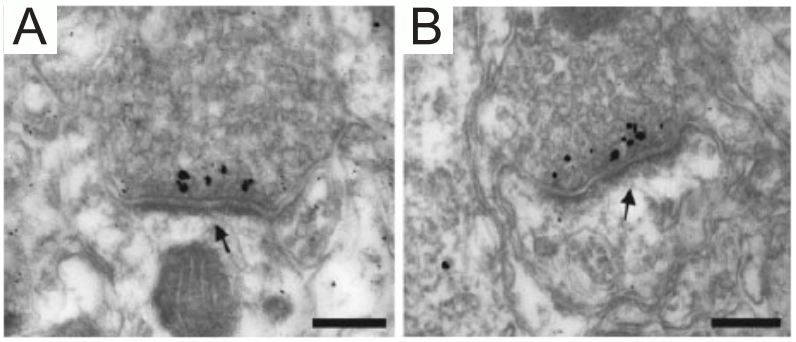

Figure 1-4. Subcellular localization of neurotrypsin in hippocampus and cerebral cortex of wild type mice. (A, B) Immuno-electron microscopy of the neuropil of the hippocampal CA1 area and the cerebral cortex localized neurotrypsin in presynaptic terminals, close to presynaptic membranes lining in the synaptic cleft. Silver-intensified gold particles reporting neurotrypsin immunoreactivity were accumulated at vesicles close to the presynaptic membrane opposite to postsynaptic density (arrows). Scale bars = 0.2 μm.

1.3 Agrin

Agrin is an extracellular matrix (ECM) protein named assigned to its key role in the aggregation of acetylcholine receptors (AChRs) which takes place during synaptogenesis in the neuromuscular junction (NMJ) (Sanes & Lichtman, 2001). The amino acid sequence of agrin has a predicted mass of 210 kDa. Due to addition of O- and N-linked carbohydrates as well as glycosaminoglycans (GAGs) in the N-terminal part of the molecule, the molecular weight of native agrin is increased to 400-600 kDa (Figure 1-6; Tsen et al, 1995). The three O-linked GAGs serve as binding sites for heparan sulfate glycosaminoglycans (HS-GAG), which classify agrin as a member of the heparan sulfate proteoglycans (HSPGs). The lamini-globular domain (LG) at the C-terminus is required for AChR-clustering at the NMJ (Gesemann et al, 1995; Cornish et al, 1999).

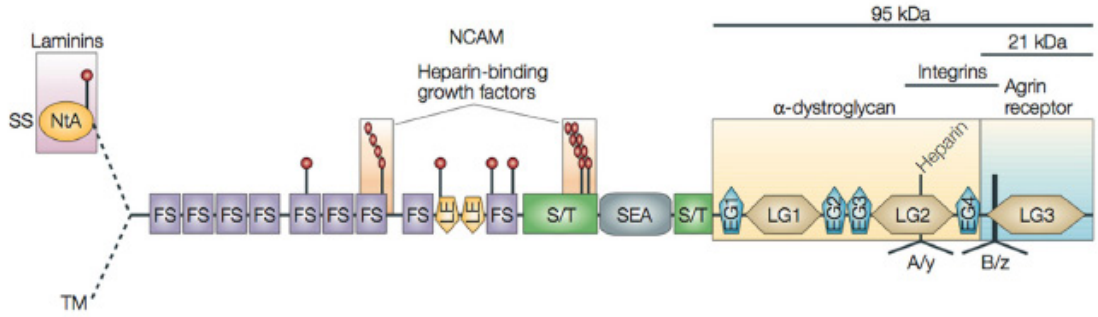

Figure 1-5. Schematic representation of agrin. Structural domains, sites of alternative mRNA splicing, andbinding regions of some of the most important partners for agrin are illustrated. Signal sequence (SS) and amino (N)-terminal agrin domain (NtA) are present in a secreted agrin isoform which is localized at the NMJ and bind to laminin in the basal lamina (NtA). The alternatively spliced type II transmembrane segment (TM) of agrin anchors this isoform at places that are devoid of basal laminae such as the ECM of the brain. The N-terminal half of agrin is highly glycosylated at Ser/Thr (S/T) attachment sites. These regions are involved in binding to NCAM L1 and heparin-binding growth factors. The C-terminal 95 kDa part of agrin is fully active in AChR aggregation and contains binding sites for α-dystroglycan, heparin some integrins and a as yet unidentified agrin receptor. The four amino acid-long insert at the A/y site encodes a separate exon. Similarly, the different inserts at the B/z site of 8, 11, and 19 amino acids are encoded by separate exons. The most C-terminal 21-kDa LG3 domain is sufficient to induce AChR aggregation although at much lower potency. Its activity requires the eight amino acid insert. FS, follistatin-like domain; LE, laminin EGF-like domain; LG, laminin globular domain; SEA, sperm protein enterokinase and agrin domain. Figure and text were modified from (Bezakova & Ruegg, 2003).

1.3.1 Alternative splicing of agrin

Agrin is encoded by a single gene but alternative RNA splicing gives rise to several isoforms with distinct tissue expression and functional characteristics. Different N-termini are either leading to a secreted form, which is mainly expressed in muscle and peripheral tissues, or to a shorter non-secreted type II transmembrane protein specifically expressed in neurons (Figure 1-5; Neumann et al, 2001; Burgess et al, 2000). Both isoforms have at least two additional splicing sites in the C-terminal part of the molecule, designated as y and z in humans (Figure 1-6). Splicing at the y-site is leading to a protein with the insertion of 0 or 4 (Lys-Ser-Arg-Lys) amino acids at the LG2 domain. The y4 variant is required for α-dystroglycan- and heparin-binding (Gesemann et al, 1996; Hopf et al, 1996). Furthermore, splicing at the z-site in the LG3 domain gives rise to proteins with 0, 8, 11, or 19 (8+11) amino acid insertions. Results from localization studies of the mRNA in adult rat brain show a broad expression of the z-transcripts throughout the CNS (O`Connor et al, 1994). While non-neuronal cells express only agrin z0, neurons express various combinations of one or more agrin transcript (Yang et al, 2001). The total mRNA expression is > 40% for agrin z0, whereas agrin z8 and z19 account for the majority of 60%. Agrin z11 constitutes a very small percentage (< 7%) of these transcripts (see Figure 1-6 (B)).

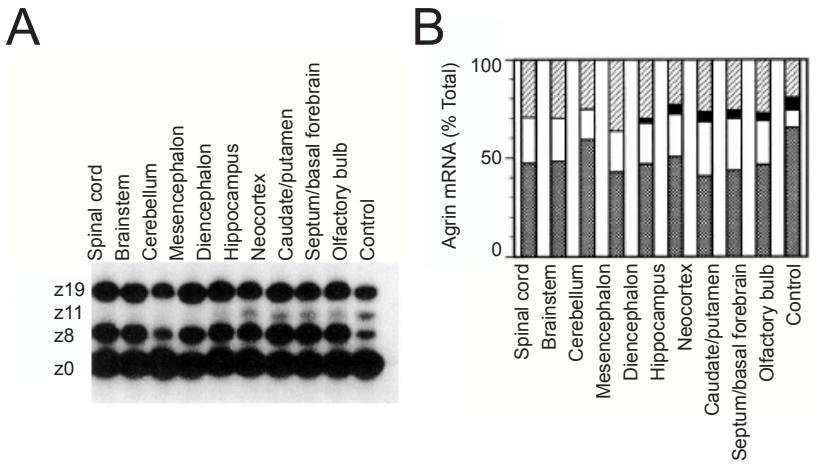

Figure 1-6. Alternatively spliced isoforms of agrin mRNA are expressed in the adult rat CNS. (A), Film autoradiogram from a typical experiment indicating each of the four agrin isoforms is expressed in the CNS. Note that one of these isoforms, agrin z11, can only be detected in RNA isolated from regions of the forebrain. The control lane represents a reaction in which RNA was omitted from first-strand cDNA synthesis. (B), Expression levels of each transcript was calculated using quantitative densitometry of film autoradiogram. They were expressed as a fraction of all four transcripts. Agrin z0 (stippled bars) comprises the largest percentage (> 40%) of these transcripts in all regions of the CNS while agrin z19 (hatched bars) and agrin z8 (open bars) account for the majority of the remaining 60%. By comparison, when agrin z11 (solid bars) is expressed, it constitutes a very small percentage (~ 7%) of these transcripts. Figure and text modified from (O`Connor et al, 1994).

Agrin mRNA is present at high levels in hippocampal regions CA3 and CA1. The transcript z11 is restricted to forebrain structures (see Figure 1-6. B). The characteristic pattern of alternative splicing is influenced by regionally specific cues and supports the idea of a physiological significant mechanism of agrin`s regulation in the adult CNS. In addition, the z+ variants are crucial for agrin`s ability to aggregate AChRs at the NMJ whereas the z0 variant is inactive (Burgess et al, 1999). AChRs are still aggregating *in vitro* when applying the 22 kDa LG3 domain (agrin-22) with z+ insertions, though with decreased potency compared to the agrin full-length form (Gesemann et al, 1995; Cornish et al, 1999).

1.3.2 Agrin and the neuromuscular junction

AChR clustering is an essential characteristic in the process of postsynaptic differentiation. At birth, AChRs are clustered underneath the nerve terminals and a single muscle fiber is innervated by several motor axons. In the adult conformation, a single axon innervates one muscle fiber. Therefore, nerve terminals are in competition and upon synapse elimination the postsynaptic apparatus is remodeled. At the end of this process of synapse maturation, AChR clusters have acquired a pretzel-like shape. Agrin was first purified from basal-lamina-containing extracts of the electric organ of the marine ray *Torpedo californa* (Godfrey et al, 1984; Nitkin et al, 1987).

At the NMJ, agrin is synthesized in motor neurons in the spinal cord and transported along motor axons to the muscle (Magill-Solc, 1988; Magill-Solc, 1990). After secretion at the nerve terminal, agrin induces tyrosine phosphorylation of the muscle-specific receptor tyrosine kinase (MuSK) (De Chiara et al, 1996; Glass et al, 1996). As agrin and MuSK could not be shown to interact directly, the linkage between these molecules was missed for a decade. Recently, a member of the family of low-density lipoprotein receptors, namely LRP4, was demonstrated to be associated with MuSK and agrin (Zhang et al, 2008; Kim et al, 2008). Further, neuronal agrin induced tyrosine phosphorylation in non-muscle cells exclusively if LRP4 was co-expressed with MuSK. These results suggest that LRP4 is the functional receptor for agrin at the NMJ. The importance of agrin for the development of the NMJ is nicely illustrated by the fact that agrin-deficient mice die directly after birth due to insufficient innervation of the respiratory muscles (Gautam et al, 1996). The motoneuron-derived form of agrin is defined as pro-synaptic molecule at the neuromuscular junction (Sanes & Lichtman, 2001; Kummer et al, 2006). Recent studies have shown that there is strong evidence for a regulatory function of agrin in the CNS (Annies et al, 2006; Mc Croskery et al, 2006; Hilgenberg et al, 2006; Matsumoto-Miyai et al, 2009).

1.3.3 Synaptic functions of agrin in the brain

Besides its role at the NMJ, in situ hybridization demonstrate that agrin mRNA is also expressed in cells of the CNS. For example, agrin could be detected at interneuronal synapses and the course of expression coincides with synapse formation. But at present its role remains still unclear (O´Connor et al, 1994; Mann & Kröger, 1996; Cohen et al, 1997). All four agrin z-isoforms are expressed in the adult CNS. However, both the level of expression and the pattern of the alternative splice variants are differentially regulated in the brain (O'Connor et al., 1994). In contrast to the situation at the NMJ, all agrin-22 z-transcripts (0, 8, 11, and 19) are equally potent agonists of the neuronal receptor and agrin-22 z0 and 8 are sufficient for receptor activation (Hilgenberg et al, 1999; Hoover et al, 2003). Subcellular localization in the hippocampus and the cerecral cortex of wild-type mice showed a perisynaptic as well as an extrasynaptic localization of agrin (Figure 1-7, Stephan et al, 2008). Agrin`s expression pattern in the CNS and its function at the NMJ suggests a similar role in synaptogenesis and has therefore been hypothized to be implicated in several brain functions. This hypothesis is mainly supported by the finding of abnormal synapse formation and generation of fewer synapses in hippocampal neuron cultures after suppression of agrin by antisense oligonucleotide treatment or the expression of non-functional agrin (Ferreira 1999; Böse et al, 2000). The perinatal death of agrin-deficient mice could be preventes by ectopic expression of agrin in motoneurons. Similar as for the experiments in neuron cultures, these mice showed reduced number of pre- and postsynaptic structures (Ksiazek, 2007). It has been biochemically shown that the α3 subunit of Na^+/K^+-ATPase (NKA) is a neuronal receptor for agrin (Hilgenber et al, 2006). Agrin binds to the α3NKA in CNS neurons and signaling is regulated by release of intracellular Ca^{2+}. Increased cytoplasmic Ca^{2+} concentration activates CaMKII and other Ca^{2+} effectors which are known as regulators of various synaptic functions and neurotransmitter turnover (Hilgenberg and Smith, 2004).

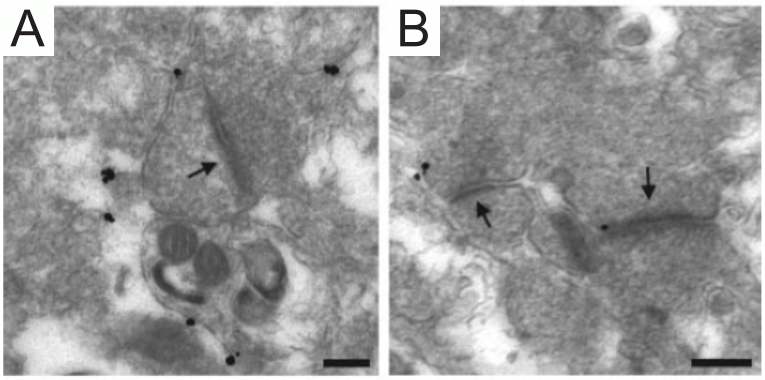

Figure 1-7. Subcellular localization of agrin in hippocampus and cerebral cortex of wild type mice. (A, B) Silver-intensified gold particles indicate for agrin immunoreactivity at perisynaptic, as well as extrasynaptic locations in the neuropil of the hippocampal CA1 area and the cerebral cortex. Arrows point to postsynaptic densities. Scale bars = 0.2 µm. Figure and text was modified from (Stephan et al, 2008).

1.3.4 Agrin in Alzheimer`s disease

Alzheimer`s disease (AD) is a neurodegenerative disorder characterized by the loss of neurons and synapses in the brain (Davies et al, 1987; Hamos et al, 1989; Martin et al, 1994). A pathologic feature of this disease is the occurrence of β-amyloid-containing senile plaques, neuro-fibrillary tangles within neurons, and cerebral amyloid angiopathy (Roses, 1996). Clinically, the disease is associated with progressive dementia and memory loss (Snow et al, 1988). Furthermore, the pathological properties of AD are associated with HSPG function (Snow & Wight, 1989, Fukiuchi et al, 1998) and HSPG levels are elevated in AD brains (Table 1-1; Horssen et al, 2003; Snow & Wight, 1989).

The presence of subtypes of heparan sulphate proteoglycan in different AD lesions

Heparan sulphate proteoglycan	Normal vessels	CAA in AD	Cerebellar diffuse SPs	Cerebellar classic SPs	Cerebral diffuse SPs	Cerebral classic SPs	Neurofibrillary tangles
Collagen XVIII	+++	+++	-	++	-	+++	-
Agrin	+++	-/+/++	+++	+++	+++	+++	+++
Perlecan	+++	-	-	-	-	-	-
Syndecan 1, 3	-	-	-	+++	++	++	++
Syndecan 2	-	+/++	-	++	+/++	++	+
Syndecan 3	++	-/+	-	+++	+/++	+/++	++
Glypican 1	-	+++	++	+++	++	+++	++
Heparans sulphate glycosaminoglycan	+++	+++	+++	+++	+++	+++	+++

CAA=cerebral amyloid angiopathy; SP=senile plaque.

Table 1-1. The distribution of HSPGs in various AD lesions. Table from (Horssen et al, 2003).

Severely affected brain regions in AD show highest agrin expression e.g. in the hippocampus and amygdala (Boew & Fallon, 1995; Braak& Braak, 1991). Agrin binds β-amyloid peptide Aβ (1-40) in its fibrillar state via a mechanism involving the heparan sulfate glycosaminoglycan chains of agrin (Cotman et al, 2000). Furthermore, agrin is able to accelerate Aβ fibril formation and protects Aβ (1-40) from proteolysis *in vitro*. Immunocytochemical studies demonstrate agrin`s presence within senile plaques and cerebrovascular amyloid deposits, and capillaries immunostained for agrin exhibit pathological alterations in AD brain (Figure 1-8; Donahue et al, 1999; Verbeek et al, 1999; van Horssen et al, 2002). Therefore it was suggested that agrin may be an important factor in the progression of Aβ peptide aggregation and Aβ persistence in the brain of AD patients.

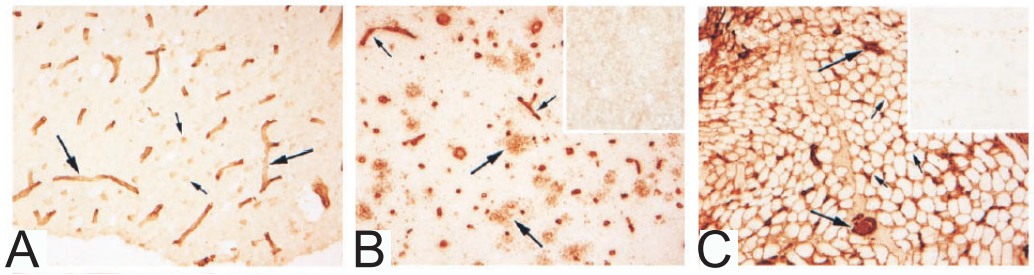

Figure 1-8. Localization of agrin in aged control and AD brain. Sections were immunohistochemically stained with either diaminobenzidine-labeled tertiary antibody (A–E). (A) Aged control brain section labeled with antiagrin antibody. Agrin immunoreactivity is prominent within the cerebral microvasculature (large arrows) and is also evident in selected neurons (small arrows). Prefrontal cortex, A10, 3200. (B) Prefrontal cortex (A10) of a patient with AD immunostained with anti-agrin antibody. Note the robust staining of neuritic and diffuse plaques (large arrows) and blood vessels. In contrast to aged control cases (e.g., A), blood vessels in AD had attenuated diameters and a more ragged profile (small arrows). No immunoreactivity was observed when the antisera were preabsorbed with 10 M agrin protein (Inset). (3200.) (C) Normal infant skeletal muscle labeled with anti-agrin antibody. Note the uniform agrin immunoreactivity of the basement membranes surrounding individual muscle fibers (small arrows) and capillaries (large arrows). (Inset) The same skeletal muscle after the primary antibody was preabsorbed with 10M agrin protein. There is complete abolishment of agrin immunoreactivity. (Quadriceps muscle, 3200.). Figure and text modified from (Donahue et al, 1999).

1.3.5 Agrin is a unique substrate of neurotrypsin

Co-transfection of wild type neurotrypsin and the transmembrane isoform of agrin in eukaryotic cells resulted in cleavage at two sites and the release of three fragments at 110, 90 and 22 kDa into the culture supernatant that are detectable by Western blot (Figure 1-9). The cleavage sites are located in the sequence PIER ↓ ASCY (α-cleavage site) and in the sequence LVEK ↓ SVGD (β-cleavage site). Neurotrypsin-dependent cleavage has been observed *in vivo* and was absent in neurotrypsin-deficient mice. The agrin-22 fragment was identified in brain and kidney. Therefore, neurotrypsin is responsible for the cleavage of agrin.

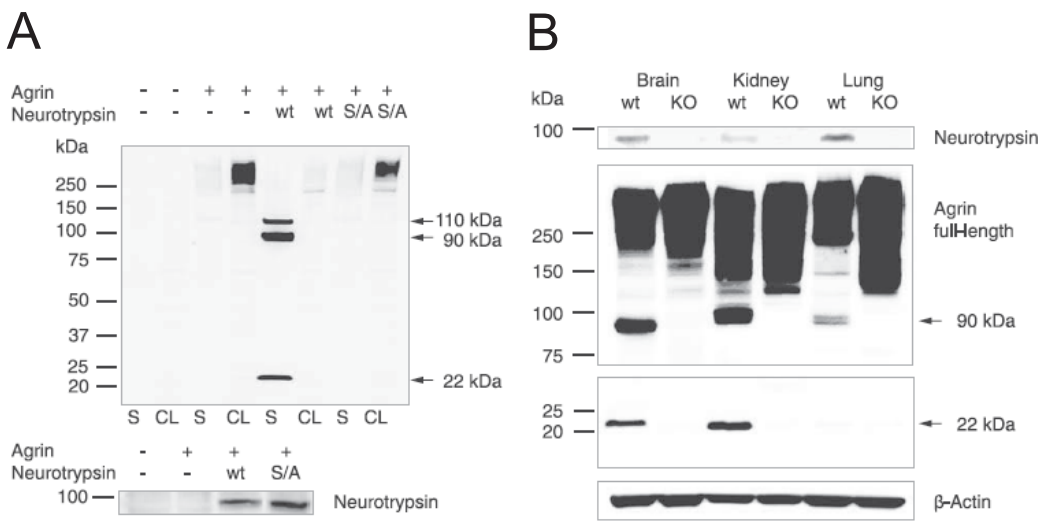

Figure 1-9. Neurotrypsin cleaves agrin in vitro and in vivo. (A) Western blot analysis of HeLa cells co-transfected with combinations of membrane-bound agrin (+), wild type neurotrypsin (wt), inactive neurotrypsin (S/A), and empty pcDNA3.1 (-). Supernatants (S) and cell lysates (CL) were analyzed with anti-agrin (R132 and G92) antibodies, directed against the C-terminus of agrin. (Top) Transfection of agrin alone resulted in a signal above 250 kDa in cell lysate. Upon co-transfection with wild type neurotrypsin, full-length agrin was cleaved resulting in fragments running at 22, 90 and 110 kDa in supernatant. No cleavage was found after co-transfection with inactive neurotrypsin. (Bottom) Control for neurotrypsin expression with G93 antibody. (B) Western blot analysis of tissue from wild type (wt) and neurotrypsin-deficient (KO) mice. The 90 kDa agrin cleavage product was detected in brain, kidney, and lung of wild type mice but was absent in neurotrypsin-deficient. Similar results were obtained for 22 kDa fragment except for lung. β-Actin was used as a loading control. Figure and text taken and modified from (Reif et al, 2007).

The heparan sulfate proteoglycan agrin is until today the exclusive substrate of neurotrypsin. Neurotrypsin cleaves agrin at two homologous sites which are highly conserved in evolution (Figure 1-10, Reif et al, 2007). It has been reported that neurotrypsin-dependent cleavage is sequence specific. Based on the terminology of Schechter and Berger (Schechter & Berger, 1967), strong preference of neurotrypsin for substrate cleavage was observed for basic amino acids in the P1 position and a strictly conserved Glu at the P2 position which is important for recognition by the S2 subsite of neurotrypsin.

	α site										β site									
Species	P5	P4	P3	P2	P1	↓	P1'	P2'	P3'	P4'	P5'	P5	P4	P3	P2	P1	↓	P1'	P2'	P3'	P4'	P5'
Homo sapiens	P	P	V	E	R	↓	A	S	C	Y	N	G	L	V	E	K	↓	S	A	G	D	V
Pan troglodytes	P	P	V	E	R	↓	A	S	C	Y	N	G	L	V	E	K	↓	S	A	G	D	V
Bos taurus	L	P	M	E	R	↓	A	S	C	Y	N	G	L	I	E	K	↓	S	A	G	D	L
Canis familiaris	P	P	M	E	R	↓	A	S	C	Y	N	G	L	I	E	K	↓	S	A	G	D	V
Rattus norvegicus	P	P	I	E	R	↓	A	S	C	Y	N	G	L	V	E	K	↓	S	V	G	D	L
Mus musculus	P	P	I	E	R	↓	A	S	C	Y	N	G	I	V	E	K	↓	S	V	G	D	L
Gallus gallus	P	A	I	E	R	↓	A	T	C	Y	N	V	I	I	E	K	↓	A	A	G	D	A
Discopyge ommata	V	P	N	E	R	↓	S	T	C	D	N	A	L	E	E	K	↓	S	A	S	G	S
Rana pipiens												A	T	I	E	K	↓	S	A	G	S	S
Danio rerio												T	I	F	E	K	↓	S	A	G	D	T
consensus	P	P	I	E	R	↓	A	S	C	Y	N	G	L	V	E	K	↓	S	A	G	D	V
	L	A	M			↓	S	T		D		A	I	I			↓	A	V	S	G	L
	V		V			↓						V	T	E			↓				S	S
			N			↓						T		F			↓					T
																	↓					A

Figure 1-10. Alignment of α- and β-cleavage sequences of agrin of different species. For comparison of amino acid residues surrounding scissile bond of α- and β-cleavage sites, terminology of Schechter and Berger was used. P1 denotes the N-terminal and P1' the C-terminal residue engaged in scissile bond. Flanking residues in N-terminal direction are denoted P2, P3,…Pn, flanking residues in C-terminal direction are denoted P2', P3',…Pn'. Figure and text are taken and modified from (Reif et al, 2007).

The temporal expression pattern suggests that cleavage is active during the late phase of synaptogenesis and decreases in adult brain (Figure 1-11). The agrin-22 fragment is only detectable in murine brain tissue until age P60 whereas the persistence of agrin-90 indicates that neurotrypsin cleavage is active at both sites throughout life. Recent observations implicate a synapse-regulating function of agrin and its neurotrypsin-dependent fragments in the CNS. It has been reported that clustering of transmembrane agrin by polyclonal anti-agrin antibodies induce a dose- and time-dependent formation of numerous filopodia-like processes extending from axons and dendrites of the CNS and PNS neurons (Annies et al, 2006). Dendritic filopodia are thin and long membranous protrusions which have been characterized as precursors of spines (Matus, 2005; Knott et al, 2006). They are able to mature into a persistent synapse within days by establishing preliminary contacts with axonal boutons or shafts. The formation of dendritic filopodia was found to be reduced in hippocampal CA1 neurons of neurotrypsin-deficient mice (Matsumoto-Miyai et al, 2009). Remarkably, exogenous application of agrin-22 fully rescued the filopodial response in the observed slice culture. In addition, presynaptic activity was documented to trigger the release of neurotrypsin, whereas additional activation of postsynaptic NMDA-receptor was required for the neurotrypsin-dependent cleavage of agrin. Western blot analyses of synaptosomes confirmed that neurotrypsin-dependent cleavage of agrin occurs locally at the synapse (Stephan et al, 2008). In addition, higher increase of the agrin-90 fragment was observed compared to the amount of agrin-22. Hence, agrin-22 appears to be more diffusible and indicates mobility by passing the non-synaptic tissue into the cerebrospinal fluid (CSF). Neurotrypsin-dependent cleavage of agrin at the synapse is thought to influence the synaptic function of agrin. The release of biological active agrin fragments may modulate the interaction with receptors which are possibly abolished for full-length agrin. Together, these results suggest the neurotrypsin-dependent cleavage of agrin as a potential pathway for activity-dependent reorganization and remodeling of synaptic circuits in the brain.

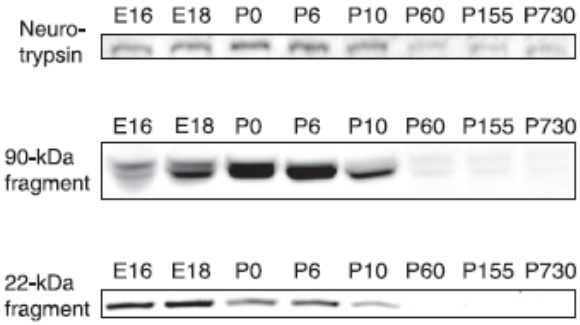

Figure 1-11. Developmental course of neurotrypsin-dependent agrin cleavage. Brain tissue from C57BL/6 mice from embryonic day E16 until postnatal day P730 were analyzed by Immunoblotting using anti-agrin (R132 and R139) and anti-neurotrypsin (G93) antibodies. Neurotrypsin expression and appearance of both 90 and 22 kDa fragments of agrin peaked during late fetal days and in first postnatal week. However, the 90 kDa fragment remained detectable at low level at all adult stages. Figure and Text taken from (Reif et al, 2007).

1.4 The Calsyntenin Family

Calsyntenin-1 was named for bindinding synaptic Ca^{2+} with its cytoplasmic domain (Vogt et al, 2001). It was identified by *in vitro* screen for targeted proteins of extracellular proteases as a transmembrane protein of the postsynaptic membrane in excitatory and inhibitory synapses in the CNS. Calsyntenin-1 has two cadherin-like repeats in its N-terminal extracellular region and a highly acidic cytoplasmic C-terminal region. Northern blot analysis and in situ hybridization illustrated the expression of three different calsyntenin members: calsyntenin-1, -2, and -3 (Hintsch et al, 2002). They show a stringent homology of their extracellular sequences, but show high variability in their architecture of the cytoplasmic domains. The N-terminus of calsyntenin-1 is released into the extracellular space after ξ-cleavage by ADAM10 and ADAM17 (Marcello et al, 2007; Hata et al, 2010). Thus, it exhibits strikingly similar features as the prominent transmembrane, amyloid precursor protein (APP), whose misregulation in proteolytic processing is thought to contribute to Alzheimer`s disease (Figure 1-12). In the case of the calsyntenin members, the transmembrane stump is internalized and accumulated in the spine apparatus of the synapse and the Ca^{2+}-binding domain is translocated from the cytoplasmic side. Hence, calsyntenin-1 is implicated in the dynamic modulation of postsynaptic Ca^{2+}-signaling. The proteolysis-dependent translocation is suggested to illustrate an independent downstream event in protease-mediated synaptic plasticity.

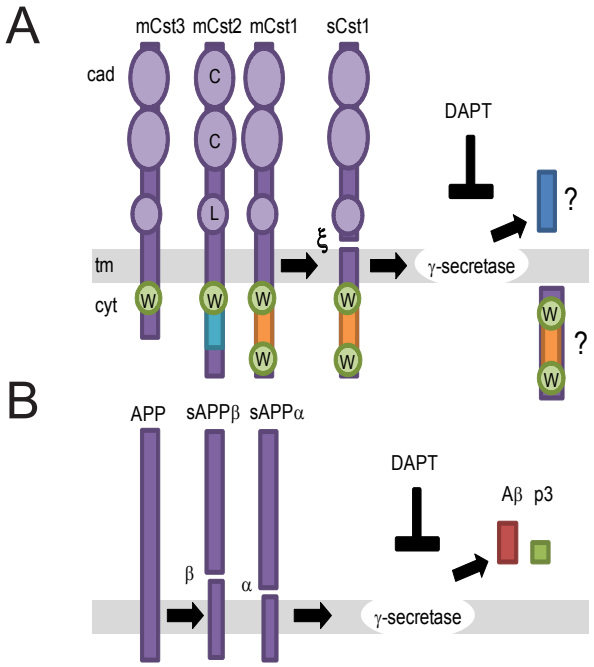

Figure 1-12. Schematic representation of the domain structure of the calsyntenin family members, of β-amyloid precursor protein and their proteolytic processing. A, Calsyntenins are type-I transmembrane proteins and possess two N-terminal cadherin domains (cad), a transmembrane domain (tm) and relatively short cytoplasmic domains (cyt). All three calsyntenins bear conserved WDDS motifs, either in two copies in calsyntenin-1 or in on copy in calsyntenin-3 and murine calsyntenin-2, respectively. All calsyntenins undergo ectodomain shedding (ξ) by ADAM10 and ADAM17, followed by γ-secretase-mediated regulated intramembrane proteolysis, at least in the case of calsyntenin-1 and -3. However, latter resulting proteolytic fragments were not yet identified in vivo. B, β-Amyloid precursor protein (APP) undergoes constitutive ectodomain shedding mediated by α-secretase (α) ADAMs 9, 10, and 17 or alternatively by β-secretase (β) BACE, both resulting in the release of soluble APP and the retention of a C-terminal transmembrane stump. Subsequent γ-secretase-mediated intramembrane proteolysis (γ) of the transmembrane stump generates p3 (α-cleavage) or Aβ (β-cleavage) peptides. Accumulation of latter peptides leads to its amyloidogenic aggregation, which is a hallmark of Alzheimer`s disease. The non-transition state inhibitor DAPT abolishes γ-secretase-mediated proteolytic processing and thus results in an accumulation of the transmembrane stumps. Figure and text taken and modified from (Steuble M., Dissertation, 2008).

Furthermore, calsyntenin-1 is mainly expressed in all CNS neurons, whereas expression levels of Calsyntenin-2 and -3 vary between neuronal subpopulations (see Figure 1-13). Pyramidal neurons in the hippocampal CA1 region show high expression of only Calsyntenin-1. In contrast, part of the Purkinje cells in the cerebellum express calsyntenin-2 and -3, but lack calsyntenin-1. The distinct pattern for each of the members suggests specific functions in distinct neuronal areas. In addition, the putative Ca^{2+}-binding region exhibits the highest degree of structural diversity between the calsyntenin members. Based on the characteristic clusters of acidic amino acids, calsyntenin-1 shows enhanced Ca^{2+}-binding capacity compared to the other family members (Lucerno et al, 1994).

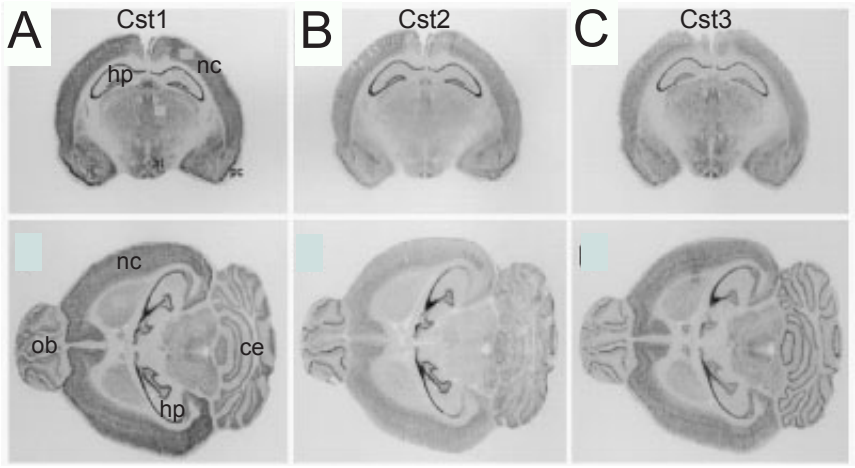

Figure 1-13. Differential expression pattern of calsyntenin members in the brain. (A-C) In situ hybridization of coronal (upper panels) and horizontal (lower panels) sections of adult mouse brain. Calsyntenin-1 and -3 are expressed in the neocortical regions (nc), hippocampus (hp), olfactory bulb (ob), and cerebellum (ce), whereas calsyntenin-2 is expressed only in the hippocampus and olfactory bulb. Figure and text taken and modified from (Hintsch et al, 2002).

Intracellular proteolysis of the type I transmembrane protein APP generates the amyloid-β-protein (Aβ) which, through aggregation and accumulation, is implemented in the pathogenesis of AD (Haass & Selkoe, 2007). The transmembrane protease is named β-site APP cleaving enzyme (BACE) and processes APP at the β-site generating a large extracellular N-terminal domain (sAPPβ) and a cellular C-terminal fragment including the entire Aβ domain. Subsequent intramembrane proteolysis of the transmembrane stump by γ-secretase gives rise to Aβ. Alternatively, a non-amyloidogenic α-secretase pathway by the metallo proteases ADAM9, ADAM10, and ADAM17 can take place (Sisodia, 1992). This process inhibits the production of Aβ by cleavage of APP within the amyloid domain.

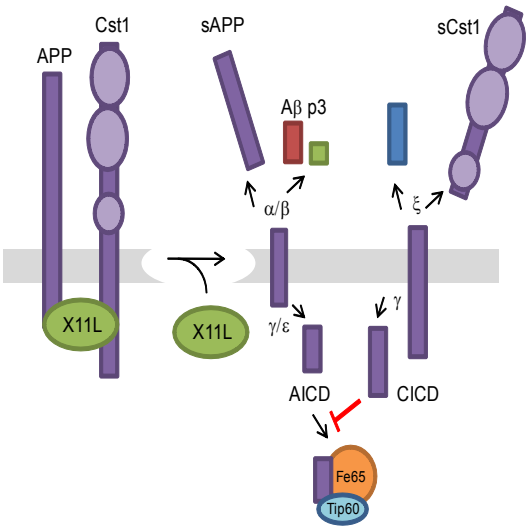

Figure 1-14. Schematic model of the interdependence between calsyntenin-1 and b-amyloid precursor protein. Calsynetnin-1 and APP associate with each other through their interaction with X11L, forming a tripartite complex, which stabilizes the metabolism of calsyntenin-1 and APP. Upon dissociation of X11L, calsyntenin-1 and APP are cleaved at their primary cleavage site (ξ and α or β, respectively) followed by cleavage at the secondary site (γ/ε). The generated intracellular fragment of APP (AICD) forms a complex with the nucleoshuttling protein Fe65 and the histone acetyltransferase Tip60, which exhibit the gene transactivation activity. The intracellular fragment of calsyntenin-1 (CICD) can as well associate with Fe65 and inhibit the Fe65-dependent gene transactivation activity of AICD (Araki et al, 2004). Figure and text taken and modified from (Steuble M. Dissertation, 2008).

Calsyntenins and APP undergo a similar coordinated proteolytic processing (Figure 1-14). Hence, they are also termed Alzheimer-related cadherin-like proteins (alcadeins; Araki et al, 2003). Recent findings demonstrate that APP and the cytoplasmic X11L/Mint2 protein form a tripartite complex with calsyntenin-1 (Araki et al, 2003). It was suggested that formation of this complex stabilizes intracellular APP metabolism and mediates suppression of the Aβ generation. The dissociation of X11L from the tripartite complex enables cleavage of calsyntenin-1 and APP at their primary cleavage sites (ξ and α or β, respectively). Followed by secondary cleavage at the ε/γ-site, an intracellular fragment of APP (AICD) is generated. The cytosolic AICD cleavage product is thought to bind the nucleo-cytoplasmic shuttling protein Fe65 and the histone acetyltransferase Tip60 and forms a transcriptionally active complex (Araki et al, 2004). Similarly, the intracellular fragment of calsyntenin-1 (CICD), which is generated after γ-cleavage, can associate with Fe65. It was suggested that CICD suppressed the Fe65-dependent gene transactivation activity of AICD, probably because CICD competes with the APP intracellular domain fragment for binding to Fe65. In addition, deficiencies in the X11L-mediated interaction and imbalance in the metabolism of calsyntenin-1 and APP may be related to neuronal disorders like AD.

Recently, it was shown in our group that proteolytic processing of calsyntenin-1 and APP is dependent on neuronal activity (Steuble M., unpublished results). The chemical LTP stimulation was performed in whole hippocampi of young mice. Both potassium-based TEA and non-potassium-based PFR chemical LTP stimulation protocols increase ectodomain shedding of the two molecules, whereas TEA elicits a stronger LTP-inducing effect than PFR (Figure 1-15).

It might well be, that there is a connection of neuronal activity and proteolytic processing. Further studies on proteolytic processing could contribute to better understand pathological mechanisms leading to neuronal disorders.

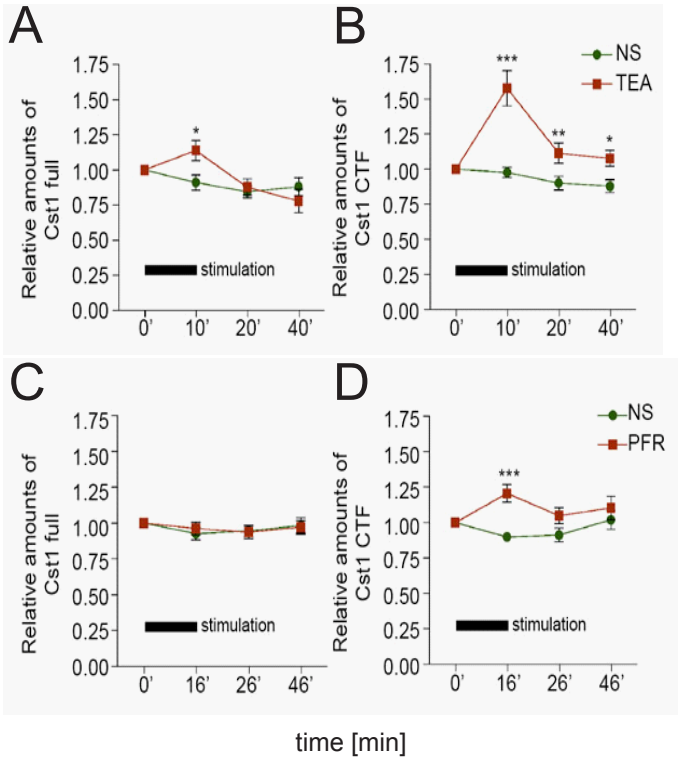

Figure 1-15. Timecourse of the relative amount of full-length calsyntenin-1 (Cst1 full) (A and C) and the cleavage product calsyntenin-1 ectodomain (Cst CTF) (B and D) during chemical LTP stimulation in whole hippocampi. LTP induction was performed by potassium-based TEA (A and B) and non-potassium-based PFR (C and D) stimulation. The hippocampi were taken from young mice (P10). Experiments were performed with in triplicates with n=5 hippocampi; normalized to β-actin; *p < 0.05; **p < 0.005; ***p < 0.001; paired *t*-test (Steuble M., unpublished results).

1.5 Mass spectrometry

Mass spectrometry (MS) is a powerful analytical tool used in chemistry, biology, pharmacy and medicine and provides insights e.g. into possible interaction partners and signaling pathways. The measurement of the accurate molecular weight of a compound provides information about the sample purity and helps to determine post-translational modifications. Fragmentation of selected proteolytic precursor ions in so called tandem MS analyses offers the possibility to obtain inormation about the sequence of biomolecules and their identification by matching the MS fragment ion spectra to sequence databases.

Nomenclature of fragment ions

The nomenclature according to Roepstorff and Fohlmann (Roepstorff & Fohlmann, 1984) is based on the idea of the breaking peptide bond (Figure 1-16. The y-fragment is the piece representing the original C-terminus. Fragment ions representing the N-terminus are named b-ions. Amino acids with functional groups (Asp, Glu, Lys, Arg, Cys) and distinctive structural features (Pro) can influence the fragmentation process of a peptide. Thus, the process of fragmentation can change within the peptide.

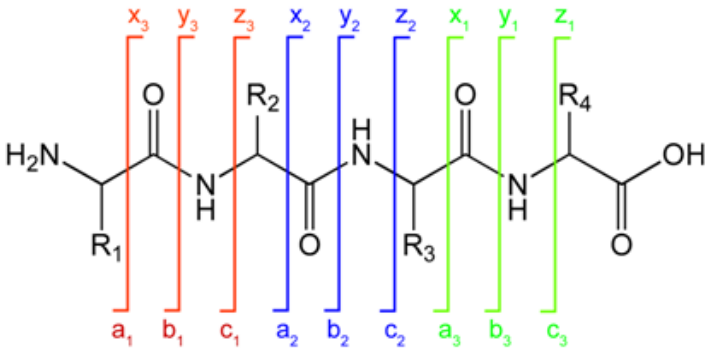

Figure 1-16. Peptide fragmentation pattern according to Roepstorff

The mass spectrometer mainly consists of four important and very flexible parts: the HPLC-interface, the ionization section, the mass analyzer, and the detector. A large variety of ionization methods and mass analyzers offers the identification of unknown compounds, the quantification of known compounds and the elucidation of the structure and chemical properties of molecules. The sections 1.5.1 and 1.5.2 will describe two predominant types of ionization and the commonly used mass analyzer in more detail.

1.5.1 Ionization

For the ionization of large biomolecules such as peptides and proteins a soft ionization method is essential, since these molecules are a polar, nonvolatile, and thermally unstable species, therefore relatively fragile and fragment easily when using conventional ionization methods. The two important ionization methods with regard to soft ionization are electrospray ionization (ESI) and matrix assisted laser desorption ionization (MALDI).

Electrospray ionization

Electrospray is a continuous ionization method coupled to the continuous analysis mass spectrometer. It uses the formation of charged liquid droplets that contain the analyte and from which the ions are desolvated or desorbed (Fenn et al, 1989). During ionization, single and multiply charged ions like $[M+H]^{1+}$ and $[M+nH]^{n+}$ are formed in solution. ESI allows the analysis of molecules with a high mass, such as proteins, because a high amount of charge i.e. protons, can be transferred to the molecule during the ionization process. Therefore large biomolecules can be detected as multiple charged ions in a moderate m/z range. As ESI is perfectly compatible with liquid separation techniques it has become one of the most widely used methods in biological analyses. The development of micro and nano ESI offers higher sensitivity, as they can be coupled to capillary reversed phase columns which run at low flow rates in the nano-liter per minute range (Griffin et al, 1991; Emmett et al, 1994; Shen et al, 2003).

Matrix assisted laser desorption ionization

Unlike ESI, the MALDI source produces mainly $[M+H]^{1+}$ ions from solid phase. The matrix in MALDI applications functions as the carrier of the charge (Karas and Hillenkamp, 1988). It absorbs the energy from the laser beam, gets ionized and transfers part of the charge to the biomolecules which have been co-crystallized with the matrix before. The absorption of the excessive energy by the matrix molecules prevents the degradation of the analyte. As matrix, low-molecular substances with high tendency for crystallization are used. Their absorption peak is in the range of the wavelength of the applied laser.

1.5.2 Mass analyzer

After a long period of research for enhancing the performance of the ionization, MS instrumentation is now dominated by the improvements of the performance of the mass analyzer. This part of the instrument enables isolation and storage of ions and separates them based on the m/z ratio. The basis consists of three different mass analyzers: (i) the quadrupole (Q) which uses m/z stability; (ii) the time-of-flight (TOF) which uses flight time and (iii) the ion trap (IT), orbitrap (OT) and ion cyclotron resonance (ICR) which is based on m/z resonance frequency (Yates et al, 2009). Through the combination of several mass analyzers, advanced MS-MS capabilities can be created. The types of mass spectrometers which are commonly used in proteomic studies are summarized in Table 1-2.

Instrument	Resolution	Mass accuracy	Sensitivity	Dynamic range
LIT (LTQ)	2.000	100 ppm	fmol	1E4
TQ	2.000	100 ppm	amol	1E6
LTQ-OT	100.000	2 ppm	fmol	1E4
LTQ-FTICR	500.000	< 2 ppm	fmol	1E4
Q-TOF	10.000	2-5 ppm	amol	1E6

Table 1-2. Performane comparison of commonly used mass analyzers in proteomics. Linear ion trap (LIT/LTQ which is the Thremo Scientific version). Figure and text taken and modified from Yates et al, 2009.

1.5.3 Separation and LC-MS coupling

On-line coupling of the nano-liquid chromatography system to the ESI source of the mass spectrometer offers a fast and powerful tool to effectively reduce the complexity of the sample mixtures (e.g. serum, urine, cerebrospinal fluid) and increase the sensitivity. It is the first step in method development and essential for analyzing molecules in the low abundant peptides (Yates et al, 2009). The reversed phase (RP) resins separate proteins and peptides according to their hydrophobicity. Development of narrow capillary RP columns showed an increase in sensitivity and dynamic range in peptide separation (Shen et al, 2002; Shen and Smith, 2002; Shen et al, 2005). Additionally, improvement of peak capacity, resolution and faster analysis was achieved by using small particle size (> 2μm) (Anspach et al, 2007). The Workflow of a typical proteomic experiment is illsutrated in Figure 1-17. Typically, proteins are digested to produce a complex mixture of peptides, which are separated by HPLC before analysis by MS. The overall process consists of a number of steps, specifically the ionization of the peptides, acquisition of a full spectrum (survey scan) and selection of specific precursor ions to be fragmented, fragmentation, and acquisition of MS/ MS spectra (product-ion spectra). Two of the predominant mass analyzers used in Proteomics will be disscussed in the following section.

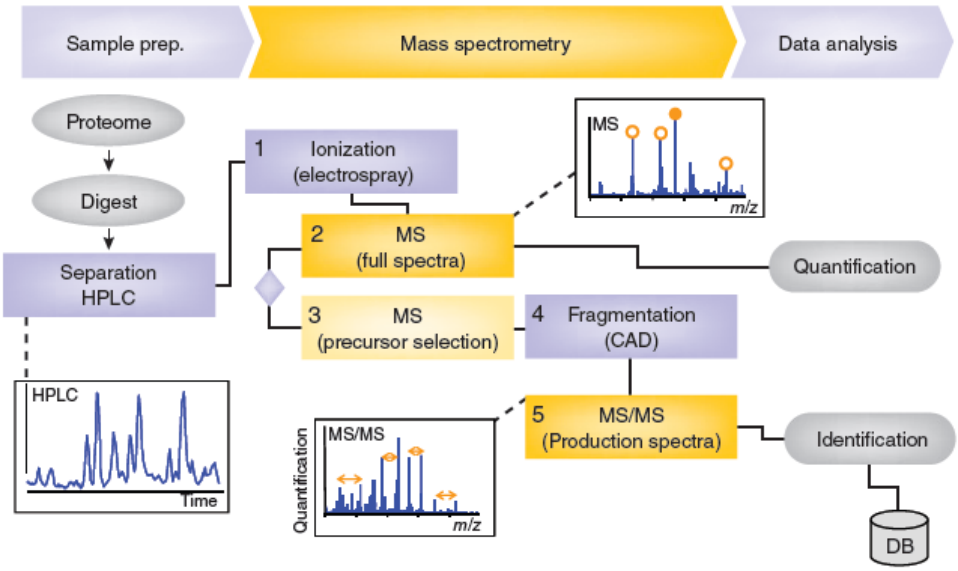

Figure 1-17. Workflow of a typical proteomic experiment. Proteins are digested to produce a complex mixture of peptides, which are separated by HPLC before analysis by MS. The overall process consists of a number of steps, specifically the ionization of the peptides, acquisition of a full spectrum (survey scan) and selection of specific precursor ions to be fragmented, fragmentation, and acquisition of MS/MS spectra (product-ion spectra). The data are processed to either quantify the different species and/or determine the peptide amino acid sequence through a database search. Figure and text taken and modified from (Domon and Aebersold, 2010).

1.5.4 Instrumentation and applications

Fourier Transform Ion Cyclotron Resonance Mass Spectrometry

Fourier transform mass spectrometry (FT MS) is based on the concept of ion cyclotron resonance (ICR). The ions are formed in an external source and trapped in the FTMS analyzer cell which is placed in a center of a strong magnetic field. The ions move in raid spirals around the magnetic field lines. The cyclotron frequency is dependent on the m/z ration of each ion as well as the magnetic field strength. When ions are passing the receiver plates, their image current signals are recorded. This results in high resolution and mass accuracy since frequencies can be recorded more precise than other physical parameters. Mass spectra are generated using Fourier transform analysis. The time-dependent transients of the ions are therefore converted into a frequency-dependent function.

Quadrupole instruments

The quadrupole mass spectrometer consists of four precisely straight and parallel rods and functions as a mass filter. As a result of the high frequency electric field, ions are oscillating in x and y direction through the quadrupole. Only resonant ions with a specific m/z ratio pass the quadrupole filter on a stable flight path, whereas all others are non-resonant and get redirected on their path. During m/z analysis, the frequency and DC voltage of the poles is varied whereby the spectrum is generated.

Targeted mass spectrometry

In contrast to shotgun or directed MS, this technique uses previously established information to develop a detection and quantification method of previously evaluated analytes in complex protein mixtures. It allows the analysis of predetermined fragment ions which are anticipated, but not necessarily detected in a survey scan (Domon and Aebersold, 2010). The experiment is mainly performed on a triple quadrupole instrument which operates in selected reaction mode (SRM, often also called MRM). For SRM approaches using TQ instruments, the first quadrupole Q1 is set for a distinct precursor ion mass, which then enters the Q2 collision cell. The Q3 is additionally set for one or several distinct fragment ion masses. In this manner, the transition of Q1 to Q3 is monitored. The workflow of a targeted MS assay is demonstrated in Figure 1-18.

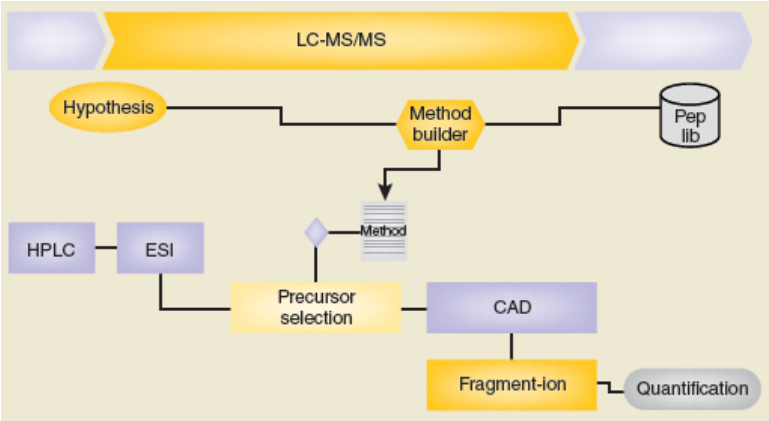

Figure 1-18. Workflow of a targeted proteomic experiment. As the experiment is hypothesis-driven, it targets a very specific subset of peptides uniquely associated with the proteins of interest. An instrument method is built using existing proteomic resources (peptide spectral libraries) required for a target analysis and is typically performed using a triple-quadrupole instrument. For each peptide, a series of transitions (pairs of precursor and fragment ion m/z values) are monitored during a time that specifically corresponds with its predicted elution time. This enables hundreds of peptides to be analyzed in a single experiment. Figure and text taken and modified from (Domon and Aebersold, 2010).

For each transition, the m/z of the precursor ion, its elution time and characteristic high-intensity fragment ions need to be defined. An initial effort is required to evaluate ideal fragmentation parameters and to generate an optimized method for each peptide (Domon and Aebersold, 2010). The method is highly specific and the most sensitive mass spectrometric strategy and therefore used to screen complex sample mixtures for distinct target proteins.

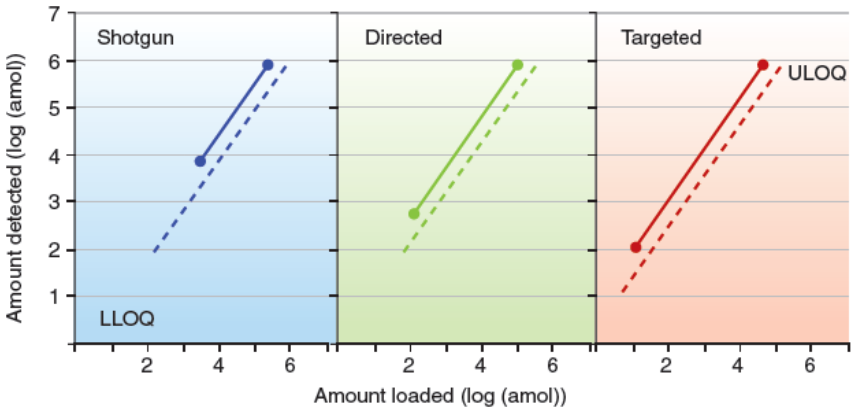

Figure 1-19. Effect of biochemical background on quantification by the shotgun (discovery), directed and targeted proteomics strategies. Whereas dotted lines indicate a low-complexity background, full lines represent a complex background, such as a full cell lysate. LLOQ, lower limit of quantification; ULOQ, upper limit of quantification. Figure and text taken and modified from (Domon and Aebersold, 2010).

The limit of detection (LOD) is defined as three times the signal-to-noise ratio, while the limit of quantification (LOQ) is defined as nine times the signal-to-noise ratio. The complexity of the sample matrix is affecting the dynamic range as well as the LOD/LDQ of a certain method (Figure 1-19). The LOD of the same peptide can be shifted by several orders of magnitude if this peptide is surrounded by a complex sample matrix and decreased signal intensities of the analyte in complex samples are recorded when compared to pure analyte (Domon and Aebersold, 2010). The differences in limit of detection and dynamic range are shown in Figure 1-20.

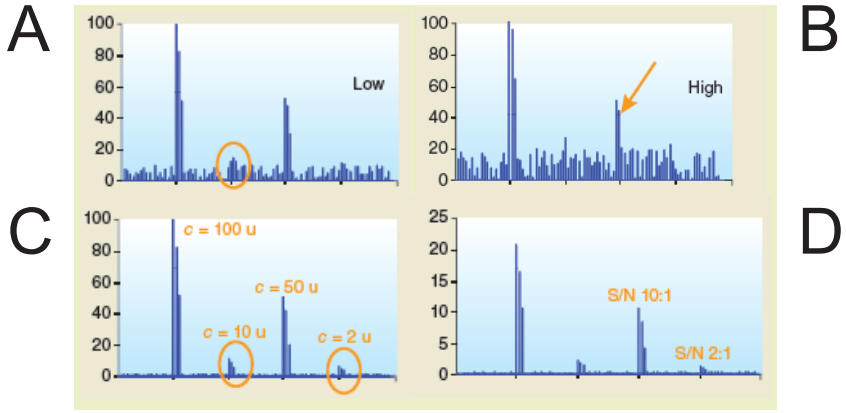

Figure 1-20. Effect of background on the detection of a peptide mixture in various concentrations (arbitrary units). (A) low/moderate background; (B) high background; (C) In-beam, no background; (D) trapping instrument, no background; note the changes in the ordinate as ion counts decrease. c, concentration; u, arbitrary units; S/N, signal-to-noise; the x and y axes correspond to m/z values and signal intensities, respectively. Figure and text taken and modified from Domon & Aebersold, 2010.

1.5.5 Quantitative proteomics

Protein quantification via isotope labeling

The reliable quantification of proteins is essential for the understanding of biological processes and evaluation of protein biomarkers in order to shed light on disease processes. A quantification model needs to be independent of protein sequence, accurate over several orders of magnitude and should not be affected by the overall sample complexity. The first quantization strategy was the comparison of spot intensities after sample separation with 2 Dimensional Electrophoresis (2DE) gels. The limitations of quantification via 2DE gels is due to a low resolution, low dynamic range and the difficulty of detecting proteins with extreme molecular mass or isoelectric point (pI) (Gygi et al, 2000). In addition, spots on a given 2DE-gel often contain more than one protein, making it difficult to quantify changes of the protein of interest since it is not clear which protein has changed in the spot. Beside the 2DE-gel approach, a various set of isotope labeling techniques have been developed: isotope-coded affinity tag (ICAT) (Gygi et al, 1999), isobaric tags for relative and absolute quantification (iTRAQ) (Ross P.L. et al, 2004), stable isotope labeling by amino acids in cell culture (SILAC) (Ong et al, 2002), absolute quantification (AQUA), metabolic $^{15}N/^{14}N$ labeling and enzymatic $^{16}O/^{18}O$ labeling. Therefore, samples are labeled separately, mixed together and analyzed by MS. The m/z ratio of the paired peptides can be distinguished by a few mass units. The first approach uses chemical modification by isotope-coded affinity tag (ICAT). Two proteomes can be analyzed and isolated proteins from experiment and control are denatured, reduced and modified with the heavy or light chemical reagent. ICAT involves cystein-directed tagging of intact proteins following tryptic digestion of the combined proteomes of labeled proteins and control. The labeled peptides are further enriched by avidine column via a biotin tag, leading to an overall reduction in sample complexity. Another MS-based approach for relative quantification of proteins is iTRAQ which relies on derivatization of primary amino groups in intact proteins. Therefore, proteins are labeled using isobaric tags that produce fragment ions 114, 115, 116

or 117 Da allowing analysis of four different proteomes in one single analysis. Differentially labeled proteins do not differ in their mass and their tryptic peptides appear as single peak in the MS spectrum. The quantitative information is provided by isotope-encoded reporter ions which are observed exclusively in the MS/MS spectra. For the absolute quantification (AQUA), samples are spiked with a synthesized set of peptides. The stable isotopes (^{13}C, ^{15}N) are incorporated in these peptides at the lysine or arginine position and result in a +8 Da or +10 Da mass shift. As the standard peptides show identical physicochemical properties, they elute with the same retention and ionize in a similar manner as the unlabeled endogenous peptides of interest. This allows for absolute quantification of the analyte, but can only be applied after identification of the biomarker of interest (Kirkpatrick et al, 2005). The constriction in all isotope labeling methods is the need for a mass spectrometer with high mass resolution and the labeling of the samples has to be complete. Statistical analysis is not necessarily possible, since the labeling is basically designed for comparative analysis of two sample sets or upon eight when using iTRAQ. Additionally, one has to keep in mind, that the isotope labels are very cost intensive. The general approaches of quantitative proteomics are depicted in Figure 1-21.

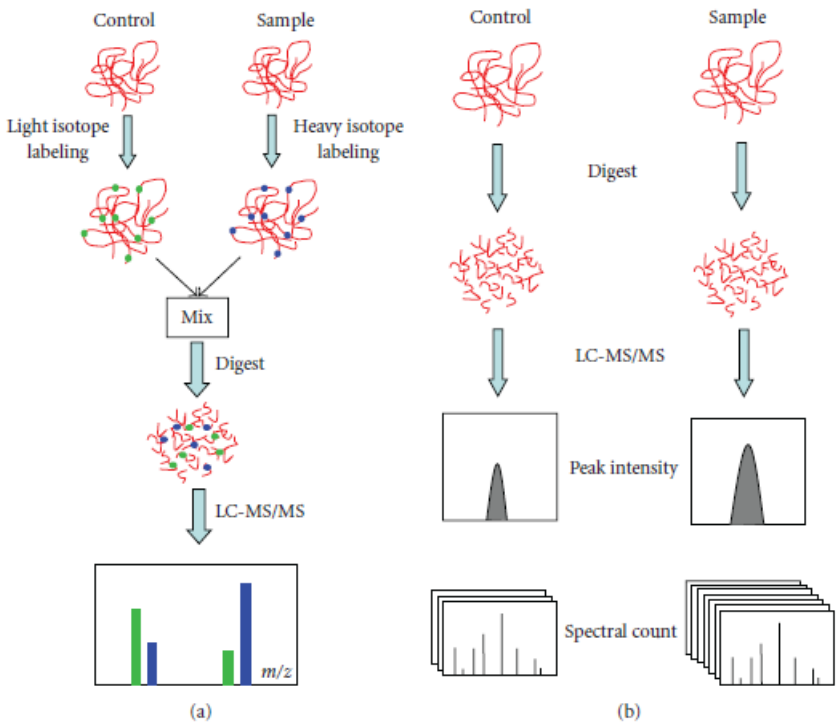

Figure 1-21. General approaches of quantitative proteomics. (a) Shotgun isotope labeling method. After labeling by light and heavy stable isotope, the control and sample are combined and analyzed by LC-MS/MS. The quantification is calculated based on the intensity ratio of isotope-labeled peptide pairs. (b) Label-free quantitative proteomics. Control and sample are subject to individual LC-MS/MS analysis. Quantification is based on the comparison of peak intensity of the same peptide or the spectral count of the same protein. Figure and text taken and modified from (Zuh et al, 2010).

Label-free protein quantification

In contrast to labeling methods, this method is simple, no extra step for sample preparation is needed, and the inclusion of statistical analysis is possible, since a high sample number can be compared. Quantification is either based on ion-intensity changes such as peak area and peak height or on spectral counting of identified proteins after MS/MS analysis.

Relative quantification by peak intensity

Early studies report relative quantification of peptides upon comparison of peptide ion peak intensities in several LC-MS runs (Chelius et al, 2002; Bondarenko et al, 2002). This method is based on the finding that peak areas linearly increase with increased concentration. It could be demonstrated that this method is reproducible even at the complexity of proteome samples when using a correlation of the peak area and retention time between replicate runs (Wang et al, 2006). The method is vulnerable to experimental variability and normalization is required. Additionally, highly reproducible LC performance is essential to accurately align chromatographic peaks. A shift in retention time and/or m/z will result in huge variability and inaccurate quantification. The TOP3protein quantification approach by Silva (Silva et al, 2006) uses precursor ion intensities of the three best performing PTPs in terms of ionization and identification of a certain protein.

Relative quantification by spectral count

The linear correlation between increasing protein abundance and resulting number of PTPs is the basis of relative quantification by comparing the number of identified MS/MS spectra (spectral count) from the same protein identified in multiple LC-MS/MS runs (Washburn et al, 2001). To normalize the influence of protein lengths on spectral count, a normalized spectral abundance factor (NSAF) was calculated (Zybailov et al, 2006).

Absolute quantification by spectral count

A modified spectral counting strategy is absolute expression (APEX) and enables for absolute protein quantification per cell (Lu et al, 2007). The fraction of expected number of peptides is proportional to the observed number of peptides when including correction factors in order to determine the APEX score.

Bioinformatics tools

There is enormous increase in developing bioinformatics tools for label-free quantitative data analysis and several computational methods like SuperHirn, APEX, Mascot-emPAI and T3PQ are available either commercially or as open-source programs (Müller et al, 2008; Grossmann et al 2010). All available software for label-free quantification enables data normalization, time alignment, peak detection, peak quantification, peak matching, identification, and statistical analysis. The workflow illustrated in Figure 1-22 depicts the steps for quantification of proteins in a complex mixture using T3PQ.

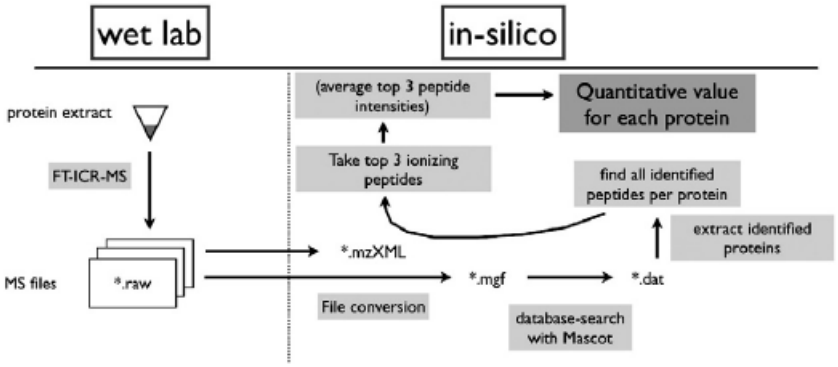

Figure 1-22. Workflow of Top 3 Protein Quantification. The figure illustrates the different steps for achieving quantitative values for proteins in a complex mixture using Top 3 Protein Quantification (T3PQ). Figure and text taken and modified from (Grossmann et al, 2010).

1.6 Biomarker discovery from body fluids via mass spectrometry

The evaluation of biomarkers as reporters of the patho-physiological status of the human body is of exceeding interest. Especially those biomarkers that would allow diagnosis at the early-onset of a disease. Their identification may result in a fast treatment and thus, in a better prognosis of the disease.

The development of novel methods in mass spectrometry offered a new path in the analysis of peptides and proteins from serum samples as source for new diagnostic markers. Initiation was the analysis of serum samples by spot detection in 2DE gels (Anderson, 2002). The implementation of so called fingerprints, peak patterns of peptides, as parameter for identification started in 2002 and shed light on the pathological processes in prostate cancer (Adam et al, 2002; Qu et al, 2002) and breast cancer (Li et al, 2002). Followed by the first SELDI-TOF experiments, where serum samples are incubated on chips providing specific surfaces (C18, immunoglobulins, ion exchange) to fractionate and enrich the proteins. Unbound molecules are removed in a wash step and subsequent application of a matrix on top of the sample spots enables the collection of mass spectra by laser ionization TOF mass spectrometry (Simpkins et al, 2006). By using the peak intensities, protein concentrations were correlated for the blood samples. Additional, first MALDI-TOF studies were based on statistical analysis of peak intensities between a set of cases with a specific disease and control subjects to designate differences in protein concentration (Villanueva et al 2004; Villanueva et al, 2006; Baumann et al, 2005; Callesen et al, 2005). These methods do not necessitate a biological knowledge of the pathological or physiological cause of the disease. Possible biomarkers do not have to be selected before the experiment. Alongside, there are critical comments on the use of mass spectrometric peptide patterns in the process of declaration of novel biomarkers. The pitfalls of the mass spectrometric workflow are threefold:

(i) High variability in experimental design and data mining

As a high number of these studies are based on the comparative analysis of two sample sets, individuals with a specific disease and healthy control subjects. In many cases, a slope in expression of proteins was due to non-specific reactions of the organism, for example the increase of acute-phase response proteins (Diamandis, 2004; Koomen et al, 2005). Another major mistake was the use of faulty algorithms for the classification of diagnostic markers. The result was over-fitting of peak patterns and generation of artifacts. The use of a larger sample number and the careful evaluation of the obtained biological model can help overcome these mistakes (Diamandis, 2004; Wagner et al, 2004; Hilario et al, 2006). Another effect was, that resulting data was not reproducible, neither in other groups nor in the same laboratory (Diamandis, 2003; Feng et al, 2004; Coombes, 2005).

(ii) Technical limitations of the instrumentation

The parameters influencing signal intensity are yet not well understood. Quantification of a certain protein in two samples with distinct compositions may lead to false alterations in protein concentration (Gillette et al, 2005; Aebersold & Mann, 2003).

(iii) The biological relevance of the data

Protein concentrations in the blood cover about 10 orders of magnitude, ranging from albumin (35-50 mg/ml in serum) to IL6 (0-5 pg/ml in serum) Figure 1-23; Anderson & Anderson, 2002). The major group of high abundant plasma proteins comprises albumin, immunoglobulins, fibrinogen, α-1 antitrypsin, α-2 macroglobulin, transferrin and lipoproteins (Schulte et al, 2005). The residual 3% are middle- to low-abundant proteins and are considered to provide information about the patho-physiological condition of the body. As the dynamic range of detection in mass spectrometry is about 2-3 orders of magnitude, it is insufficient to target the overall range of proteins in blood samples. Another effect of high-abundant proteins is suppression of signals of low-abundant proteins (Diamandis, 2004; Gillette et al, 2005; Koomen et al, 2005). Therefore, observed spectral patterns have to be carefully investigated, as they may be caused by artifacts from the analytical process or the natural fluctuations of the blood. A common way to eliminate these disadvantages is the selective depletion of most abundant proteins or the fractionation of the sample. One current depletion technique is the use of resins with efficient binders or antibodies against the high-abundant proteins (Omenn et al, 2005; Echan et al, 2005; Zolotarjova et al, 2005; Huang et al, 2005). Other procedures are ultrafiltration (Rezaee et al, 2006) or adding organic solvents like ACN to enrich globular proteins and albumin in a pellet (Mitchell et al, 2005). Until today, all these methods applied for the depletion of high-abundant proteins remove as well some middle- and low-abundant proteins from the sample (Shen et al, 2005; Granger et al, 2005; Moritz et al, 2005).

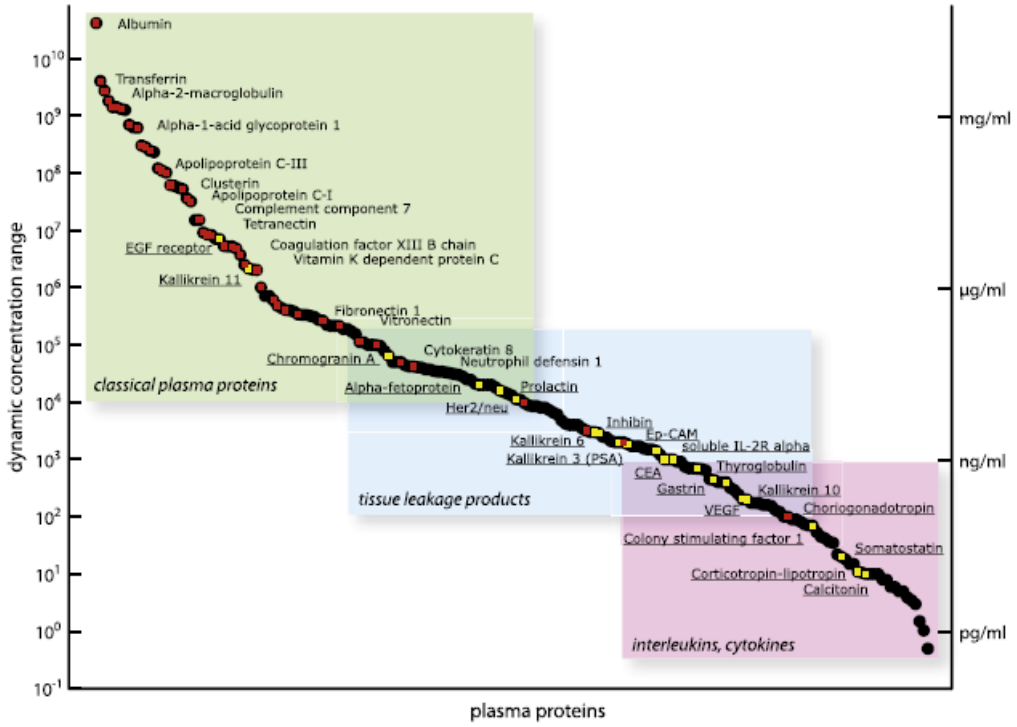

Figure 1-23. Depicted are the plasma protein concentrations as described by Anderson and Anderson (2002). The proteins can be grouped in three main categories (classical plasma proteins, tissue leakage products, interleukins/cytokines). Red dots indicate proteins that were identified by the HUPO plasma proteome initiative (States et al, 2006) and yellow dots represent currently utilized biomarkers (Polanski and Anderson, 2006). Figure and text taken and modified from (Schiess et al, 2009).

1.6.1 Diagnostic markers in serum

Serum is a very interesting source for such diagnostic markers since its proteome carries information about the physiological and pathophysiological state of the human body. It is influenced by the status of various organs and disease-dependent changes. Thus, it delivers biomarkers to monitor the clinical status of the patient. The various proteins cover a wide range of concentrations, for example the amount of serum albumin is in the mg/ml range compared to the pg/ml range of cytokines (Bishop, 2000). Serum albumin covers about 50-70% of the total serum proteins and immunoglobulin heavy and light chains take additional 25%. Whereas sample supply is relatively easy, it is among the most difficult samples to analyze when using LC-MS instrumentation (Anderson and Anderson, 2002). The presence of high-abundant proteins can mask others and results in a loss of resolution in LC-MS approaches. Removal of highly abundant proteins is essential prior to LC-MS analysis (Colantonio, 2005).

1.6.2 Cerebrospinal fluid - a source for biomarkers

The human cerebrospinal fluid (CSF) is one important source for diagnostic markers of neurological diseases. It is produced in the choroid plexus and gets its inputs from extracellular space of the spinal cord and the brain (Mc Comb, 1983). CSF is accumulated in the four ventricles and is an important determinant of the extracellular fluid (ECF) surrounding neurons and glia in the CNS. The CSF has a low protein concentration (150–450 mg/ml) and a high salt concentration (4150 mmol/l). Despite the low total protein concentration, the concentration of albumin (60% of the total CSF protein) and immunoglobulin is extremely high in the CSF (Hammack et al., 2003). The changes of proteins which are involved in biochemical pathways may be reflected in CSF. For example the level of total-tau protein and the light subtype of the neurofilament proteins (NF-L) after acute ischemic stroke (Hesse et al., 2001). The collection of CSF is predominantly performed by lumbar puncture (Figure 1-24). A spinal needle is inserted between the lumbar vertebrae L3/L4 or L4/L5 through the dura and the arachnoid mater into the subarachnoid space. CSF is a multifunctional body fluid and it for example physically protects the CNS and actively regulates CNS activity via circulating hormones and neuropeptides (Stopa et al, 2001; Chodobski, 1998). The physiological and pathological status of the CNS can be monitored (Carrette et al, 2003; Davidsson et al, 2005). Thus, CSF serves as ideal biological source for identification of neurological biomarkers to describe the status of the brain. For several years, various groups used the CSF proteome to characterize diagnostic markers in the context of brain diseases (Abdi et al, 2006; Zhang et al, 2005).

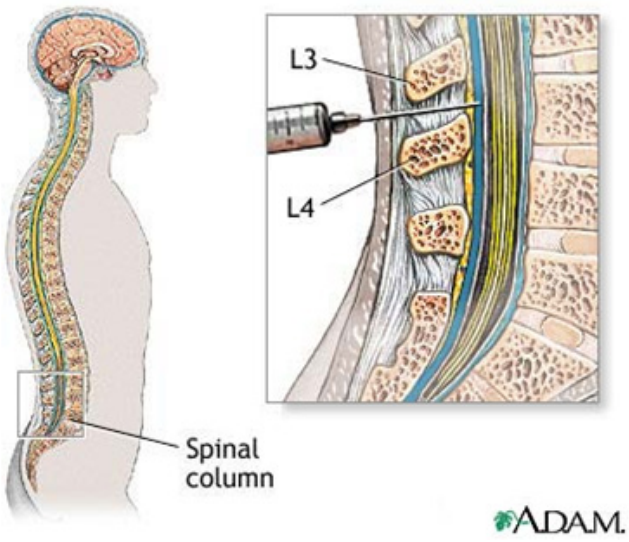

Figure 1-24. CSF collection by lumbar punture. Figure taken from (Olson & Pawlina, 2008)

As there is a high variability between results of several laboratories studying the CSF proteome, there are some factors which have to be carefully discussed when working with CSF. The main influences on heterogeneity between results are: variability of patients, experimental design, sample processing and the proteomics technology.

Variability of patients

The total CSF volume in an adult is about 150 ml. As CSF is renewed every 6-8 hours, the overall daily production is about 500 ml. In addition, there is a bulk flow of molecules, regardless of the molecular size, from extracellular fluid of the spinal cord and the brain to CSF (Cserr et al, 1981). Besides, plasma proteins enter the CSF upon diffusion with respect on their molecular size (Thompson, 1995). In the lumbar cisterna, highest protein concentrations of about 2.5 times compared to the ventricular zone are found (Huhmer et al, 2006). Therefore, it is of high importance for the quantification assay, that CSF is collected always in the same way. In our case we included only human CSF collected by lumbar puncture, which is a conventional method. In some biomarker studies, only later fractions (15-25th ml) were used, because concentrations of brain-derived proteins should be highest with regard to the caudorostral gradient (Abi et al, 2006; Zhang et al, 005; Pan et al, 2006). Other factors on protein concentrations in CSF are age and circadian rhythm. The CSF turnover decreases with age (Preston, 2001) and the secretion rate is reported to be about doubled at night when compared to the afternoon in healthy subjects (Nilsson et al, 1992). Timing of the lumbar puncture and the age of a subject thus affect quantitative proteomics. Hence, we included the correlation of agrin-22 levels to age for each subject. Agrin and neurotrypsin expression shows age-dependency.

Sample storage

It has been reported, that protein degradation occurs when they have undergone multiple freezing/thawing and when stored at -20°C (Carrette et al, 2005). CSF samples should be stored at -80°C in aliquot samples to avoid freeze/thaw cycles. Since there is no information about suitable protease inhibitors, addition of inhibitor cocktails is not recommended.

Sample processing

Relatively high salt concentrations in CSF require a desalting step in the beginning of sample preparation. According to the documentation of Zhang (Zhang, 2007), desalting of CSF is achieved best with dialysis in terms of protein recovery. The dynamic range of CSF proteins is comparable to blood (Blennow et al, 1993). Therefore, depletion of high-abundant proteins and enrichment of low abundant proteins is required.

2 Aim

The approach towards developing a biomarker for monitoring activity of the drug target neurotrypsin was based on identifying and quantifying the product of neurotrypsin`s proteolytic activity in bodyfluids, i.e. the 22 kDa fragment of its unique substrate agrin. This was supposed to be achieved by quantitative mass spectrometry as well as Western blot analysis. The cleavage of agrin by neurotrypsin releases its C-terminal domain agrin-22 into the serum and CSF. Hence, the level of this fragment in these bodyfluids gives rise on the proteolytic activity of neurotrypsin in the brain as well as in the periphery. The following work is aimed in detecting and quantifying the agrin-22 fragment in murine serum of neurotrypsin overexpressing as well as neurotrypsin deficient mice and human CSF at different ages and various neurological diseases. The level of this fragment could report about the activity of neurotrypsin at the synapse. Its concentration might have a diagnostic value or serve for the monitoring of therapeutically interventions. Since it was shown that the release and activation of neurotrypsin follows an activity dependent mechanism, the focus was set on diseases with uncommon neuronal activity e.g. epilepsy and Alzheimer's disease. The activity of neurotrypsin and therefore the level of the cleavage fragment agrin-22 in CNS could serve as diagnostic biomarker for neurological diseases. Besides, neurotrypsin's unique substrate agrin has been extensively studied at the neuromuscular junction, where a synapse promoting effect could be observed. As the role of agrin in the CNS is not well understood, it is conceivable to have a synapse stabilizing effect in the brain as well. Hence, the work was as well aimed to improve the understanding of the functional role of agrin-22 in the CNS.

Furthermore, proteolytic ectodomain shedding of the transmembrane protein calsyntenin-1 was identified and quantified. Calsyntenins and APP undergo a similar coordinated proteolytic processing. After ectodomain shedding (ξ) by ADAM10 and ADAM17, cleavage by γ-secretase regulateds intramembrane proteolysis. The transmembrane stump of calsyntenin-1 is internalized and accumulated in the spine apparatus of the synapse. Thus, proteolysis-dependent translocation is suggested to illustrate an independent downstream event in protease-mediated synaptic plasticity. Furthermore, the similar metabolism of calsyntenin-1 and APP may be related to neuronal disorders like AD and it was recently shown that calsyntenin-1 ectodomain-shedding is increased by induction of synapse activity. Further studies on the proteolytic processing could contribute to better understand pathological pathways leading to neurological diseases.

3 Results

The generation, reorganization and elimination of synaptic circuits is an essential mechanism during learning and memory tasks in the central nervous system (CNS). It is known that extracellular proteases are involved in these structural changes in neurons. The neuronal serine protease neurotrypsin is expressed in many brain areas during neuronal development. A four base pairs deletion in the coding region leads to an inactive form of neurotrypsin and causes severe mental retardation in humans. Therefore, neurotrypsin was linked to adaptive synaptic functions. Neurotrypsin cleaves agrin at two well-defined sites and one released fragment, agrin-22, shows a promoting effect on filopodia generation. To address the cleavage activity of neurotrypsin, agrin-22 was quantified by Western blots of murine serum from mice either overexpressing or lacking neurotrypsin. To investigate the role of agrin-22 in the CNS, human cerebrospinal fluid (CSF) from patients of different ages, with Alzheimer's disease (AD) and epilepsy compared to healthy control subjects, was analyzed by Western blot. The main focus of this project was the development of a targeted mass spectrometry assay to quantify the four agrin-22 isoforms z0, 8, 11, and 19, since they are not distinguishable in Western blot analysis. Additionally, quantification of calsyntenin-1 ectodomain was included in the studies of human CSF samples. There was supporting evidence that ectodomain shedding of calsyntenin-1 is dependent on neuronal activity and thus could provide a diagnostic marker for AD as well as epilepsy.

3.1 Isolation and identification of agrin-22

In this paragraph, I am going to identify and describe the presence of the neurotrypsin-dependent agrin-22 fragment in murine serum and rat cerebrospinal fluid (CSF). I will start with the identification of agrin-22 using data-dependent LC-MS/MS measurements and give an overview about the activity of neurotrypsin in association with the age and the genotype of different mouse groups. So far, neither murine serum nor rat CSF were subjected to detailed analysis, therefore nothing was known about the distribution of agrin-22 isoforms in these body fluids.

3.1.1 Neurotrypsin-dependent processing in murine serum and rat cerebrospinal fluid

As a result of the relatively low agrin and neurotrypsin expression, enrichment of agrin-22 was essential. Immuno-affinity isolation was performed, pooled elution fractions were trypsinized and analyzed by mass spectrometry. Analysis was achieved using an inclusion list for agrin-22 z0, 8, 11, and 19, which enabled selection of peptide ions with particular mass-to-charge (m/z) ratio for collision-induced dissiociation (CID) in the LTQ mass spectrometer. The mapped tryptic peptides from LC-MS/MS are shown below and confirmed the presence of the neurotrypsin-dependent cleavage fragment agrin-22 in murine serum (Figure 3-1) and rat CSF (Figure 3-2). All tryptic peptides match the very C-terminal part in the LG3 domain of agrin.

SVGDLETLAF DGRTYIEYLN AVIESEKALQ SNHFELSLRT EATQGLVLWI GKVGERADYM ALAIVDGHLQ LSYDLGSQPV VLRSTVKVNT NRWLRVRAHR EHREGSLQVG NEAPVTGSSP LGATQLDTDG ALWLGGLQKL PVGQALPKAY GTGFVGCLRD VVVGHRQLHL LEDAVTKPEL RPCPTL

Mascot search results:
Database: UniRef100 20020206
Agrn protein [Mus musculus] Q99KT4, Mass: 28364, Score: 276, Queries matched: 9

Figure 3.1. Identification of the neurotrypsin-dependent cleavage fragment agrin-22 in murine serum samples. The identified tryptic peptides from LC-MS/MS analysis are highlighted in colors.

SVGDLETLAF DGRTYIEYLN AVIESEKALQ SNHFELSLRT EATQGLVLWI GKAAERADYM ALAIVDGHLQ LSYDLGSQPV VLRSTVKVNT NRWLRIRAHR EHREGSLQVG NEAPVTGSSP LGATQLDTDG ALWLGGLQKL PVGQALPKAY GTGFVGCLRD VVVGHRQLHL LEDAVTKPEL RPCPTP

Mascot search results:
Database: UniRef100 20051018
Agrin precursor [Rattus norvegicus] UPI00005038EA, Mass: 206096, Score: 251, Queries matched: 6

Figure 3-2. Identification of the neurotrypsin-dependent cleavage fragment agrin-22 in murine serum samples. The identified tryptic peptides from LC-MS/MS analysis followed by Mascot database search are highlighted in colors.

The absence of N-terminal parts of agrin in serum and CSF was confirmed by Western blot analysis using the antibodies R139 against the C-terminal LG3 domain of agrin and the antibody R132 against the N-terminal part of agrin (not shown). The identified tryptic peptides are not proteotypic for one specific z-isoform of agrin-22. Hence, no suggestion can be given for the distribution pattern or neurotrypsin`s favorable substrate in case of agrin-22 splice variants. Neither full-length agrin (smear at 250-200 kDa) nor one of the other neurotrypsin-dependent cleavage products agrin-90 or agrin-110 could be detected. Therefore it was concluded, that agrin-22 is released into the blood and CSF and can serve as reporter on neurotrypsin`s proteolytic activity.

3.1.2 Neurotrypsin-dependent cleavage of agrin is linked to the genotype

To confirm the neurotrypsin-dependent processing of agrin, mouse serum was compared by Western blot. Serum of transgenic mice overexpressing neurotrypsin (tg/+, Muslik 533) and of homozygous neurotrypsin-deficient mice (KO/KO, NT-KO) of different ages (P4 and P10) was analyzed. As reference, sera of wild type littermates from each mouse group were included. The control sera used for signal normalization were from wild type mice (+/+, NMRI) of the age E18 (Figure 3-3).

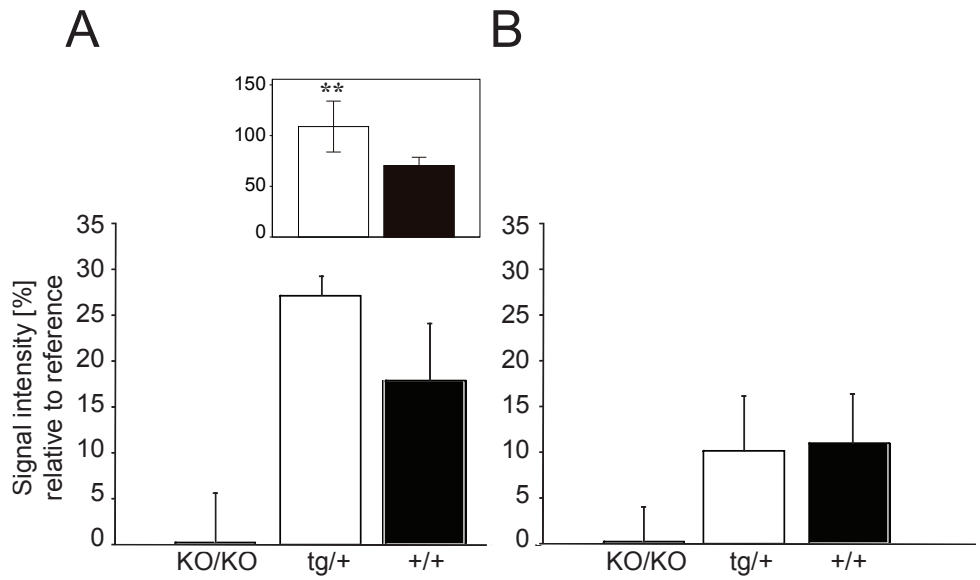

Figure 3-3. Evaluation of agrin-22 in homozygous neurotrypsin-deficient mice (KO/KO), transgenic neurotrypsin-overexpressing mice (tg/+) and wild type littermates (+/+). (A) Agrin-22 levels at P4. (B) Agrin-22 levels at P10. Murine serum was separated by 4-12% NuPAGE gels and quantitative Western Blot was performed from the same sample in triplicates. Error bars represent STDEV. The small insert in (A) shows the result of the t-test for five independent samples of (tg/+, open bars) and (+/+, black bars). ** $p < 0.005$. Western Blot was performed in triplicates. Error bars represent STDEV.

The neurotrypsin-dependent processing of agrin is particularly active during neuronal development. Additionally, neurotrypsin-overexpressing animals show significantly increased amounts of agrin-22 at P4 compared to wild type animals ($p < 0.005$). The increase in signal intensity in serum of neurotrypsin-overexpressing animals displays a higher accumulation of agrin-22 which is likely due to higher expression of neurotrypsin and thus due to increased proteolytic processing of agrin. At P10, signal intensity was clearly reduced in both neurotrypsin-overexpressing mice as well as their wild type littermates. There is no difference in agrin-22 levels compared to P4. This might be explained by a decreased expression of neurotrypsin and particularly of endogenous agrin with increased age of the animals (see also next chapter). In contrast, the agrin-22 signal was clearly absent in homozygous neurotrypsin-deficient animals at both ages. This reflects most likely the lack of neurotrypsin-dependent cleavage. Furthermore, it supports the finding that the presence of agrin-22 is exclusively dependent on cleavage of agrin by neurotrypsin. The full length form of agrin was not present in murine serum neither in neurotrypsin overexpressing animals nor in serum from their wild type littermates (data not shown). The unprocessed full-length agrin variants are therefore thought to accumulate in the tissues. Distribution into the blood stream is abolished as a result of agrin`s high molecular weight or agrin remains N-terminally linked to the tissue. On 4-12% NuPAGE gels followed by Western blots the four isoforms of agrin-22 were not resolved, but appeared as one band at the molecular weight level of 22 kDa. The differentiation of agrin-22 splice variants is not possible when using Western blot, because the antibody R139 against the C-terminal part of agrin, which is used in this study, does not distinguish between the splice inserts.

3.1.3 The appearance of agrin-22 is linked with aging and neuronal development in mice

The amount of neurotrypsin and agrin at the mRNA and protein level is particularly high from the late embryonic phase throughout the first postnatal week (Wolfer et al, 2001, Stephan et al, 2008) and therefore it is linked to early neuronal development. Thus, neurotrypsin`s cleavage activity in relation to age was examined and the presence of the agrin-22 fragment in murine serum of increasing age was analyzed. For this purpose, murine serum samples ranging from P1 until P30 were collected. Again, the concentration of agrin-22 was monitored using heterozygous littermates from neurotrypsin-overexpressing transgenic mice, knock-out littermates from neurotrypsin-deficient mice and wild type siblings. The data shown in figure 3-4 are based on quantification of Western blots with antibody R139 to detect the neurotrypsin-dependent cleavage fragment agrin-22.

The agrin-22 values in murine serum of transgenic neurotrypsin-overexpressing mice as well as the wild-type animals show a decrease following a similar age-dependent course as previously described for endogenous neurotrypsin and full-length agrin. The expression and cleavage activity of neurotrypsin and its substrate agrin is similarly and developmentally regulated (Reif et al, 2007). Highest expression of neurotrypsin was reported to take place around E18 and P10. The results from murine serum samples are in accordance with these previously reported findings on mRNA as well as on protein level.

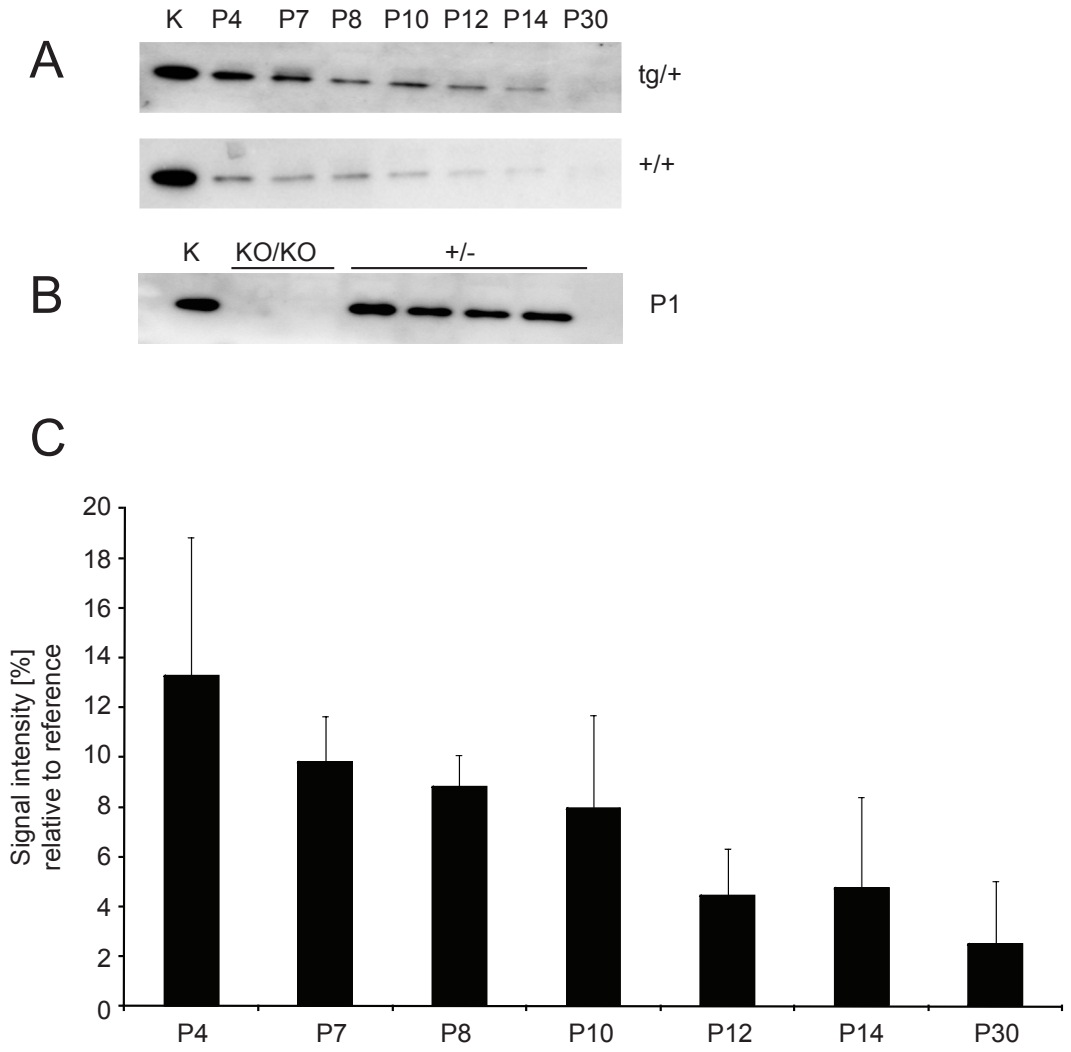

Figure 3-4. Age-dependent agrin-22 levels. (A) Western blot of sera from transgenic neurotrypsin-overexpressing mice (tg/+) and their wild type littermates (+/+) from P4 to P30. (B) Western blot of sera from homozygous neurotrypsin-deficient mice (KO/KO) and their heterozygous littermates (+/-) at P1. Serum from E18 aged wild type mice (K) is loaded as reference for quantification. All serum samples were diluted 1:10 in PBS and 10 µl of this dilution were seperated with 4-12% NuPAGE gels and analyzed by Western blot with antibody R139. (C) Quantitative analysis of Western blots from wild-type sera from P4 to P30. Western blots were perfromed in triplicates using the same sample. Error bars represent STDEV.

3.2 Evaluation of sample preparation for mass spectrometry

Blood, serum, CSF as well as other body fluids can be obtained relatively easily and thus serve as a useful source for the detection and quantification of novel biomarkers. To quantify the four splice variants of agrin-22 in murine serum with mass spectrometry, depletion of the complex protein matrix was necessary. Various high-abundant proteins suppress the signals of low-abundant proteins when using chromatography for protein separation and mas spectrometry (MS) for protein identification. In general, low sample volumes (10-300 µl) are used in liquid chromatography-MS (LC-MS) analysis. Thus most expressed proteins are not present in sufficient quantities and remain undetectable (Fountoulakis, 2001). However, less abundant proteins are often of great interest as they are most likely drug targets and diagnostic markers. Therefore, the removal of highly abundant proteins is essential (Colantonio, 2005).

I am going to describe the advantages and disadvantages in conjunction with depletion. Four depletion columns and three fractionation techniques were tested to deplete murine serum prior to LC-MS analysis (Table 3-1).

Depletion device (supplier)	Loading capacity (in µl serum)	Method	Performance/ Agrin-22 Recovery
ProteomeLab IgY-12 (Beckman Coulter)	10	Affinity column	-
ProteoPrep Immunoaffinity Albumin/IgG Depletion Kit	25	Affinity spin column	-
ProteoSpin Abundant Serum Protein Depletion Kit (Norgen)	10	Ion-exchange spin column	-
ProteoExtract Albumin/IgG Removal Kit (Calbiochem)	15	Affinity gravity column	-
Microcon YM-30 Microcon YM-50 (Millipore)	200	MWCO filter	-
Ammonium Sulfate	5	Precipitation	+
Gelfiltration Superose 12 (10/30)	100	Size-exclusion column	+

Table 3-1. Depletion columns and fractionation techniques used for serum depletion prior to analysis with LC-MS.

3.2.1 ProteomeLab IgY-12

The depletion column was tested with 10 µl murine serum (wild-type, E18). Protein concentrations were monitored with the Bradford protein assay. The fractions of depleted serum, wash and bound proteins were TCA-precipitated, separated by 12,5% SDS-PAGE for silver staining or loaded on a 4-12% NuPAGE gel for Ponceau staining followed by Western blot analysis with antibody R139 (Figure 3-5).

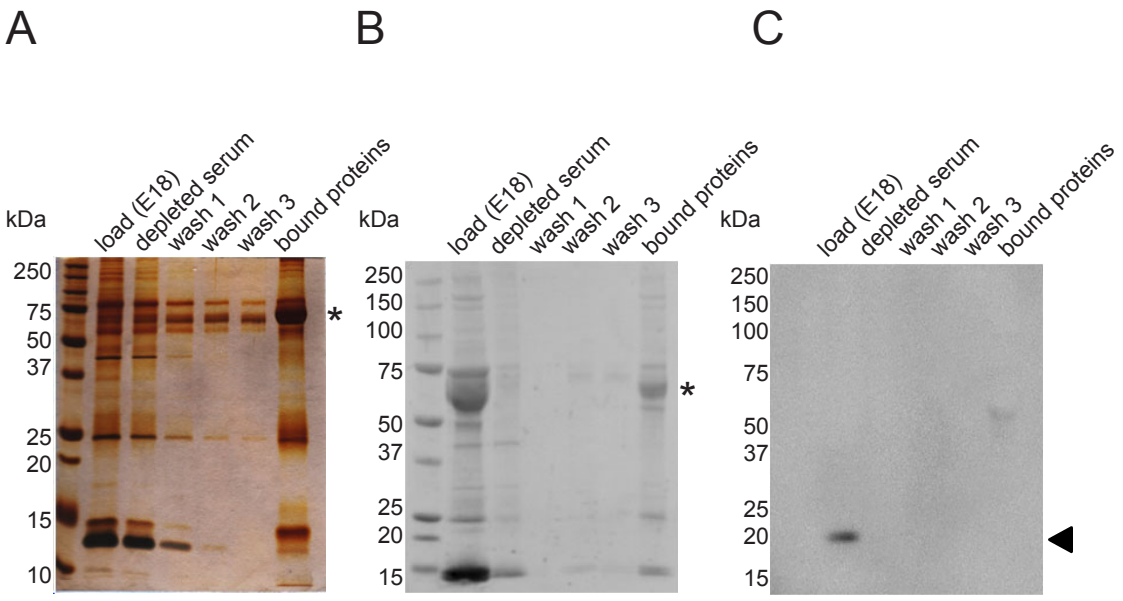

Figure 3-5. Murine serum proteins (wild-type, E18) after depletion of high-abundant proteins using ProteomeLab IgY-12 column. Protein amounts after TCA precipitation were separated by 12,5% gels for (A) silver staining and by 4-12% NuPAGE Bis-Tris gels for (B) Ponceau staining and (C) Western blot with antibody R139. Agrin-22 is marked by an arrowhead. Asterisks on the right indicate the relative position of albumin.

The protein bands in the silver gel show an accumulation of low-molecular weight proteins in the depleted serum fractions. Additionally, high-molecular weight proteins like albumin and immunoglobulins are enriched in the elution fraction of bound proteins. This suggests that depletion of high-abundant serum proteins and enrichment of low molecular weight molecules is possible with the depletion column. The Western blot in panel (C) Figure 3-5 shows a signal for agrin-22 in the load but, the signal was absent in the depleted serum as well as in all other fractions (bound proteins and wash fractions). Thus, agrin-22 could not be eluted from the column neither in the depleted serum nor in the bound protein fractions or wash. This result may indicate that agrin-22 is lost through unspecific binding to the column material.

3.2.2 ProteoPrep Immunoaffinity Albumin and IgG Depletion Column

To monitor the protein recovery with a well-defined input, recombinant agrin-22 z19 was included into the column test. Depletion was performed with 25 µl murine serum (wt, E18) and 25 µl murine serum with addition of recombinant agrin-22 z19 (275 ng, protein concentration measured by UV-absorbance). The samples were previously diluted in 75 µl equilibration buffer before their concentration was determined. Depleted serum fractions are obtained as flow-through after 10 minutes of incubation followed by centrifugation. Elution of bound proteins was performed with the same volume as the load. Samples were precipitated with chloroform-methanol (Wessel & Flügge, 1984), followed by separation using 4-12% NuPAGE gels and analyzed by Western blot (Figure 3-6).

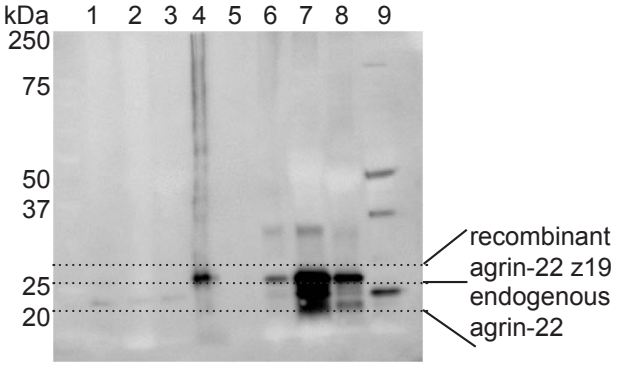

Figure 3-6. Murine serum proteins after depletion of high-abundant proteins using ProteoPrep Immunoaffinity Albumin and IgG depletion kit. Proteins after chloroform-methanol precipitation were separated by 4-12% NuPAGE Bis-Tris gels and Western blot using antibody R139 was performed. Lanes: 1-2, depleted serum; 3, bound proteins eluted from depletion column; 4, control (recombinant agrin-22 z19); 5, empty; 6-7, bound proteins eluted from depletion column; 8, depleted serum; 9, control murine serum (wt, E18).

The signal for agrin-22 was visible as a faint band in all fractions, the depleted serum, wash fractions and elution fractions of bound proteins. This indicates that isolation of agrin-22 in the fraction of the depleted serum failed. Addition of recombinant agrin-22 z19 in the second experiment results in a high signal for agrin-22, which was detected in all fractions. Additionally, the signal for endogenous agrin-22 was detected in all fractions and is highest in the fraction of the bound proteins. The signal intensity was much higher in all fractions compared to the previous experiment where recombinant agrin-22 z19 was absent. It is therefore believed, that the presence of recombinant agrin-22 z19 prevents unspecific binding of the endogenous agrin-22 to the resin of the column. Due to the unspecific binding of agrin-22, the depletion kit is found to be not suitable for the purposes.

3.2.3 ProteoSpin Abundant Serum Protein Depletion Column

This depletion column provides a fast and simple procedure for the effective depletion of major serum proteins. It is based on an ion-exchange mechanism and not on the use of specific antibodies. The complexity of the sample is reduced, allowing for the detection of less-abundant proteins. The eluted samples are ready for use in downstream applications including LC-MS. The depletion column was tested with 10 µl murine serum (wt, P5), which was diluted in activation buffer. Binding takes place during centrifugation, whereby high-molecular weight proteins are not retained to the flow-through. Elution of depleted serum is performed in two portions of 100 µl elution buffer after neutralization. The efficiency of depletion was controlled by a silver-stained 4-12% NuPAGE Bis-Tris gel as well as by Western blot using antibody R139 (see Figure 3-11 in the paragraph "Sample preparation for murine serum"). Taken together, the kit shows a high efficiency in depletion, as high-molecular weight proteins were clearly accumulated in the flow-through fraction as shown in the silver gel. Nevertheless, the elution fraction of depleted serum appears as a smear which is distributed throughout all molecular weight regions in the gel. Besides, the signal intensity for agrin-22 in the Western blot was poor, indicating a low recovery for the protein of interest when compared to the same murine serum sample (non-depleted, wt, P5). The depletion column is therefore another unsuited method for the isolation of agrin-22.

3.2.4 ProteoExtract Albumin/IgG Removal Kit

The gravity column is based on a novel albumin affinity resin and a unique immobilized protein-A polymeric resin. Depletion was achieved using 15 µl murine serum (wt, P5) which was diluted to a volume of 350 µl with binding buffer before being applied on the column. The depleted serum is obtained by washing the resin two times with 600 µl binding buffer, while bound proteins remain trapped in the column after elution. The depleted serum was loaded on 4-12% NuPAGE Bis-Tris gel and analyzed via silver staining and Western blot with antibody R139 as shown in Figure 3-11 in the paragraph "Sample preparation for murine serum". The kit shows satisfying performance in the depletion. High-molecular weight proteins were clearly reduced in the wash fraction. Nonetheless, overall signal intensity for endogenous agrin-22 in the depleted serum is very poor when compared to the column input and the control sample (non-depleted, wt, P5). In conclusion, this finding reveales that this depletion kit is not convenient for sample preparation.

3.2.5 Microcon YM-30, 50

In order to separate serum protein mixture by their size, Microcon centrifugal filter devices were tested. The idea was to enrich albumin and immunoglobulins in the supernatant to obtain a low-molecular protein mixture in the flow-through fraction. First experiments were performed with recombinant agrin-22 splice variant z19. Protein concentration was measured by UV-absorbance on a nano-Drop spectrophotometer. Measurements were performed for the load, flow-through and the supernatant of the recombinant protein solution. The results are shown in Figure 3-7.

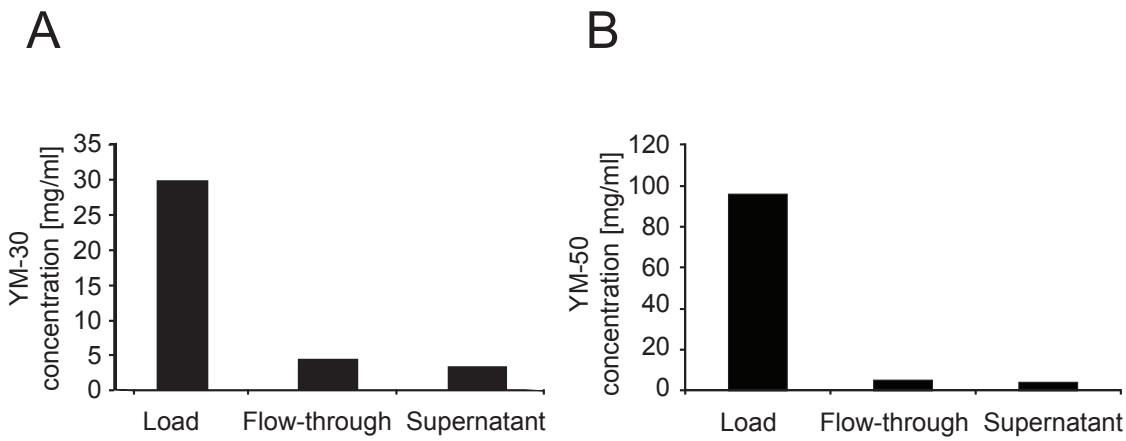

Figure 3-7. Protein recovery for depletion with Microcon centrifugal filter devices: (A) YM-30 (30 kDa MWCO) and (B) YM-50 (50 kDa MWCO). Each bar represents protein concentration measured by UV-absorbance for the load, flow-through and supernatant.

The low protein concentration after centrifugation indicates the absence of the agrin-22 z19 in the depleted flow-through fraction as well as in the supernatant. Protein recovery was not possible as indicated by the drop in concentration. To monitor the performance on endogenous agrin-22, microcon YM-50 device was additionally tested with 200 µl rat CSF Figure 3-7, B).

Analysis with Western blot confirms that the isolation of endogenous agrin-22 in the depleted serum (flow-through fraction, Figure 3-8.) was not possible with the filter devices. Moreover, agrin-22 can be found in the supernatant which contains high-abundant proteins as well. In conlusion, the depletion of murine serum and the parallel isolation of agrin-22 is not possible with this method.

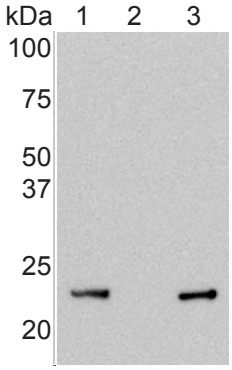

Figure 3-8. Rat CSF proteins after depletion according to the molecular mass using YM-50 centrifugal filter devices with MWCO 50kDa. Proteins were separated with 12,5% SDS-PAGE and Western blot was performed using antibody R139. Lanes: 1, load; 2, depleted CSF; 3, supernatant.

3.2.6 Gel filtration

Besides the commercial depletion columns, gel filtration was considered as an alternative method for serum depletion. This chromatographic method is based on size-exclusion and molecules are mainly separated according to their stokes`s radius. Larger molecules elute faster as they are less or not retained at all in the pores of the column material. In contrast, small molecules have a high ability to diffuse into higher number of pores, thus elute after the high-molecular weight fraction. The column used was a Superose 12 (10/30) and 100 µl murine serum (wt, P10) was applied without any previous dilution. The elution fractions were analyzed with silver-stained 4-12% NuPAGE Bis-Tris gel and Western blot using antibody R139 (Figure 3-9).

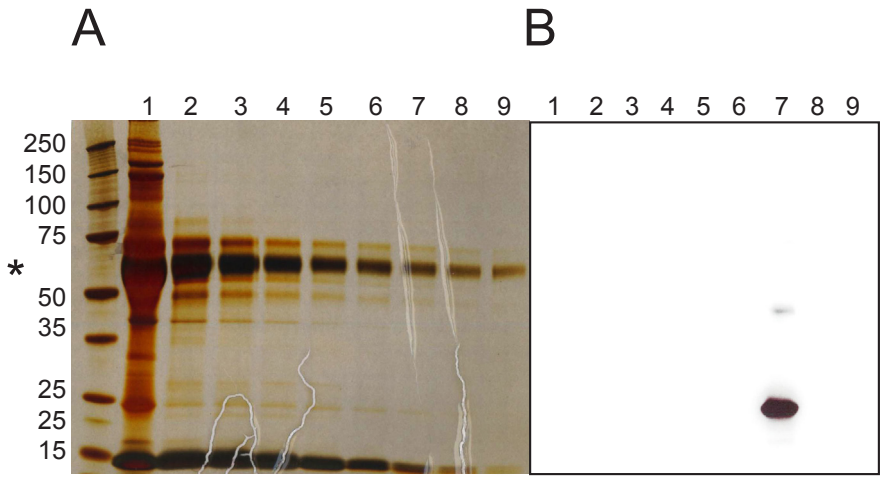

Figure 3-9. Murine serum proteins (P10) after separation by gel filtration. Elution fractions were loaded volume-adjusted (20µl) and separated by 4-12% NuPAGE Bis Tris gels. (A) Silver stain; (B) Western blot with antibody R139. Lanes: 1, Load (P10); 2-9, elution fractions. Agrin-22 is found in fraction 7. The Astersik on the left indicates the relative postion of albumin.

Silver staining clearly indicated the accumulation of high-molecular weight proteins in earlier elution fractions. Size-exclusion chromatography lead to very good depletion of the murine serum sample compared to the column input. Agrin-22 could be isolated and eluted in fraction 7, which additionally shows a high degree of depletion of serum proteins. These data support that gel filtration is a possible method to deplete serum samples and to isolate endogenous agrin-22 in one fraction of depleted serum.

3.2.7 Ammonium sulfate precipitation

The solubility of a protein in a solvent is defined by its interaction of the charged functional groups with the molecules of the solvent. This interaction can be manipulated and proteins will precipitate by the following additives: inorganic salts, organic solvent, basic proteins, pH variation and temperature change. The common method to achieve protein isolation, enrichment and purification is the fractionated precipitation by addition of inorganic salts like $(NH_4)_2SO_4$. The ability of a protein to precipitate is a result of the number and special distribution of hydrophobic groups at the surface (functional groups of Phe, Tyr, Trp, Leu, Ile, Met and Val). For proteins like very nonpolar functional groups, small amounts of inorganic salts are sufficient to precipitate them. To deplete the murine serum samples, I tested the protein fractionation according to polarity by precipitation using ammonium sulfate. Here, 5 µl murine serum (wt, E18) was diluted 1:2 in PBS. The ammonium sulfate solution (4 M) was added stepwise starting at 10% (v/v) saturation with increasing the amount until 100% (v/v) saturation. In order to avoid high local concentrations of ammonium sulfate, addition of the stock solution was performed with continuous shaking. The precipitate and the supernatant were analyzed in parallel with 4-12% NuPAGE Bis-Tris gels and Western blot using antibody R139 (Figure 3-10).

The signal for agrin-22 was exclusively detected in the supernatant containing 10% $(NH_4)_2SO_4$. Thus, isolation of agrin-22 is possible with ammonium sulfate precipitation. Additionally, it can be claimed that the fraction comprising agrin-22 should not contain big amounts of high-molecular weight proteins. This can be suggested by the Ponceau staining of the respective pellet after precipitation since it shows a higher accumulation of high-molecular weight proteins compared to the supernatant (Figure 3-10, B). Taken together, the data supports that serum depletion and isolation of agrin-22 in one of the depleted fractions is possible.

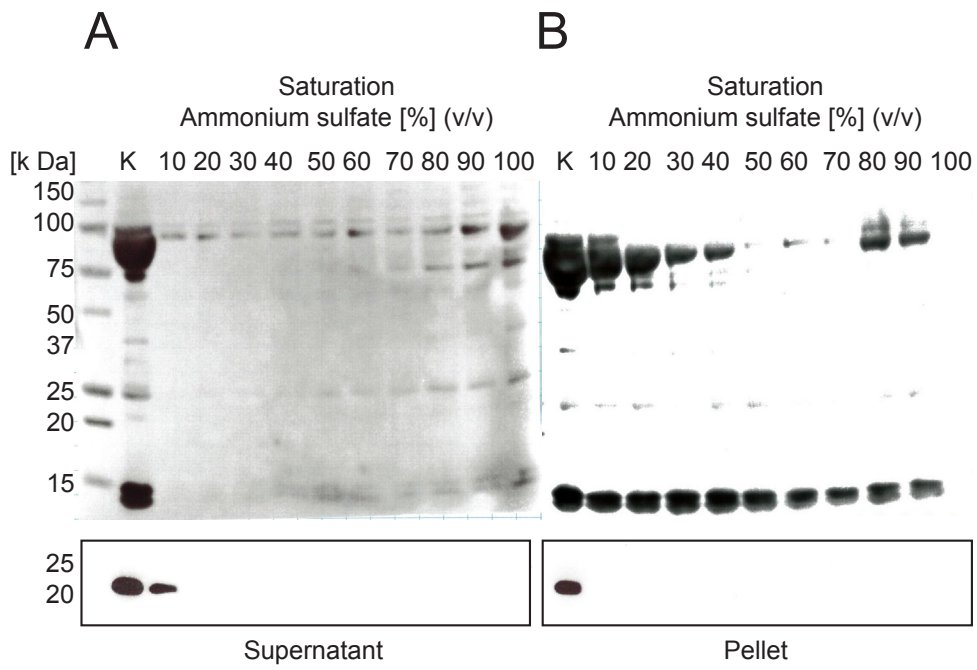

Figure 3-10. Murine serum samples (5µl) after precipitation with ammonium sulfate. Samples were separated on 4-12% NuPAGE gels and immunoblot was performed with antibody R139. Upper panels show Ponceau red-stained blotting membrane, lower pannels the corresponding immunoblots using antibody R139. (A) Supernatant and (B) Pellet after precipitation with the indicated ammonium sulfate concentration. Murine serum (wild-type, E18) is used as reference sample (K).

3.2.8 Direct comparison of the three best enrichment methods

The removal of high-abundant proteins in murine serum samples was expected to improve the signal intensity of agrin-22 by SDS-PAGE and Western blot as well as the quantification by LC-MS analysis. The results display that all seven depletion techniques tested removed albumin and IgG with high efficiency. Based on reproducibility and binding specificity, size-exclusion separation via gel filtration offered the best depletion. The depleted sera of the three best depletion techniques, (i) Proteo-spin Abundant Serum Protein Depletion Kit, (ii) ProteoExtract Albumin/IgG Removal Kit, and (iii) gel filtration were further evaluated with silver-stained SDS-PAGE, Western blot and LC-MS analysis (Figure 3-11). The analysis was carried out on all fractions (load, depleted serum, wash and elution of bound proteins) to study the binding efficiency, recovery and possible unspecific interactions.

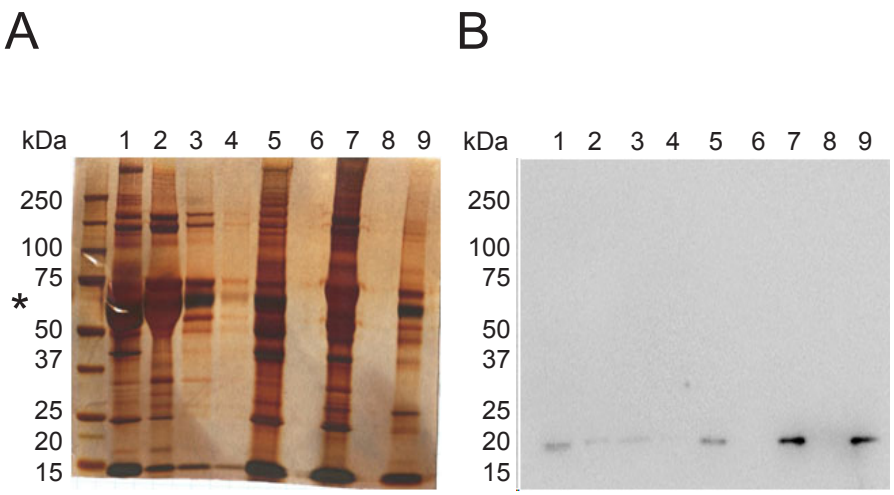

Figure 3-11. Murine serum proteins after depletion of high-abundant proteins using different depletion columns. Proteins after chloroform-methanol precipitation were separated by 4-12% NuPAGE Bis-Tris gels. (A) Silver stain; (B) Western blot with antibody R139. Lanes: 1, control (E18); 2-5, Proteo-spin Abundant Serum Protein Depletion Kit; 2, depleted serum; 3-4, wash; 5, bound proteins eluted from depletion column; 6, empty; 7, ProteoExtract Albumin/IgG Removal Kit, depleted serum; 8, empty; 9, Gel filtration, elution pool. The asterisk on the left indicates the relative position of albumin.

Based on the recovery and signal intensity of agrin-22, the ProteoExtract Albumin/IgG Removal Kit displayed promising results. It shows high protein recovery and specificity. Nevertheless, I chose the separation via size exclusion by gelfiltration for sample preparation before LC-MS analysis. Gel filtration allows the preparation of high amounts of serum (100 µl). The high sample volume is essential for the identification of agrin-22 due to its low concentration in serum and it shows the best performance in the removal of hig-abundant serum proteins, which is a crucial prerequisite for a successful analysis with LC-MS. Additionally, the recovery of agrin-22 after depletion with gel filtration was very good and highly reproducible.

After this comparative study, I wanted to test the depletion for human cerebrospinal fluid samples as well. Due to the low sample volume, the previous tested depletion kits were not compatible. The CSF has a low protein concentration (150–450 mg/ml) and a high salt concentration (4150 mmol/l). The high salt concentrations in CSF require a desalting step at the beginning of sample preparation. Desalting of CSF is achieved best with dialysis in terms of protein recovery (Zhang, 2007). The dynamic range of CSF proteins is comparable to blood (Blennow et al, 1993). Therefore, depletion of high-abundant proteins and enrichment of low abundant proteins is indeed needed. I choose a fractionation method via graduated ACN addition because of the low sample volumes available and the extensive dilution which would result after gel filtration. No significant variations were found in protein concentration in terms of precipitation when using this approach (Zhang et al, 2005). In order to evaluate differences between serum and CSF, I similarly performed dialysis followed by ACN fractionation of 100µl murine serum (wt, E18) and 100µl human CSF. Pellet P1 and supernatant S1 were collected after addition of 1.5 volumes (v/v) ACN. Pellet P2 and supernatant S2 were obtained after addition of 3 volumes (v/v) ACN to supernatant S1. Supernatant S2 was dried in a speed-vac. The resulting pellets (P1 and P2) and supernatant (S2) were loaded on a 4-12% NuPAGE gel followed by Western blot analysis. The Western blot was stained with Ponceau red to visualize

the quality of protein separation and depletion before incubation with antibody R139 for the detection of agrin-22.

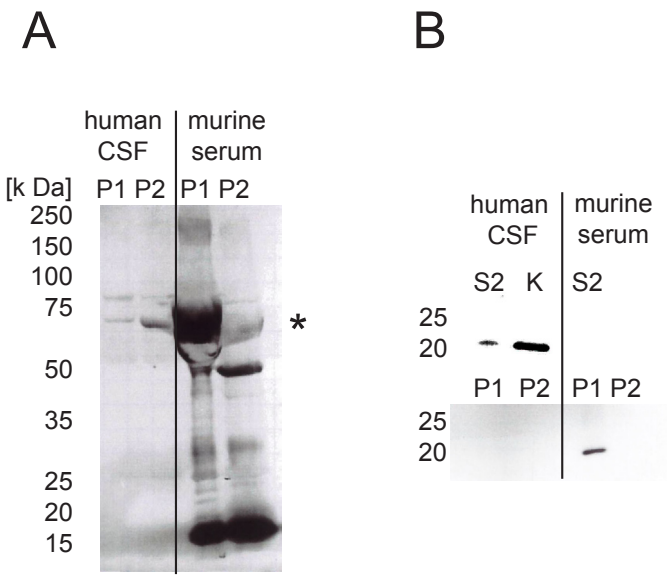

Figure 3-12. Fractionation of human CSF in comparison to murine serum with ACN precipitation. Samples (30 µl) were separated on 4-12% NuPAGE gels. (A) Ponceau red staining of the blotting membrane corresponding to the Western blot in the lower panel of figure (B). (B) Western blots after incubation with antibody R139. Upper panel shows the signals of agrin-22 in the supernatant (S2) of human CSF and murine serum and reference samples for human CSF (K). Lower panel displays the signals of agrin-22 in the pellets (P1 and P2) for human CSF and murine serum. The asterisk on the right indicates the relative position of albumin.

Ponceau red staining indicates a clearly higher protein amount for pellets P1 and P2 of murine serum in comparison to relatively low protein amounts for the same fractions of human CSF (Figure 3-12). The signals for agrin-22 in murine serum were found in precipitated protein fractions P1. This fraction contains additionally accumulated high-abundant proteins like albumin and immunoglobulins. In contrast, agrin-22 was enriched in the supernatant S2 in human CSF. The S2 fraction represents a depleted CSF portion and includes low-abundant proteins (data not shown). The depletion upon fractionation and simultaneous isolation of agrin-22 was achieved for human CSF. Depletion and isolation of agrin-22 in murine serum was not possible by ACN.

3.2.9 Data-dependent LC-ICR-FT-MS analysis of depleted murine serum

For examining the improved signal intensity after depletion, murine serum was prepared according to the two most suited depletion strategies, gel filtration and protein precipitation by ACN. Sera were divided into two parts. One part was depleted by gel filtration, another one by protein precipitation with ACN. For the experiments murine serum obtained from E18 wild type mice (wt, E18) was chosen, because the level of agrin-22 was shown by Western blot to be the highest at this age compared to P1-P30. As previously shown for the identification of agrin-22 in murine serum samples by LC-MS (see section 3.1), SDS-PAGE followed by in-gel digestion was a suitable sample preparation. After gel filtration, samples were thus further separated by SDS-PAGE. The gels were Coomassie blue stained and eight protein bands in the molecular weight region from 15-25 kDa were cut out and in-gel digestion was performed separately for each piece. In parallel, depleted samples using precipitation were digested in-solution. Both sample sets were subjected to sample clean-up with ZipTipC18 columns followed by LC-MS analysis for tryptic peptides with a standard gradient from 5-80% ACN. The designed steps of sample preparation are shown in Figure 3-13.

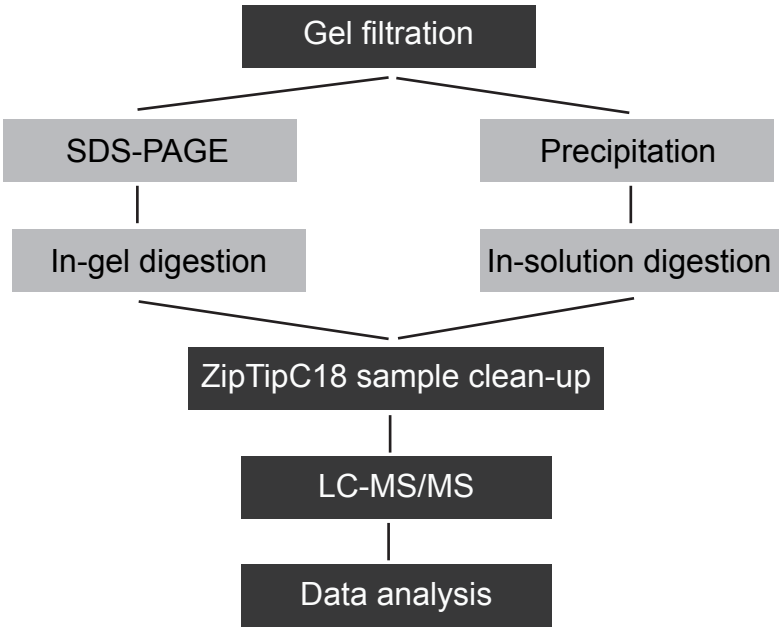

Figure 3-13. LC-MS workflow for evaluation of sample preparation.

LC-MS analysis was performed with LTQ-ICR-FT instrumentation followed by protein identification with Mascot. Peptide sequence information was generated by using an inclusion list for agrin-22 z0, 8, 11, and 19, which enables selection of peptide ions with particular mass-to-charge (m/z) ratio tandem MS. Using sthe Mascot search engine (Perkins et al, 1999), the resulting CID spectra were automatically correlated with a sequence database to identify the protein from which the peptide originated. In order to enable identification of all four agrin-22 z-isoforms, the database was extended by the sequence entry for agrin-22 z8, 11, and 19 splice variants because only the sequence of agrin-22 z0 was included in the original database. Comparison of multiple sample preparations was achieved by statistical data analysis of all MS/

MS spectra with the software Scaffold (Proteome Software, Inc., USA). This software enables graphic comparison of protein expression between samples and displays correct protein identifications in a probability score. It uses results from the Mascot and Sequest searches and established statistical algorithms in order to calculate the protein abundance in the biological sample. Results from statistical analysis using Scaffold are shown in Figure 3-14.

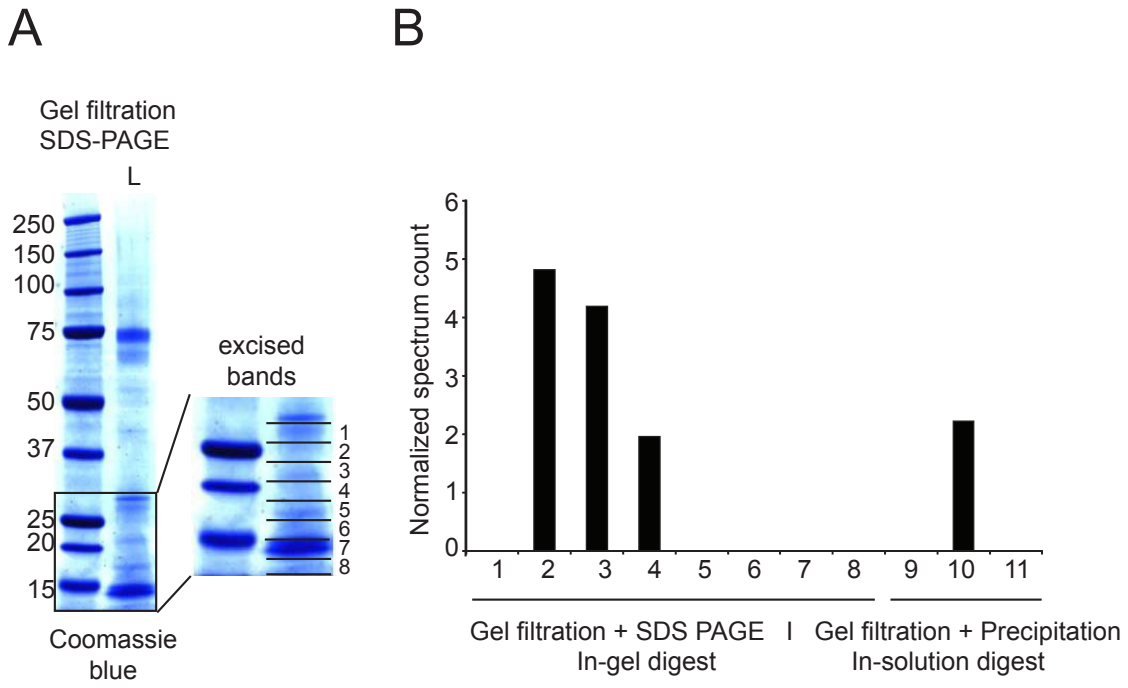

Figure 3-14. LC-MS workflow for sample preparation evaluation. Samples were depleted with gelfiltration. (A) SDS PAGE and Coomassie blue staining of the elution fraction (L) of agrin-22 in murine serum after gel filtration. Selected protein bands for in-gel digestion are enlarged. (B) Scaffold statistical analysis of sample preparation. The diagram shows the normalized spectrum count for all analyzed samples. Lanes 1-8 , normalized spectrum count according to gel bands 1-8 shown in (A). Lanes 9-11, normalized spectrum counts for precipitated samples; 9, supernatant; 10, pellet 1; 11, pellet 2.

Agrin-22 z0 was identified with 42% sequence coverage, but no specific peptides to differentiate between the other splice variants were detected in murine serum or below the detection limit for the LC-MS instrumentation. Highest amounts of agrin-22 z0, with regard to normalized spectrum counts of each LC-MS run, were found in the gel pieces 2-4. Piece 2 of SDS-PAGE gel showed the best accumulation of agrin-22 z0. Better detection of agrin-22 was achieved using in-gel digestion when compared to in-solution digestion.

3.3 Quantification of agrin-22 via targeted mass spectrometry

The basic method and the "gold standard" used for targeted protein quantification to date is enzyme-linked immunosorbent assay (ELISA). However, its limiting step is the availability of highly specific antibodies. Most of the novel discovered biomarkers in recent proteomics studies are lacking these antibodies. Therefore, the concept of targeted quantitative proteomics has been implemented into the field of mass spectrometry (Haab et al, 2006). Mass spectrometry became the alternative approach to precisely detect peptides and proteins with high mass accuracy, selectivity and specificity (Pan et al, 2009). The most popular platform used is the triple quadrupole instrument with multiple (or selected) reaction monitoring (MRM, SRM) technique (Bower et al, 1993; Anderson et al, 2004; Janecki et al 2007). This method is so far the only selective and specific tool that allows for isoform-specific identification of low-abundant proteins without a specific antibody. As the four agrin-22 isoforms differ only in the insertion of 8, 11, and 19 amino acids, analysis and differentiation is not easy. For the distinction and quantification of these isoforms, SDS-PAGE and subsequent Western blot analysis was not viable due to the lack of antibodies or even peptibodies, enabling differentiation of the four splice variants. In addition to the implementation of a less complex source for the biomarker, improvement of the detection of specific tryptic peptides for quantification of the four isoforms of agrin-22 was the aim. To this end, a triple quadrupole mass spectrometer with higher sensitivity than the FT-ICR and the possibility to perform selected reaction monitoring (SRM) was considered.

In the SRM approach, only peptides of interest are isolated in the first quadrupol of the instrument, fragmented and resulting spectra consist exclusively of the specific selected fragments. Each agrin-22 isoform has one unique tryptic peptide (proteotypic peptide, PTP) and corresponding CID fragments can be selected to monitor the protein of interest and to quantify the amount based on the area under the eluting chromatographic peak of the selected fragment ions. I wanted to study neurotrypsin-activity in association with age and neuronal diseases. Only small amounts of CSF (100-200 µl/subject) could be obtained from the clinics for age-related studies, patients with epilepsy and Alzheimer`s diesease as well as healthy control subjects for each disease group. As the main interest was based on inter-subject variabilities, the CSF samples could not be pooled and I wanted to test whether it is possible to detect agrin-22 isoforms in a small sample volume. Using targeted mass spectrometry, I measured different sample sets. Comparison of the obtained SRM spectra indicated that the measurements were not reproducible and the probability to detect and quantify the four agrin-22 isoforms remained difficult (data not shown). Hence, I wanted to experimentally determine the optimally suited parameter settings to get reproducible data and enhance PTP recovery for the quantification assay. In this paragraph, I will report about experimental investigations to identify and describe the impact of PTP selection, resolution of the first mass analyzer (Q1), LC parameters and matrix effects.

3.3.1 Selection of unique proteotypic peptides for agrin-22 isoforms

For the quantification of neurotrypsin-dependent agrin-22 via SRM I wanted to target the unique PTPs of the four isoforms of agrin-22. To this end, the amino acid sequences of all four agrin-22 isoforms were in-silico digested using trypsin (/K/R-\P), Asn-C (/N) and GluC (/E) specificity to identify PTPs which are unique for each splice variant. Only trypsin results in one unique PTP for each variant at acceptable molecular mass values which can be used for identification of the protein of interest. The sequence information was further evaluated with Pinpoint software (Thermo) which can be used as a method builder and for data analysis of the SRM spectra. It enables in-silico identification of estimated CID fragments of the PTPs via a peptide library or by direct input of FASTA files. Software settings used for peptide fragmentation are based on theoretical and empirical rules, e.g. the predicted break of a peptide bond at proline. Therefore, transitions with proline as the first amino acid are preferably selected by the software. The charge state 2+ is as well preferred for the precursor selection and resulting fragments cover automatically the z-ion series. The generated list of all predicted transitions and fragmentation parameters was directly transferred into the instrument method using Xcalibur software. PTPs for each protein were selected based on the criteria to be unique for each isoform of agrin-22. Therefore, reasonable ionization efficiency and fragmentation based on empirical MS/MS data was not considered as main element in the selection of the PTPs. The proteins and their respective peptides are shown in Table 3-2.

Splice site z (0)

```
         10          20          30          40          50          60
ARVNHHHHHH HHSAGDVDTL AFDGRTFVEY LNAVTESEKA LQSNHFELSL RTEATQGLVL
         70          80          90         100         110         120
WSGKATERAD YVALAIVDGH LQLSYNLGSQ PVVLRSTVPV NTNRWLRVVA HREQREGSLQ
        130         140         150         160         170         180
VGNEAPVTGS SPLGATQLDT DGALWLGGLP ELPVGPALPK AYGTGFVGCL RDVVVGRHPL
        190
HLLEDAVTKP ELRPCPTP
```

Splice site z (8)

```
         10          20          30          40          50          60
ARVNHHHHHH HHSAGDVDTL AFDGRTFVEY LNAVTESELA NEIPVEKALQ SNHFELSLRT
         70          80          90         100         110         120
EATQGLVLWS GKATERADYV ALAIVDGHLQ LSYNLGSQPV VLRSTVPVNT NRWLRVVAHR
        130         140         150         160         170         180
EQREGSLQVG NEAPVTGSSP LGATQLDTDG ALWLGGLPEL PVGPALPKAY GTGFVGCLRD
        190         200
VVVGRHPLHL LEDAVTKPEL RPCPTP
```

Splice site z (11)

```
        10          20          30          40          50          60
ARVNHHHHHH HHSAGDVDTL AFDGRTFVEY LNAVTESPET LDSGALHSEK ALQSNHFELS
        70          80          90         100         110         120
LRTEATQGLV LWSGKATERA DYVALAIVDG HLQLSYNLGS QPVVLRSTVP VNTNRWLRVV
       130         140         150         160         170         180
AHREQREGSL QVGNEAPVTG SSPLGATQLD TDGALWLGGL PELPVGPALP KAYGTGFVGC
       190         200
LRDVVVGRHP LHLLEDAVTK PELRPCPTP
```

Splice site z (19)

```
        10          20          30          40          50          60
ARVNHHHHHH HHSAGDVDTL AFDGRTFVEY LNAVTESELA NEIPVPETLD SGALHSEKAL
        70          80          90         100         110         120
QSNHFELSLR TEATQGLVLW SGKATERADY VALAIVDGHL QLSYNLGSQP VVLRSTVPVN
       130         140         150         160         170         180
TNRWLRVVAH REQREGSLQV GNEAPVTGSS PLGATQLDTD GALWLGGLPE LPVGPALPKA
       190         200         210
YGTGFVGCLR DVVVGRHPLH LLEDAVTKPE LRPCPTP
```

Table 3-2. Amino acid sequences of the four z-isoforms of agrin-22. The unique PTP for each variant is highlighted in red. The splice insert is underlined.

The four proteins were expressed in HEK-Ebna cells as recombinant N-terminally His-tagged fusion proteins and affinity-purified by Ni^{2+}-select column. All four proteins were separately digested according to the in-solution tryptic digestion protocol. The resulting mixture of PTPs for each agrin-22 isoform was used to further optimize MS parameters for SRM experiments of the specific PTPs. In addition, the four synthetic PTPs were purchased to allow the specific analysis of their performance in the SRM assay and to use them as internal standards for the quantification. The proteotypic peptides and their selected fragments and respective collision energy (CE) are shown in the chapter Materials and Methods in Table 5.2.

3.3.2 Influence of resolution on PTP detection

The first SRM experiments for the identification of the most intense fragments for each PTP were performed using the listed set of transitions (Table 3-3). Two concentrations of 10fmol/µl and 100fmol/µl were injected (8 µl) for each agrin-22 isoform. The mass peak width for the first quadrupole (Q1) full width half maximum (FWHM) was tested for two settings: the unit resolution where Q1 is set to 0.7 and the enhanced resolution were Q1 is set to 0.1. The thrid quadrupole (Q3) FWHM was in all cases set to 0.7, scan width to 0.002 m/z and scan time to 0.05 sec (16 transitions = 0.8 sec/cycle). The enhanced resolution method with Q1 FWHM at 0.1 requires a critical review of precursor mass settings. In figure 3-15, the resulting spectra for these transitions are shown.

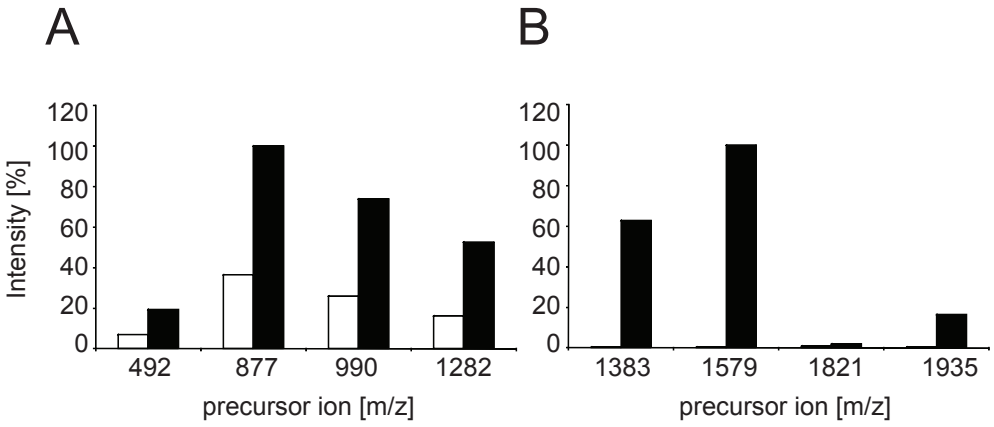

Figure 3-15. Change in response as a function of Q1 mass peak with of (A) recombinant agrin-22 z0 and (B) recombinant agrin-22 z19. Open bars: Q1 = 0.1 FWHM; black bars: Q1 = 0.7 FWHM.

In general, spectra obtained with unit resolution for Q1 (0.7 FWHM) show much higher signal intensities for all transitions of all isoforms. The enhanced resolution (0.1 FWHM) was leading to the loss of detection for two transitions of agrin-22 z19. The results are described in more detail in Figures 3-16 and 3-17.

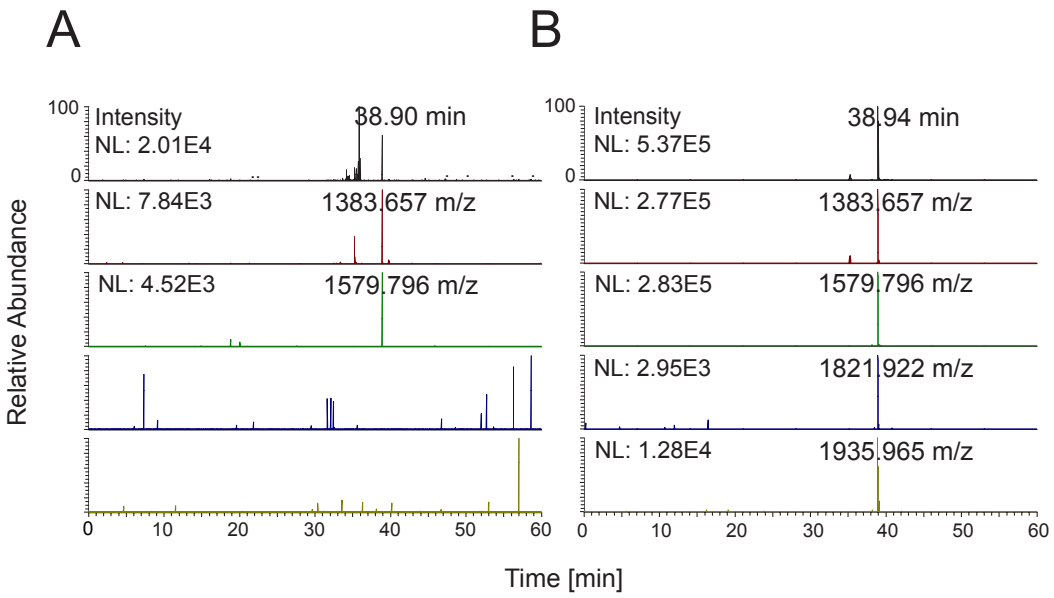

Figure 3-16. Q1 resolution agrin-22 z19. (A) Q1=0.1. (B) Q1=0.7. Mass spectrometric measurements were recorded in the targeted mode for selected reaction monitoring (SRM). The upper pannels show the total ion count (TIC) in black. In the lower pannel the extracted ion chromatograms (XIC) for all four transitions of the agrin-22 z19 isoform are shown in colour.

The spectra show that parameter setting in the enhanced resoltuion mode (Q1=0.1) makes it impossible to isolate all transitions for the agrin-22 z19 isoform (Figure 3-16, A). Only two transitions (1382 m/z and 1578 m/z) have been isolated and detected. These transitions are, with regard to the relative abundance in the unit resolution (Q1=0.7) experiment, the most intense transitions (Figure 3-16, B). In contrast, unit resolution enables the isolation and detection of all transitions for agrin-22 z19. Therefore, unit resolution is considered to serve as better resolution mode.

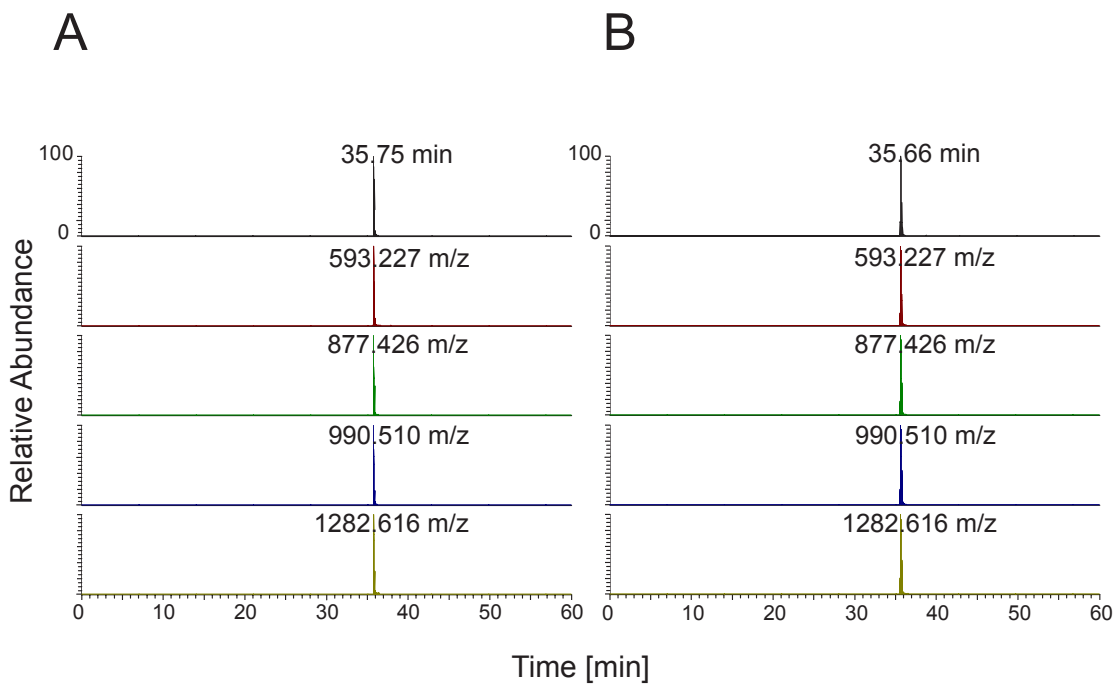

Figure 3-17. Q1 resolution agrin-22 z0. (A) Q1=0.1. (B) Q1=0.7. Spectra were measured in the targeted mode for selected reaction monitoring (SRM). The upper pannels show the total ion count (TIC) in black. In the lower pannel the extracted ion chromatograms (XIC) for all four transitions of the agrin-22 z0 isoform are shown in colour.

Comparison of the measurements of the agrin-22 z0 transitions in the enhanced and unit resolution mode represented less differences as observed for the transitions of agrin-22 z19. All four transitions of the z0 variant were detected in both modi with satisfiable abundance (Figure 3-17). The loss of intensity as sustained for the z19 isoform was not observed. The enhanced resolution of Q1 (0.1 FWHM) is suggested to increase the mass accuracy for the precursor isolation. Therefore, background signals decreased and in parallel the signal-to-noise (S/N) rate raises. However, enhanced resolution was selected and the decrease in sensitivity has to be taken as a matter of fact. As agrin-22 belongs to the low-abundant protein fraction, unit mass resolution is suggested to be the more prosperous modus for the detection.

3.3.3 Evaluation of PTP recovery in the context of ionization

ESI ionization: Performance characteristics of PTPs via selected ion monitoring

I wanted to further confirm whether discrepancies in peptide recovery are due to different accessibilities of the four splice variants for in-solution digestion or due to distinctive abilities to be ionized by ESI. Thus, we decided to measure PTPs with selected ion monitoring (SIM) on the triple quadrupole instrument. The SIM offers the possibility to selectively record spectra for the ion of interest. The S/N rate is markedly reduced. It provides an alternative to quantify the PTPs for each isoform in separate experiments. To ensure that PTPs are not lost, dilutions for each tryptic peptide mixture of the recombinant agrin-22 isoforms were introduced into the MS via direct infusion using 50% ACN without installing a chromatographic column.

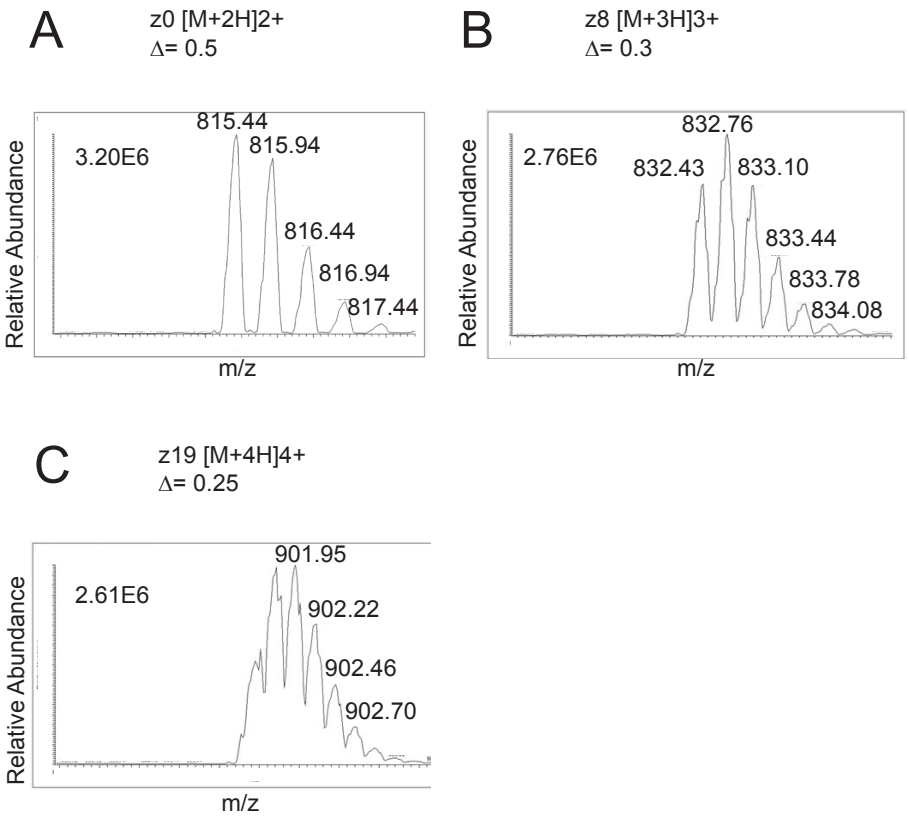

Figure 3-18. Selected ion monitoring (SIM) spectra were manually recorded via direct injection of agrin-22 z0 (A), z8 (B) and z19 (C) on the TSQ mass spectrometer. Spectra show the relative abundance, isotope pattern and the corresponding charge state for each variant.

The selected ion monitoring (SIM) spectra confirm that all isoforms are present at the same concentration and show similar ionization behavior (Figure 3-18). All PTPs show comparable signal intensities. Main differences between agrin-22 isoforms are found in the distribution of the most intense ion species resulting from the ionization process with regard on their charge state. While the dominant species for agrin-22 z0 was the [M+2H]2+, for agrin-22 z8 it was [M+3H]3+ and for agrin-22 z19 [M+4H]4+. This charge distribution depends on the amino acid sequence and previous measurements on the LTQ did show a different distribution. The 2+ charge state is automatically selected by the Pinpoint software for the precursor setting. In conclusion, the SIM spectra provided a good basis in the selection of the most abundant PTPs.

Fragmentation of the PTPs

Besides quantization of PTPs via SIM and definition of the dominant charge states, the pattern of fragmentation was concomitantly analyzed. Isolation of the precursor was performed with a collision energy (CE) set to 10 V followed by the stepwise icrease in the CE until the precursor was fragmented to 100%. In this experiment, significant differences could be detected in the fragmentation characteristics between the agrin-22 splice variants, using the CE which are automatically selected by the software. Thus, I decided to manually define the CE for all PTPs to tune fragmentation to a point at which 10% of the precursor ion is still observed. Fragmentation of agrin-22 z0, z8, and z11 showed ideal performance whereas the isoform agrin-22 z19 showed almost no ability for fragmentation (Figure 3-19).

The efficiency of fragmentation is directly related to the quality of the product ion spectra. The experiments present a possible explanation for the poor signal intensity and PTP recovery. As fragmentation ability is likely a matter of the amino acid composition of the peptide, signal intensity and peptide recovery have to be improved in this particular case using other methods.

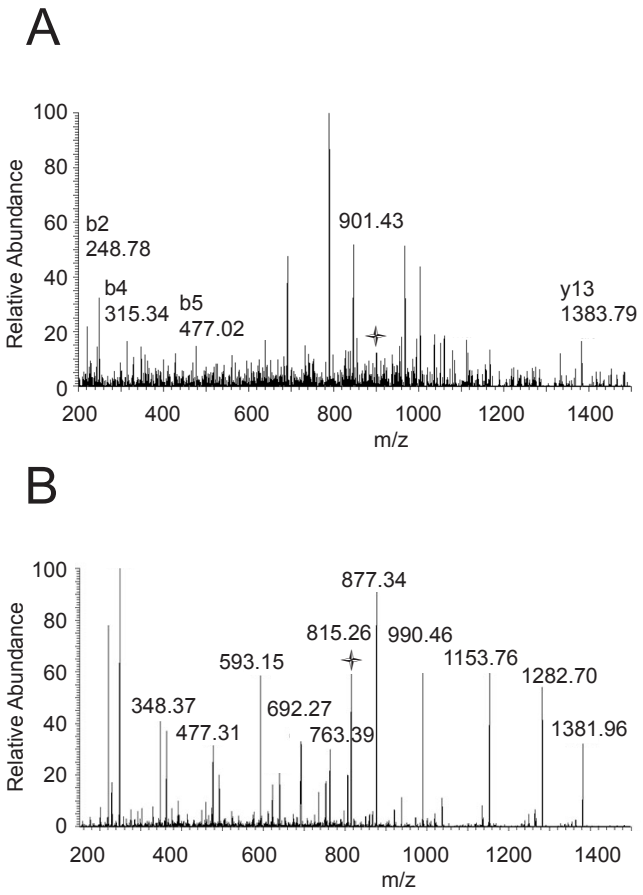

Figure 3-19. Fragmentation ability of (A) recombinant agrin-22 z19 and (B) recombinant agrin-22 z0. Spectra were recorded via direct injection without using a chromatographic system. All fragment ions are labeld with their m/z values and precursor ions are additionally marked with an asterisk.

MALDI-ionization

To exclude the possibility that the ionization method highly influences signal intensity MALDI-TOF/TOF mass spectrometry was perdormed. Furthermore, I wanted to ensure that the digestion is sufficient and adress the question whether ZipTipC18 sample clean up leads to an enhancement of the spectra quality. Samples were prepared according to standard proteomics digest (1) (see in Materials and Methods) and separated into two parts. One portion was directly spotted on the MALDI target plate without further sample clean up. For the second portion, ZipTipC18 sample clean up was performed to desalt the sample. The results indicate that the recombinant agrin-22 isoforms z0, 8, and 11 undergo efficient digestion and detection of the PTPs of these isoforms was possible. Overall, a number of 2 to 4 tryptic peptides for the identification of agrin-22 can be detected in all digestion solutions. For agrin-22 z0, 8, and 11, the specific PTPs for each splice variant can be detected in both sample sets, with and without ZipTipC18 clean-up. However, the PTP for the isoform agrin-22 z19 could not be identified with either method (Table 3-4) . The direct comparison of spectra from both sample sets showed a strong reduction of signal intensity for all tryptic peptides in case of ZipTipC18 sample clean up indicating significant sample loss on the ZipTipC18 resin (data not shown).

The resulting spectra did not show any improvement in quality when samples were processed with ZipTipC18. Taken together, tryptic peptides can be ionized with MALDI as well and the quality of digestion could be shown to be adequate.

Agrin-22 Isoform	MH+ Total mass (Mo)	Sequence
z0	1414.757	ALQSNHFELSLR
	1629.805	**TFVEYLNAVTESEK**
	2911.579	ADYVALAIVDGHLQLSYNLGSQPVVLR
z8	1389.736	TEATQGLVLWSGK
	1414.757	ALQSNHFELSLR
	2495.257	**TFVEYLNAVTESELANEIPVEK**
	2911.579	ADYVALAIVDGHLQLSYNLGSQPVVLR
z11	1389.736	TEATQGLVLWSGK
	1414.757	ALQSNHFELSLR
	2737.335	**TFVEYLNAVTESPETLDSGALHSEK**
	2911.579	ADYVALAIVDGHLQLSYNLGSQPVVLR
z19	1389.736	TEATQGLVLWSGK
	1414.757	ALQSNHFELSLR

Table 3-4. Tryptic peptides of agrin-22 isoforms identified with MALDI-TOF/TOF. The unique PTP for each agrin-22 isoform is highlighted in bold. Tryptic peptides which could not be detected after ZipTipC18 sample clean up are highlighted in red.

3.3.4 Estimation of peptide recovery in the context of their elution ability

The ability to ionize was identical in the SIM measurements for all agrin-22 isoforms. No differences with regard to amino acid sequence composition could be observed. Therefore, poor peptide recovery might be caused by other physico-chemical properties. It is well known that peptides with high hydrophobicity have a high surface interaction with some materials used for tubings and fittings in the chromatographic systems. I therefore wanted to test the affinity of the peptides to the material of the LC equipment by bypassing the chromatographic column. The setup without analytical column allowed for the detection of objectionable interactions and retentions of the analyte in the system. The experiments were carried out on the LTQ using flow injection analyses (FIA). To test the affinity of the analyte with tubing, I used a low concentration of 5% ACN, which is a basic condition at the beginning of a standard gradient in liquid chromatography of peptides and proteins, and raised the ACN concentration to 20% and 50% in separate experiments. In order to quantify the signal intensities of the analyte in each run, the solvent peak 444.6948 m/z, which can serve as internal standard, was used as reference. The resulting spectra are displayed in Figure 3-20.

The study clearly indicated highly unspecific interaction of agrin-22 isoforms z8, z11, and z19 with the surface at low ACN concentrations when compared to z0. Even at concentrations of 20% ACN, these isoforms displayed massive retention in the chromatographic system. Usually, a concentration of 10 - 30% is sufficient for the elution of peptides from reversed phase C18 materials. The high affinity of agrin-22 z8, z11 and z19 could only be prevented using high ACN concentration of 50%. These findings could be further supported by in-silico calculations using prospector. This program calculates a theoretical C18 retention index at given ACN concentrations (%) based on predicted elutions (Browne, 1982). Additionally, Bull-Breese indices for the hydrophobicity (%) of the peptides were calculated based on surface tension of amino acid solutions (Bull, 1974) using the same program.

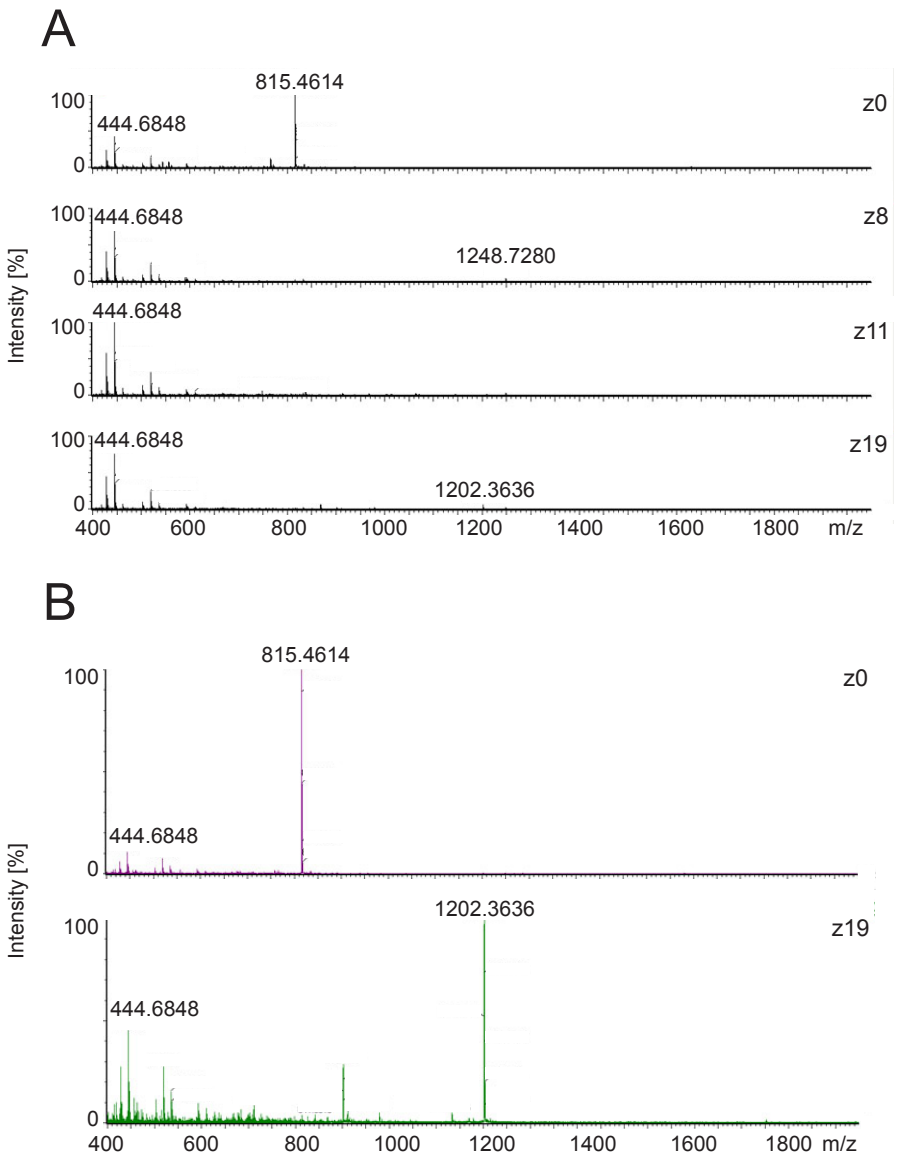

Figure 3-20. Full scan spectra of the flow injection experiments. (A) Agrin-22 z-isofroms measured in 5% ACN and (B) agrin-22 z0 and z19 with 50% ACN. The spectra were recorded on a LTQ mass spectrometer bypassing the chromatographic system. The ion with m/z value 444.6848 was chosen as reference to calculate the relative intensity for the agrin-22 isoforms in each spectrum.

PTP-sequence	Bull-Breese index Hydrophobicity (%)	RT-index ACN (%)
TFVEYLNAVTESEK	41.4	26.2
TFVEYLNAVTESELANEIPVEK	42.4	48.8
TFVEYLNAVTESPETLDSGALHSEK	38.1	57.9
TFVEYLNAVTESELANEIPVPETLDSGALHSEK	39.6	80.5

Table 3-5. Bull-Breese and retention time (RT) indices of the four agrin-22 z-isoforms. Hydrophobicity is given in (%) based on surface tension of amino acid solutions. The RT-index is based on the theoretically predicted elution at given ACN concentration (%).

The retention index of 26.2% ACN for the PTP of agrin-22 z0 represents normal elution behavior. However, retention indices for other agrin-22 isoforms indicate very poor elution probabilities from C18 materials. Especially agrin-22 z19 requires extremely high concentration of eluent predicted with 80.5% ACN. The bull breese indices for hydrophobicity are in the same range for all PTPs and indicate medium hydrophobicity.

3.3.5 Validation and refinement of LC conditions and sample delivery for PTPs

After experimental and theoretical evaluation of the increased retardation of agrin-22 PTPs, the influence of different elution gradients used for LC separation was tested in order to enhance peptide elution from C18 material. Therefore, the ACN concentration for starting conditions of the LC-gradient was increased from 5% to 10%, 20% and 40% ACN (see Materials and Methods). To further enhance the elution efficiency, 10% isopropanol was added to each eluent solution. Samples of synthetic PTPs (amount on column: z0, 8 and 11 = 100 fmol; z19 = 800 fmol) were prepared with similar solvent composition for each new starting condition. After each analysis stringent wash with injection of 10% isopropanol was applied to prevent carry-over of PTPs. Mass spectra were recorded using the triple quadrupole mass spectrometer (TSQ, Thermo) in SRM mode. The spectrum for each transition was analyzed with pinpoint software (Figure 3-21). For each run, signal intensities with regard to peak areas of transitions were quantified.

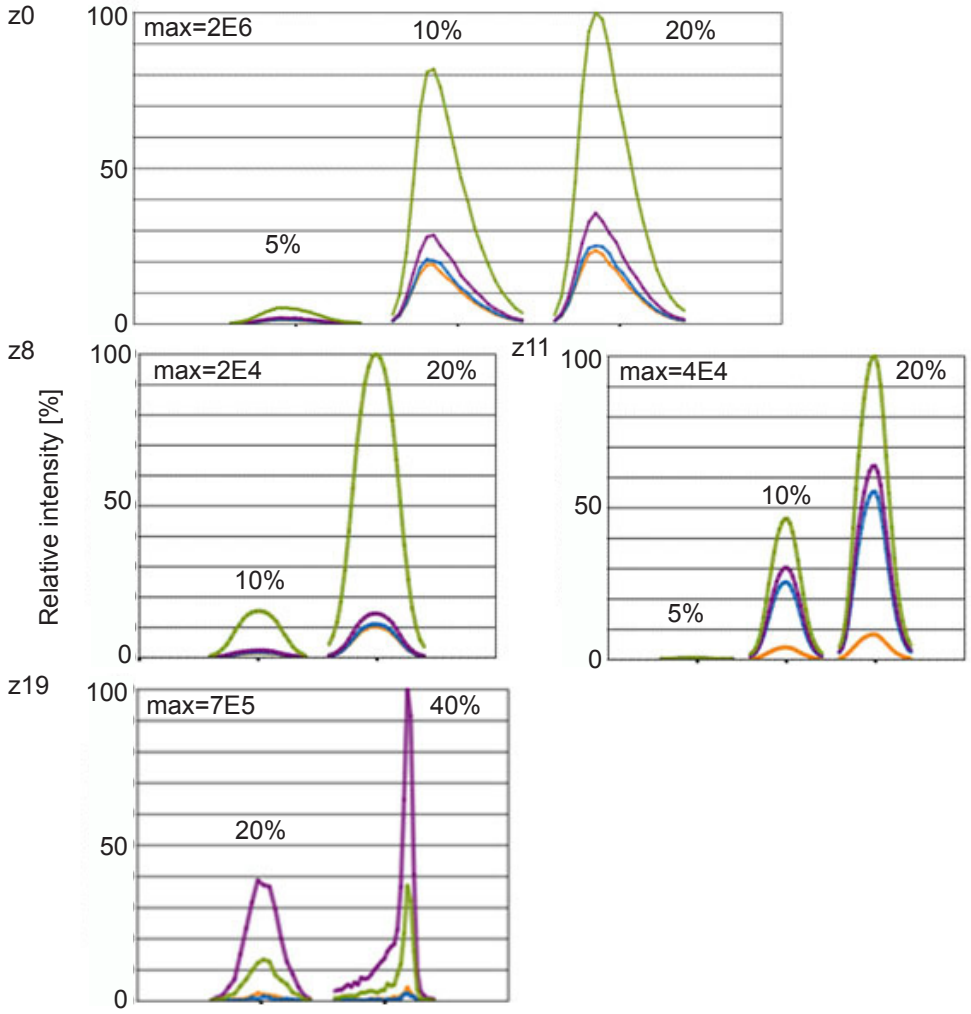

Figure 3-21. Pinpoint data analysis. The synthetic PTPs of all four agrin-22 isoforms (amount on column: z0, 8 and 11 = 100 fmol; z19 = 800 fmol) were measured with targeted mass spectrometry at different starting conditions of the LC-gradient. Transitions are given in different colours and ACN concentration for the measure is highlighted above the relative intensity pattern of the transisions. The calculated maximum of the relative intesity is given for each isoform.

The standard gradient (detailed information on the gradient composition can be found in the Chater Materials and Methods) which starts at 5% ACN results in poor signal intensities for agrin-22 z0 and z11 and is insufficient for elution of isoforms z8 and z19. A strong increase in relative signal intensity is achieved for agrin22 z0 when using the 10% gradient. This effect is only slightly enforced with the 20% gradient. Agrin-22 z8 can be eluted using the 10% gradient and shows massive enhancement when using the 20% gradient. The same is true for agrin-22 z11. The isoform z19 is detectable with the 20% gradient and elution improves by applying the 40% gradient. However, the analysis of agrin-22 z19 was not reproducible in three replicates. In parallel, all other agrin-22 transcripts did not show any retardation when the 40% gradient was tested. They eluted directly when the gradient developed. Taken together, the 20% gradient is suggested as ideal condition for the optimized elution of all PTPs.

3.3.6 Implementation of elevated temperature to enhance the elution of PTPs

Retardation is a sophisticated process when working with peptides and proteins because they are multifunctional molecules. The interaction of these large molecules is basically driven by the adsorption of their hydrophobical foot. But this mechanism can be as well influenced by additional, non-specific interactions with functional sites on the stationary phase like silanols and alkyl groups. The molecular shape and ion-pairing equilibrium contribute as well (Hancock et al, 1994). Elevated temperature leads to a reduction in viscosity and bigger solute diffusion and therefore results in more narrow and symmetrical peaks (Boyes, et al, 1993). However, a sufficient flow rate must be presented to overcome less effective diffusion (Zhu et al, 2004). Using a digested solution of fetuin (10fmol/µl) as a standard (see Figure 3-22) and a mixture of synthetic PTPs (10fmol/µl) of agrin-22 z0, 8, 11, and 19 (see Figure 3-23), I tested the influence of elevated temperature on the elution efficiency and retention time shift. Samples were analyzed using an Thermo Fisher LTQ ion trap mass spectrometer with standard LC-gradient from 5 to 80% ACN. The effects on retention time and recovery of hydrophobic peptides were tested at three temperatures: 40, 50, and 60°C.

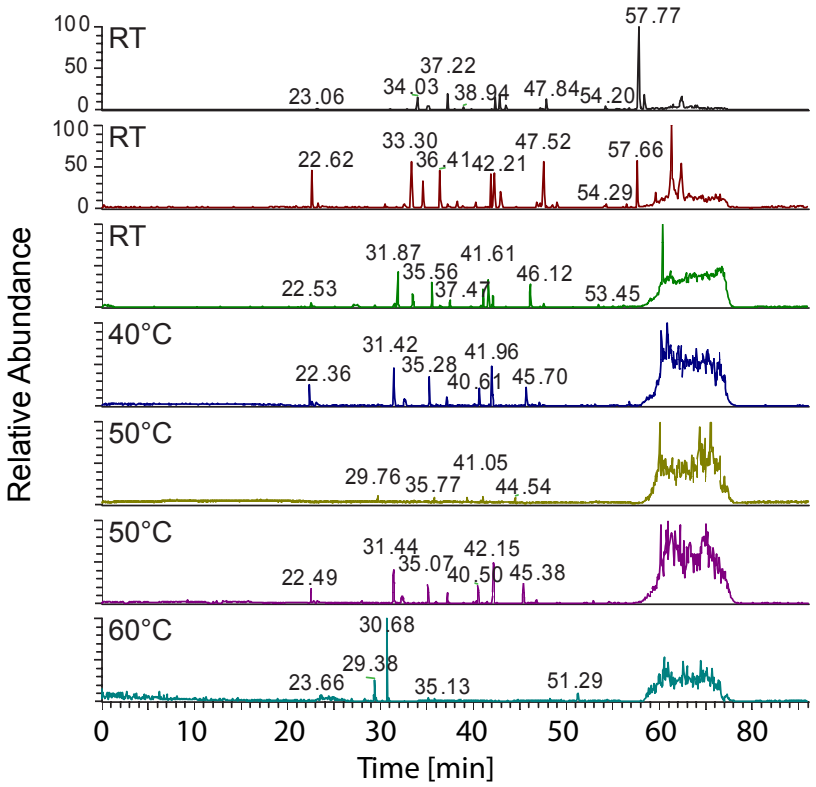

Figure 3-22. Base peak chromatograms for the comparison of retention times on RP-C18 material for a fetuin digest (stock 10fmol/µl) at RT, 40, 50, and 60°C using standard LC-gradient from 5-80% ACN. The full scan spectra were measured on an LTQ mass spectrometer. The base peak chromatograms show the retention time and m/z values for the most intense ions detected in the run.

The increased temperature of 40 and 50°C resulted in a shift towards shorter retention time of about two minutes for typical most abundant tryptic peptides of fetuin (40fmol on column). No specific signals of the tryptic peptides of fetuin were detected at 60°C. This is a possible result of the spray instability at this elevated temperature.

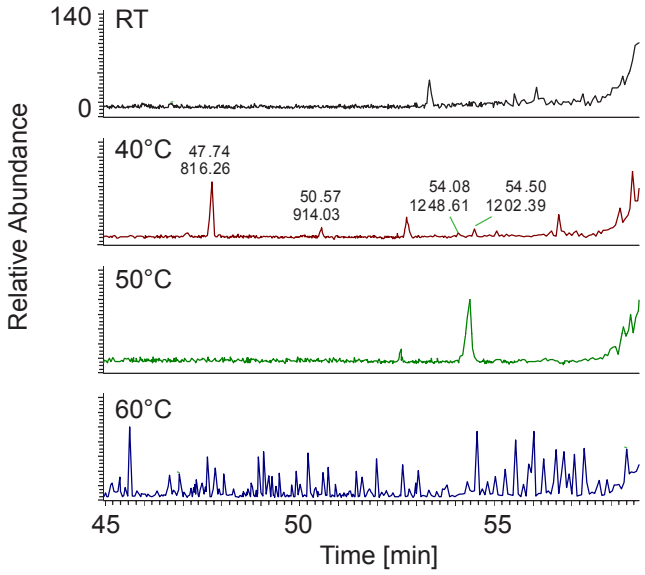

Figure 3-23. Base peak chromatograms for comparison of retention times on RP-C18 material for agrin-22 digest (stock 10fmol/µl) at room temperature (RT), 40, 50, and 60°C using standard LC-gradient from 5-80% ACN. The full scan spectra were recorded on an LTQ mass spectrometer. The base peak chromatogramms show retention time and m/z falues for the most intense ions detected in the run.

The synthetic PTPs of the four agrin-22 isoforms were exclusively detected in the full scan measurement at 40°C, but no specific signals for the tryptic peptides of interest were obtained using room temperature or higher temperatures of 50 and 60°C. For comparison of the retention times bewteen the runs, the flow rate was kept constant throughout all temperatures. This resulted in a decreased back pressure with higher temperature. Furthermore, instability in the spray performance was recognized at 50 and 60°C. A high number of unspecific signals with a high relative abundance was observed by applying a column temperature of 60°C. However, peptide recovery and retention time were not significantly improved with heated chromatography.

3.3.7 Linear range and limit of quantification of agrin-22 z0

To ensure accuracy in quantification of agrin-22 z0, the linear concentration ranges and limits of quantification of the instrument were determined for pure, synthetic proteotypic peptide of agrin-22 z0 in 20% ACN. The response for agrin-22 z0 was found to be linear (R2 = 0,9984) over 4 orders of magnitude. The limit of quantification was approximately 80 amol (~1 pg) of peptide injected on-column. The linear concentration range and limit of quantification are affected by matrix complexity as well as instrument sensitivity. For example, if the ion suppression in

the matrix is significant, the limit of quantification of the given target in the complex matrix will differ from the limit of quantification of the pure peptide. Hence, the linear concentration range and limit of quantification were also determined for agrin-22 z0 spiked into human CSF. As expected, the linear concentration range was greater and the limits of quantification were generally lower using pure peptide compared to the spiked peptide, since matrix complexity causes some degree of ion suppression. Three replicate measurements were performed and agrin-22 z0 was not detected (data not shown).

3.3.8 Analysis of poor recovery of PTPs in the context of matrix effects

A comparative study of diluted human CSF was performed to elucidate the effect of the peptide matrix in fractionated human CSF samples on PTP recovery. In the first experiment, CSF samples were prepared according to the digestion protocol with 50% methanol followed by incubation of three hours at room temperature (see digest 2 in Materials and Methods). The digested CSF was further spiked with the synthetic PTP for agrin-22 z0 (25 fmol/µl) and dilutions of CSF (1:10, 1:100) with 20% ACN were prepared. Targeted mass spectrometry of agrin-22 z0 was performed and the resulting spectra are displayed in Figure 3-x. Targeted mass spectra show a shift to shorter retention time of ten minutes in case of the 1:100 diluted CSF sample. Based on this result the presence of a strong matix effect was claimed in human CSF samples.

In a second experiment, a comparative study of a set of three samples was performed to elucidate the effect of the peptide matrix in fractionated human CSF samples on PTP recovery. Therefore the CSF digest from the previous experiment was split into two parts: (i) digested CSF as it is and (ii) digested CSF spiked with digested recombinant agrin-22 z0 (10fmol/µl). The digest of recombinant agrin-22 z0 was in parallel used as standard in order to visualize the matrix effect induced by the CSF peptide matrix. The PTP with the amino acid sequence TEATQGLVLWSGK from agrin-22 was included, which is not unique for one isoform and could later provide information about the entire agrin-22 level. From previous shotgun LC-MS/MS experiments with the ICR-FT-MS, it was known that this tryptic peptide is highly abundant. Concluding from this, additional interferences in LC-MS analysis, like extensive retention on the C18 column, were absent for this peptide. Thus, it was a perfect candidate for evaluating the matrix effect by itself. The three samples were used to test whether different dilutions of CSF (1:10, 1:20, 1:30 and 1:40) with 20% ACN have an effect on retention time and PTP recovery.

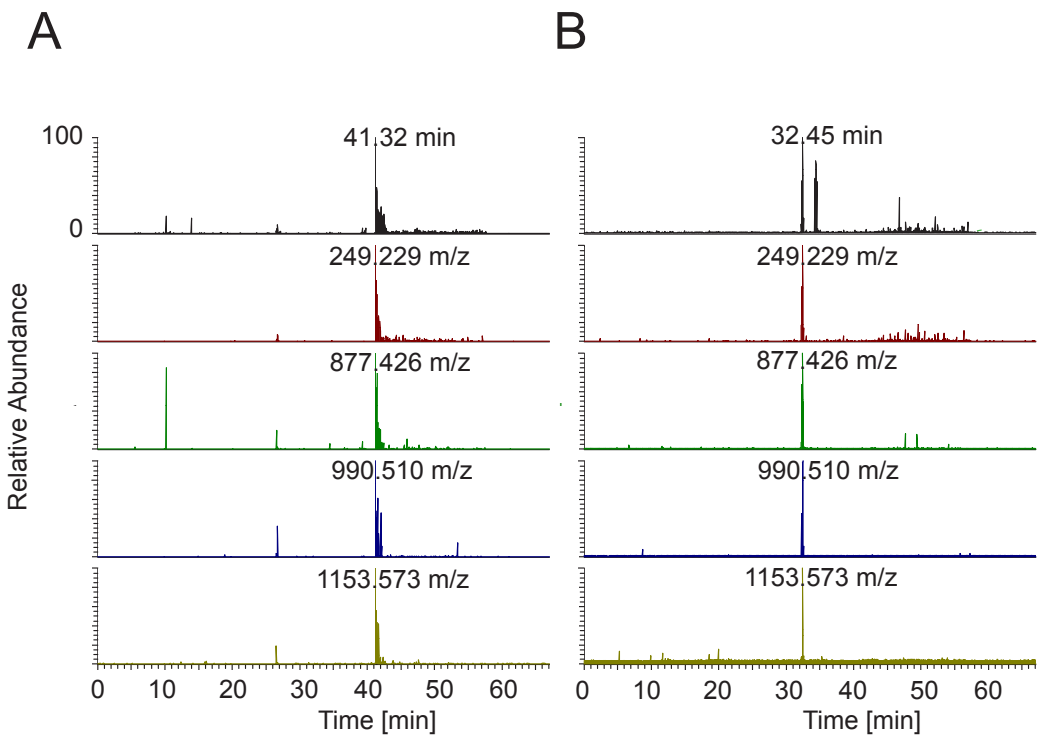

Figure 3-24. Targeted mass spectrometry of agrin-22 z0 in human CSF spiked with the synthetic PTP of the z0 variant to document the matrix effect on the retention time. In the upper part, the total ion count (TIC) is shown in black. The lower panels show the four extracted ion chromatograms (XIC) for each fragment ion in colour. (A) 1:10 and (B) 1:100 dilution in 20% ACN.

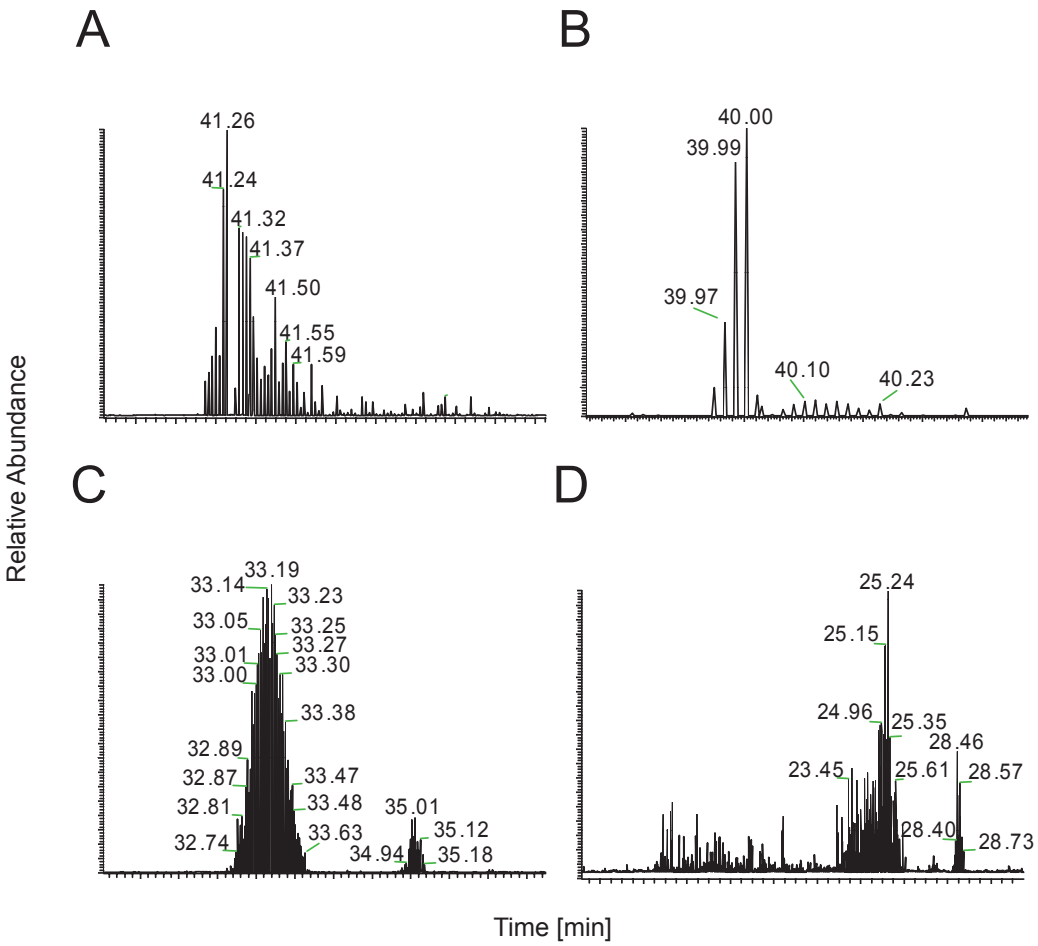

Figure 3-25. Targeted mass spectrometry of transitions for agrin-22 z0 and the peptide TEATQGLVLWSGK which is identical for all agrin-22 isoforms. The measured sample was digested human CSF spiked with a digest of recombinant agrin-22 z0 to document the matrix effect on the retention time. All chromatograms show the total ion count (TIC). (A) 1:10 dilution. TEATQGLVLWSGK elutes at 41.26 minutes, agrin-22 z0 at 41.50 minutes. (B) 1:20 dilution. TEATQGLVLWSGK elutes at 40.00 minutes, agrin-22 z0 at 40.10 minutes(C) 1:30 dilution. TEATQGLVLWSGK elutes at 33.19 minutes, agrin-22 z0 at 35.01 minutes (D) 1:40 dilution TEATQGLVLWSGK elutes from 6.00-25.24 minutes, agrin-22 z0 at 28.46 minutes. All dilutions are prepared with 20% ACN.

The experiments clearly show that there is an effect on signal intensity and retention of the two PTPs induced by the complex peptide matrix (Figure 3-25). The signal suppression for the agrin-22 z0 PTP was about 95% comparing signal intensities between the most abundant transition in the pure digestion of recombinant agrin-22 z0 (10 fmol/µl; intensity for the most abundant transition: 4.05E3) and the 1:10 dilution of CSF spiked with the same digestion (10 fmol/µl; intensity for the most abundant transition: 2.37E2). This effect could not be eliminated by diluting the CSF matrix. The 1:40 dilution of CSF still displays strong signal suppression for the most abundant transition (intensity for the most abundant transition: 1.00E1). Comparison of the retention time for all samples as well indicates a dramatic impact between digestion alone and spiked CSF samples. All four transitions for agrin-22 z0 elute at

27.41 minutes using pure digestion solution. Addition of 1:10 diluted CSF increases retention to 41.50 minutes. Dilution of CSF to 1:20 is without any improvement on retention time (40.10 minutes) whereas dilution to 1:30 shows a slight decrease in agrin-22 z0 retardation (35.05 minutes). The 1:40 dilution recovers retention (28.46 minutes) and a shift back to the value observed for the pure digestion solutions was demonstrated. A similar situation is indicated for the tryptic peptide TEATQGLVLWSGK. The shift of retention time in the 1:10 diluted CSF to 41.26 minutes accentuates the high impact of matrix effects on the elution behavior of tryptic peptides in complex samples. This effect cannot be rescued when diluting CSF to 1:20 (40.00 minutes). A slight decrease in retardation is indicated for the 1:30 dilution (33.09 minutes). In the 1:40 dilution peak fronting is observed for this tryptic peptide. The elution starts at 6 minutes, thus clearly indicating that no retardation of the peptide on the C18 material takes place. Additionally, this PTP showed poor interaction with the C18 column when analyzing the agrin-22 z0 digestion mixture without CSF, which clearly shows its low hydrophobic nature. This tendency is expected for tryptic peptides when using higher proportions of ACN as starting conditions for the LC-gradient. The experiments suggest evidence of strong matrix effects in addition to the high affinity of the agrin-22 z0 isoform to the C18 in comparison to the TEATQGLVLWSGK peptide.

To further examine the positive impact on the PTP recovery using diluted CSF, the 1:30 diluted CSF was analyzed with LC-ICR-FT-MS. As shown in the previous experiment, the 1:30 dilution was measured with and without agrin-22 z0 digest (10 fmol/µl). The resulting spectra are shown in Figure 3-26. The elution time for the agrin-22 z0 PTP is shifted to 42.57 minutes. Additionally, identification of agrin-22 was not possible in the unspiked 1:30 CSF dilution using Mascot database search algorithm. Taken together, very strong matrix effects were observed which cannot be circumvented.

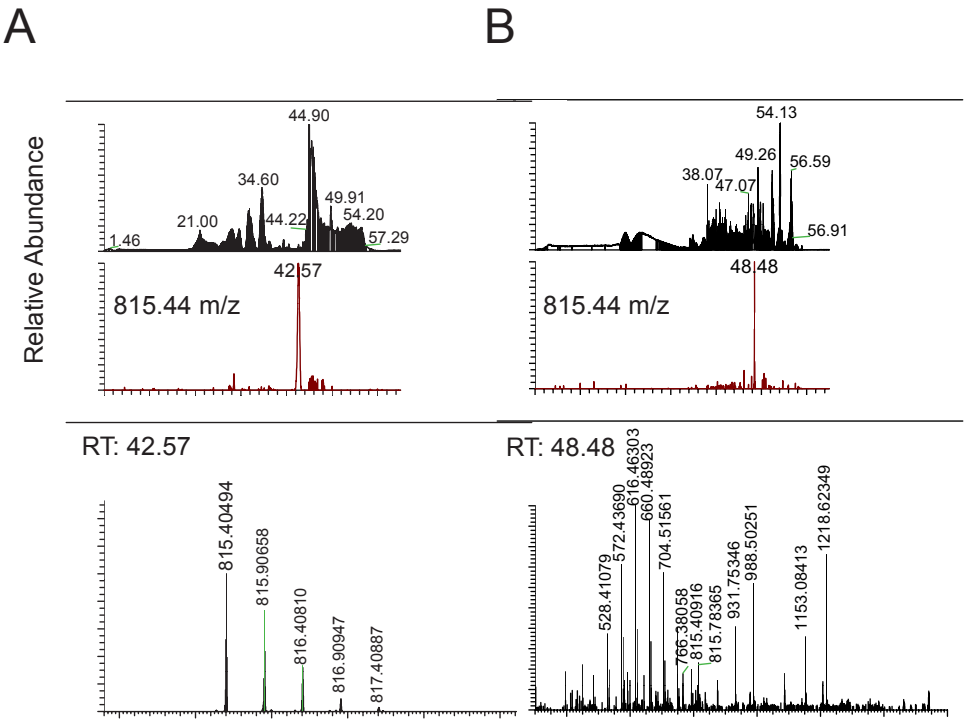

Figure 3-x26. FT-ICR spectra were recorded in the data dependent mode using an inclusion list for agrin-22 z0. (A) human CSF (1:30) spiked with agrin-22 z0 digest (10 fmol/µl) and (B) human CSF (1:30) alone. In the upper part the base peak chromatograms are shown in black, extracted ion chromatograms (XICs) are shown in dark red. The lower parts show the mass spectra at the specific retention times concluded from the XIC for the m/z value 815.3500-815.4500.

3.4 Identification of neurotrypsin-dependent cleavage of agrin in human cerebrospinal fluid

The former studies on agrin-22 in the previous paragraphs documented the difficulties in agrin-22 isolation and recovery. CSF has a less complex protein composition, hence it can be directly used for analysis by Western Blot, whereas serum has first to be depleted or diluted. In addition, previous studies showed that the concentration of agrin-22 is lower in serum compared to CSF (unpublished observation). Physiologically, agrin-22 values in the CSF can give useful informations about neurotrypsin activity in the brain. Considering these criteria, I decided to chose CSF as sample system, which offers the possibility to quantify the agrin-22 level without additional manipulations.

I am going to identify and describe the activity of neurotrypsin in human CSF samples using quantitative Western blot analyses. I will start with the identification of agrin-22 in the context of aging and present the data in association with Alzheimer`s disease (AD)and epilepsy.

3.4.1 Age-related agrin cleavage can be monitored in human cerebrospinal fluid

As shown in paragraph 3.1, murine serum samples reflect an age-dependent appearance of the neurotrypsin-dependent agrin-22 fragment. Concerning this finding, it is likely that agrin-22 amounts in the brain follow as well physiologically and age-associated properties. To obtain a detailed view on neurotrypsin`s activity in the human brain, a large set of 84 human CSF samples of different age (2 months – 35 years old, samples were ontained from from Prof. Blau, Children`s Hospital, Zurich) was analyzed without considering any status of disease. Equal amounts of CSF were resolved by 4-12% NuPAGE gels and analyzed by Western blot using antibody R139 against the C-terminal part of agrin. Normalization of signal intensities of agrin-22 was in all cases achieved by comparing agrin-22 CSF levels with a reference sample (murine serum, wt, E18).

The analysis demonstrates an age-dependent regulation of neurotrypsin-dependent processing of agrin (Figure 3-27). The agrin-22 level was strongest in the samples from 2 months old subjects and its intensity declined with aging and ongoing development. Amounts of cleavage product notably decrease at the age of 6 months. The decrease of signal intensity correlates well with neurotrypsin and agrin expression and the pattern of cleavage products in murine brain (Reif et al, 2007). Only a slight difference was obtained between subjects of the age 10 to 35 years. The proteolytic activity is likely to persist at a basal level throughout adulthood. However, several CSF samples show relatively high levels of agrin-22 independent of age. This variability in agrin-22 values is likely to represent a specific or unspecific elevation of either neurotrypsin`s activity or the expression of both proteins due to individual changes in the brain. These changes can be due to physiological- or diseased-based mechanisms. Nonetheless, variances in agrin-22 levels underlying the particularly high activity of neurotrypsin are currently not understood. To provide evidence that neurotrypsin activity and cleavage of agrin-22 could give useful information on the course of neuronal diseases, I analyzed human CSF samples from epilepsy patients and patients with Alzheimer`s disease (AD).

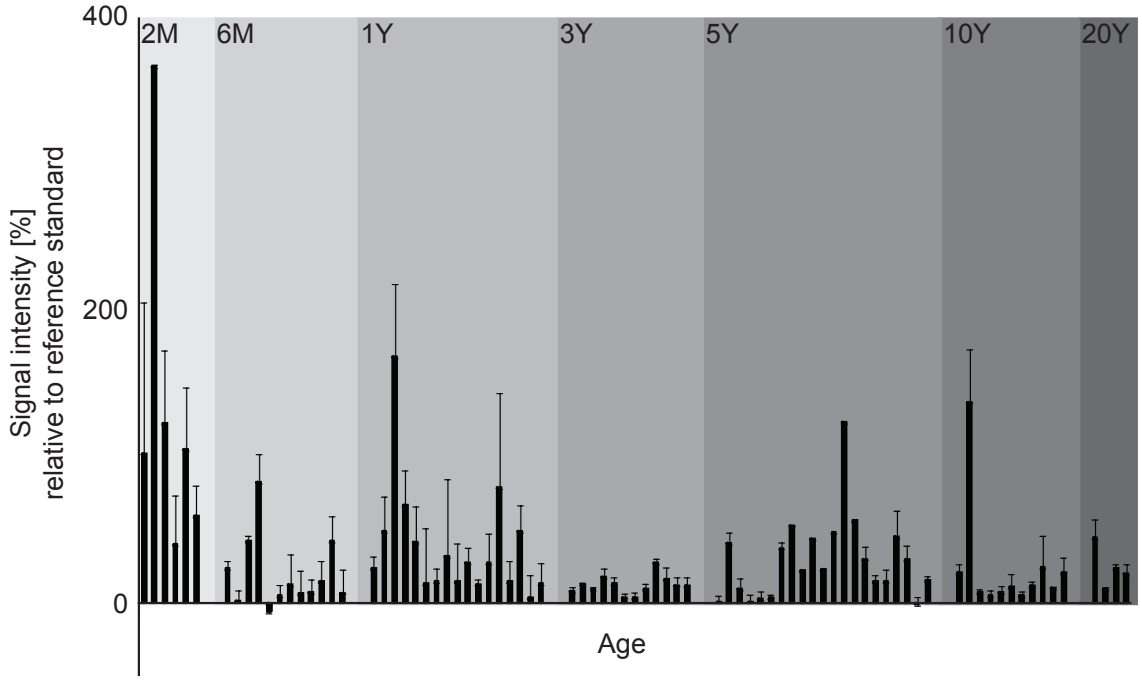

Figure 3-27: Age-dependent agrin-22 level in human CSF. Months: M, years: Y.

3.4.2 Quantification of neurotrypsin-dependent cleavage in Epilepsy

Experiments with green-fluorescent-protein tagged neurotrypsin in cultured hippocampal neurons indicated an activity-dependent release of neurotrypsin into the synaptic extracellular space (Frischknecht et al, 2008). Hence, I wanted to address the question whether the agrin-22 level is significantly different in CSF of patients with epilepsy. To analyze neurotrypsin activity in the context of the diseases and to further shed light on the phenomenon of variances observed in the previous age-dependent study, quantitative Western blot analyzes of human CSF samples from epilepsy patients were performed compared to healthy controls as well as correlation to the levels in the age-dependent samples set. Comparative Western blot analyses of CSF samples from 17 epilepsy patients and 19 controls as well as an age-matched comparison with the 84 CSF samples were accomplished. CSF samples (30 µl) were separated by 4-12% NuPAGE gels and Western blot performed with antibody R139. The results obtained by Western blot analysis were normalized to the corresponding agrin-22 signal in a murine serum reference sample (wt, E18). One big disadvantage in the study was that CSF samples from healthy controls were grouped towards higher age. Therefore the direct comparison of agrin-22 levels was deceptive, since the previous study showed the decline of neurotrypsin-dependent cleavage. Nevertheless, comparison to the set of 84 age-associated samples revealed relatively high correlation of agrin-22 levels in epilepsy with the control samples of the same age with unknown status of diseases (Figure 3-27). Still, epilepsy patients show increased signal intensities in a higher number of cases. The direct identification of agrin-22 levels at four specific ages as well as comparison of the average level for these samples demonstrated

a tendency for enhanced neurotrypsin activity in epilepsy patients (Figure 3-28). However, due to the low sample number at matching ages, statistical analysis could not be performed. Differences in agrin-22 signal intensities were apparent but do not allow for a significant distinction between values in the CSF of epilepsy patients and controls.

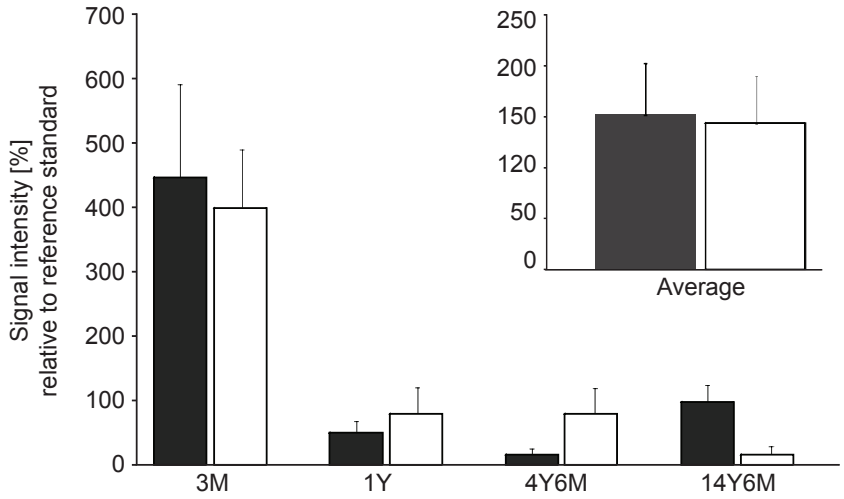

Figure: 3-28. Quantitative analysis of neurotrypsin activity in human CSF from epilepsy patients (black bars) compared to samples from the age-dependent study (open bars) at corresponding age. Samples were separated with 4-12% NuPAGE gels and Western blots were performed of the same sample in triplicates for quantification. Error bars show STDEV. The small insert displays the total average signal intensity of the four samples analyzed for each group.

3.4.3 Agrin-22 as reporter for neurotrypsin activity in Alzheimer`s disease

There are various reports about the interaction of agrin and β-amyloid precursor protein (APP) (Boew & Fallon, 1995; Braak & Braak, 1991; Cozman et al, 2000; van Horssen et al, 2002). It was shown that agrin is able to accelerate Aβ fibril formation and to protect Aβ (1-40) from proteolysis in vitro. Immunostainings suggested the presence of agrin within senile plaques. Thus, agrin may play an important role in the progression of Aβ peptide aggregation and in its persistence in the brain of AD patients. In addition, several cases of memory impairment in epilepsy encourage the idea of epilepsy-derived Alzheimer`s disease (AD) (Ito et al, 2009). AD patients seem to have a high risk to develop unprovoked seizures. In a study of Hogh (Hogh et al, 2002), a set of three patients with progressive memory dysfunction linked to AD underwent neuroimaging analysis and no loss of brain regions could be assigned. However, therapy with anti-epileptic medication showed improvement in memory performance. This phenomenon indicates that seizures are not necessarily a result of AD and that the connection of dementia and epilepsy is not unidirectional. Hence, there is emerging evidence that dementia could be a result of epilepsy due to simultaneous onset of seizures and dementia (Abou-Khalil, 2010). The activity-dependent release of neurotrypsin into the synaptic extracellular space (Frischknecht

et al, 2008) and the controversial results for agrin-22 levels in the context of epilepsy led us to investigate neurotrypsin`s activity in the context of AD.

To test for differences in agrin-22 levels and whether they correlate with AD, quantitative Western blot analyses of CSF from 10 AD patients and 10 healthy controls were performed. Neurotrypsin`s and agrin`s strong age-dependent association, it could not be considered in this measurement because infomation on the patient`s age was not available due to legal regulations. The CSF samples (30 µl) were separated by 4-12% NuPAGE gels and Western blot was performed using antibody R139.

The comparison of agrin-22 levels revealed a slight decrease of neurotrypsin-dependent processing of agrin in the context of AD patients (Figure 3-29). However, statistical analysis confirmed the absence of a significancy between AD and healthy controls for agrin-22 values. This finding rendered it impossible to clearly decide whether neurotrypsin activity in AD is reduced.

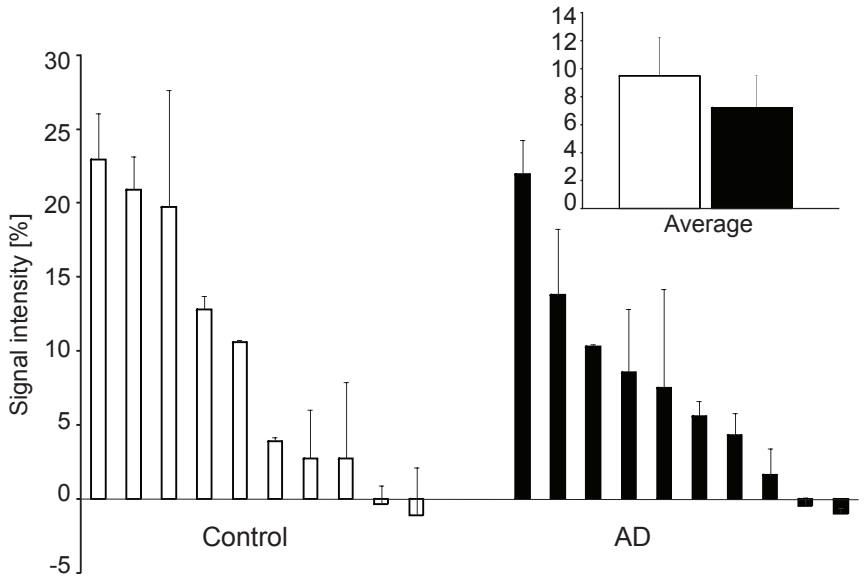

Figure 3-29. Comparison of agrin-22 levels in human CSF samples from 10 healthy controls (open bars) versus 10 AD patients (black bars). Samples were separated on 4-12% NuPAGE gels and Western blots were performed of each sample in triplicates for quantification. Error bars show STDEV. The insert shows the average signal intensity of all samples analyzed for each group.

3.5 Quantification of calsyntenin-1 ectodomain in human CSF

Neuronal excitation either increases production or activates the matrix metalloproteases ADAM10 and ADAM17 reported to cleave calsyntenin-1 and to release its soluble ectodomain into the extracellular space (Marcello et al, 2007, Hata et al, 2010). After proteolytic processing, the resulting ectodomain is accumulated in cerebrospinal fluid (Vogt et al, 2001). At the same time, its transmembrane stump is internalized. In addition, it could be shown by chemical induction of long term potentiation (LTP) in acute whole hippocampi that ectodomain shedding of calsyntenin-1 is enhanced in comparison to non-stimulated hippocampal tissue (unpublished results). The synaptic activity was chemically enhanced by blockade of K^+ channels with tetraethylammonium chloride (TEA) or a combination of picrotoxin, forskolin, and rolipharm (PEA) which induces LTP in the hippocampal CA1 region in an NMDA-R-dependent manner. Both, potassium-based TEA as well as non-potassium-based PFR stimulation protocols enhance calsyntenin-1 ectodomain shedding. Thereby, induction of LTP by TEA showed a stronger effect as compared to PFR stimulation (see introduction).

In this paragraph, I am going to identify and describe the accumulation of calsyntenin-1 ectodomain in human CSF using quantitative Western blot approach. I will start with the identification of specific antibodies for calsyntenin-1, discuss the identification of calsyntenin-1 in human CSF using data-dependent and targeted LC-MS/MS measurements, give an age-associated overview of the calsyntenin-1 ectodomain level, before presenting the data in the context of epilepsy and AD.

3.5.1 Antibody specificity

To examine the specificity of the polyclonal antibodies against calsyntenin-1 ectodomain, recombinant proteins of mouse calsyntenin-1, -2 and -3 were expressed either with myc-tag or fused to EGFP in adherent HeLa cells. The cell lysate was chloroform-methanol precipitated and 20 µg protein was loaded on a 4-12% NuPAGE gel and Western blot analysis was performed with four different antibodies. The tested antibodies were R130 (IgG) raised against the P3-immunogen of calsyntenin-1, R131 (IgG) 2nd and 3rd boost raised against P3-immunogen and R85 (affinity purified) raised against the P1-immunogen of calsyntenin-1. The P1-immunogen lies in the N-terminal part of the extracellular domain of calsyntenin-1, whereas the P3-immunogen is targeting the more C-terminal region in the extracellular space of calsyntenin-1 which is located proximal to the membrane. Figure 3-30 displays representative Western blots with the antibodies R85 and R131 3rd.

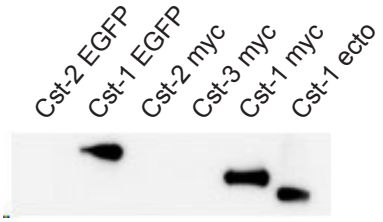

Figure 3-30. Western blot analysis of recombinant calsyntenin family members in order to test the specificity of antibody R131 3rd boost. Cell lysates were chloroform-methanol precipitated and each 20 µg protein was analyzed with 4-12% NuPAGE gels. Recombinant calsyntenin-1 ectodomain was used as reference.

The experiments indicated the specificity of the antibody R130 for calsyntenin-1. In contrast, no signal could be obtained for the calsyntenin-1 ectodomain. Antibody R85 shows a broad interaction with all three calsyntenin family members, whereas antibody R131 (2nd and 3rd boost) is highly specific for calsyntenin-1. As signal intensities of calsyntenin-1 were highest with R131 3rd boost, this antibody was chosen for evaluating calsyntenin-1 ectodomain levels in human CSF samples using quantitative Western blot analyses.

3.5.2 Identification of calsyntenin-1 in human CSF with mass spectrometry

The three members of the calsyntenin family are predominantly expressed in neuronal regions (Hintsch et al, 2002). Interestingly, they show a different distribution pattern in the brain which suggests specialized functions in distinct regions. In order to identify the presence of the calsyntenin members in human CSF, 4ml CSF of three independent subjects were denatured and reduced (25mM ammonium bicarbonate, 1% SDS, 5mM DTT) followed by concentration (Vivaspin 5 kDa MWCO) and 40 µl were separated on 4-12% NuPAGE Bis-Tris gel. The gel was stained with Coomassie brilliant blue, protein bands at corresponding molecular masses were cut out and in-gel tryptic digestion 2 (see Materials and Methods) was performed. Extracted tryptic peptides were purified with ZipTip C18 prior to mass spectrometric analysis. Data-dependent mass spectrometry was carried out on the FT-ICR using standard LC-gradient (see Materials and Methods) and an inclusion list of calsyntenin-1, -2 and -3 for all tryptic peptides [M+2H]2+covering the m/z-range 300 – 1600. Identification was achieved with Mascot database search using Swissprot-d. The presence of calsyntenin-1 could be confirmed in three independent CSF samples. The eleven identified tryptic peptides are restricted to the extracellular N-terminal part of calsyntenin-1, in detail to the ectodomain (Figure 3-31). This finding suggests the possibility to monitor calsyntenin-1 ectodomain shedding in human CSF samples. The variants calsyntenin-2 and -3 were not identified, presumably due to their reported low expression in the brain (Hintsch et al, 2002).

```
   1 MLRRPAPALA PAARLLLAGL LCGGGVWAAR VNKHKPWLEP TYHGIVTEND
  51 NTVLLDPPLI ALDKDAPLRF AESFEVTVTK EGEICGFKIH GQNVPFDAVV
 101 VDKSTGEGVI RSKEKLDCEL QKDYSFTIQA YDCGKGPDGT NVKKSHKATV
 151 HIQVNDVNEY APVFKEKSYK ATVIEGKQYD SILRVEAVDA DCSPQFSQIC
 201 SYEIITPDVP FTVDKDGYIK NTEKLNYGKE HQYKLTVTAY DCGKKRATED
 251 VLVKISIKPT CTPGWQGWNN RIEYEPGTGA LAVFPNIHLE TCDEPVASVQ
 301 ATVELETSHI GKGCDRDTYS EKSLHRLCGA AAGTAELLPS PSGSLNWTMG
 351 LPTDNGHDSD QVFEFNGTQA VRIPDGVVSV SPKEPFTISV WMRHGPFGRK
 401 KETILCSSDK TDMNRHHYSL YVHGCRLIFL FRQDPSEEKK YRPAEFHWKL
 451 NQVCDEEWHH YVLNVEFPSV TLYVDGTSHE PFSVTEDYPL HPSKIETQLV
 501 VGACWQEFSG VENDNETEPV TVASAGGDLH MTQFFRGNLA GLTLRSGKLA
 551 DKKVIDCLYT CKEGLDLQVL EDSGRGVQIQ AHPSQLVLTL EGEDLGELDK
 601 AMQHISYLNS RQFPTPGIRR LKITSTIKCF NEATCISVPP VDGYVMVLQP
 651 EEPKISLSGV HHFARAASEF ESSEGVFLFP ELRIISTITR EVEPEGDGAE
 701 DPTVQESLVS EEIVHDLDTC EVTVEGEELN HEQESLEVDM ARLQQKGIEV
 751 SSSELGMTFT GVDTMASYEE VLHLLRYRNW HARSLLDRKF KLICSELNGR
 801 YISNEFKVEVN VIHTANPME HANHMAAQPQ FVHPEHRSFV DLSGHNLANP
 851 HPFAVVPSTA TVVIVVCVSF LVFMIILGVF RIRAAHRRTM RDQDTGKENE
 901 MDWDDSALTI TVNPMETYED QHSSEEEEEE EEEEESEDGE EEDDITSAES
 951 ESSEEEEGEQ GDPQNATRQQ QLEWDDSTLS Y
```

Database:Mascot(swissprot)
Match to: **CSTN1_HUMAN** Score: **301**
O94985) Calsyntenin-1 precursor - Homo sapiens (Human)
Found in search of 20091022_dklingler_01_CSF_A4_100kD.mgf

Figure 3-31. Amino acid sequence of calsyntenin-1. The signal peptide is highlighted in green, identified tryptic peptides are highlighted in red. The transmembrane part is underlined.

To further confirm the presence of calsyntenin-1 in human CSF samples, targeted mass spectrometry was used. Here, the Mascot sequence information from the data-dependent MS/MS spectra search was converted into a spectral library using the pinpoint software (Thermo). To define the proteotypic precursors and their most abundant fragments, Mascot library scores were taken as reference to target the mainly expected transitions. The SRM method was created using pinpoint software and implemented into the Xcalibur instrument method on the TSQ. The selected peptides for targeted analysis of calsyntenin-1 were: (i) IPDGVVSVSPK (549 m/z) and (ii) EGLDLQVLEDSGRGVQIQ (715 m/z). For the peptide separation and elution of the two proteotypic peptides from RP-C18 column, a standard LC-gradient from 5-80% ACN was used (see Materials and Methods). The results from targeted mass spectrometric analysis are displayed in Figure 3-32.

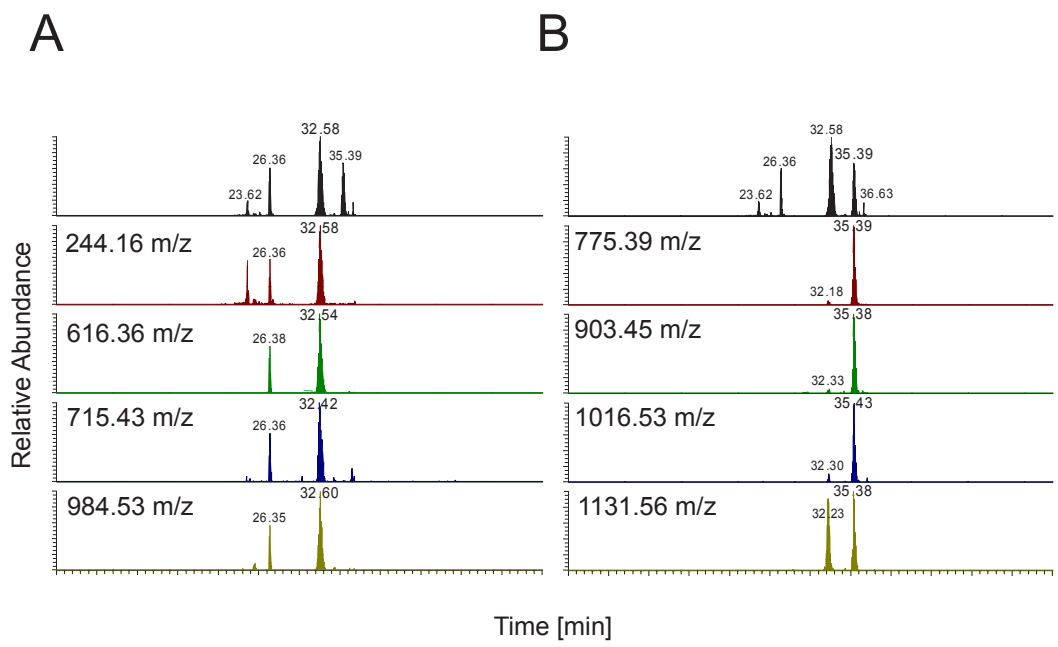

Figure 3-32. Targeted mass spectrometry of human CSF for two PTPs of calsyntenin-1. (A) IPDGVVSVSPK (549 m/z) (B) EGLDLQVLEDSGRGVQIQ (715 m/z). The upper panel shows the TIC in black. In the lower panels, the XIC spetra for the four transitions of each peptide are shown in colour.

All four selected transitions for the two highly abundant tryptic peptides of calsyntenin-1 have been detected using targeted mass spectrometry. The relative signal intensities of the transitions show enhanced response for the peptide IPDGVVSVSPK (549 m/z) at 32.58 minutes and the peptide EGLDLQVLEDSGRGVQIQ (715 m/z) at 35.39 minutes. The analysis was reproducible in a set of four independent samples proving the presence of calsyntenin-1 in human CSF. Given the high sensitivity of this measurement, the presence of calsyntenin-1 in human CSF was fully proven.

3.5.3 Age-related processing of calsyntenin-1

To investigate the proteolytic ectodomain shedding of calsyntenin-1 and to test whether there is an age-dependent regulation, human CSF samples from 84 subjects were loaded on a 4-12% NuPAGE gel and quantified by Western blot analysis using antibody R131 3rd boost.

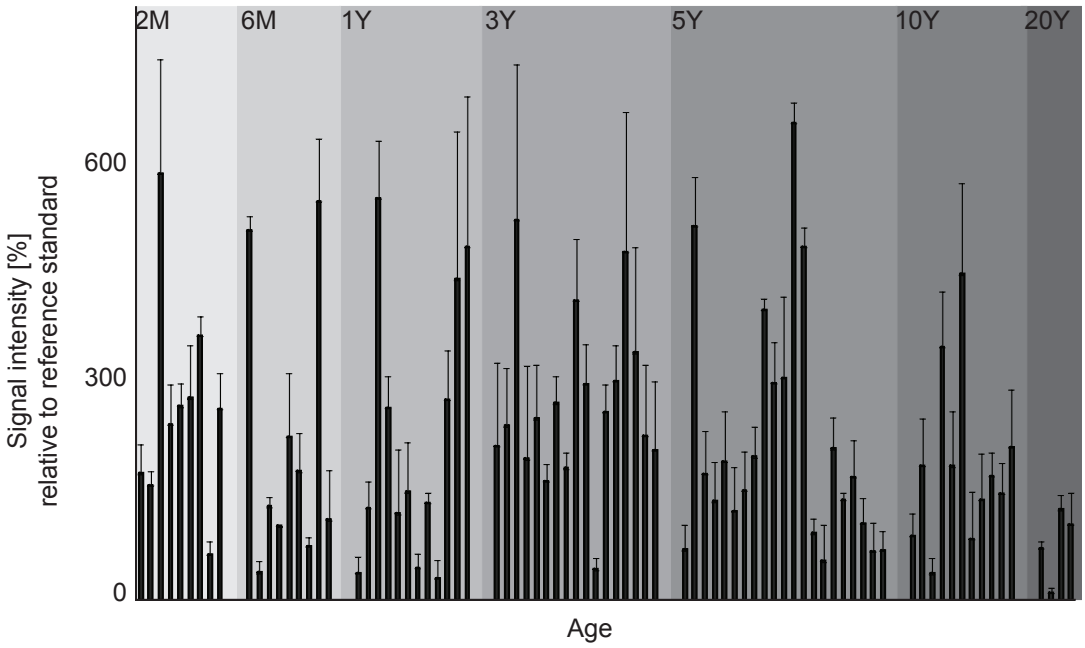

Figure 3-33. Age-dependent calsyntenin-1 ectodomain level in human CSF.

Altogether, the level of calsyntenin-1 ectodomain remains at a certain basal level from age 2 months throughout adulthood. No specific changes in calsyntenin-1 expression or proteolytic processing could be assessed in the context of its accumulation in CSF. However, several CSF samples show strong accumulation of calsyntenin-1 irrespective of the subject`s age.

3.5.4 Quantification of calsyntenin-1 ectodomain in Alzheimer's disease

Calsyntenins and amyloid precursor protein (APP) undergo a similar coordinated proteolytic processing (Araki et al, 2003). Recent findings suggest that the formation of a tripartite complex of APP and calsyntenin-1 with the X11-like (X11L) protein stabilizes intracellular APP metabolism and mediates suppression of the amyloid-β-protein (Aβ) generation. The dissociation of X11L from the tripartite complex enables cleavage of calsyntenin-1 and APP at their primary cleavage sites (ξ and α or β, respectively). Followed by secondary cleavage at the ε/γ-site, the intracellular fragments of both, APP (AICD) and calsyntenin-1 (CICD) are generated. It was suggested that CICD suppressed the Fe65-dependent gene transactivation activity of AICD, probably because CICD competes with the APP intracellular domain fragment for binding to Fe65. In addition, deficiencies in the X11L-mediated interaction and imbalance in the metabolism of calsyntenin-1 and APP may be related to neuronal disorders like AD. As calsyntenin-1 was reported as a potential biomarker in the diagnosis of AD (Hata et al, 2002), this prompted us to evaluate whether calsyntenin-1 ectodomain shedding is increased or decreased in the context of AD. To answer this question, CSF samples (30 µl) from 10 AD patients compared to 10 healthy control subjects were loaded on a 4-12% NuPAGE gel and Western blot was achieved with antibody R131 3rd boost. The signal intensities were normalized to a reference sample (pooled human CSF). The group of AD patients does not reflect a strong change in ectodomain shedding compared to healthy control subjects (Figure 3-34).

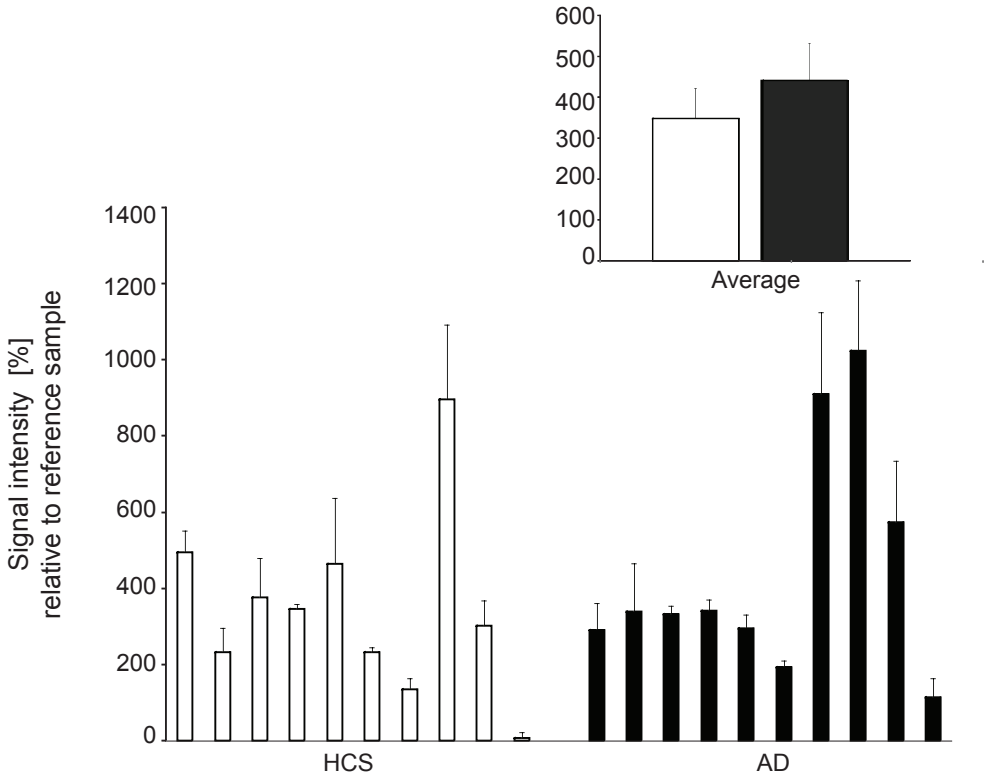

Figure 3-34. Comparison of calsyntenin-1 ectodomain levels in human CSF samples from 10 healthy controls (HCS, open bars) versus 10 AD patients (black bars). Samples were separated on 4-12% NuPAGE gels and Western blots were performed for the same sample in triplicates for densitometric quantification. Error bars show STDEV. The inset shows the average signal intensity of all samples analyzed for each group.

3.5.5 Calsyntenin-1 ectodomain shedding in Epilepsy

Recently, it could be shown by chemical LTP induction in acute whole hippocampi that both potassium-based TEA as well as non-potassium-based PFR stimulation protocols enhance ectodomain shedding of calsyntenin-1 in comparison to non-stimulated hippocampal tissue. Thereby, induction of LTP by TEA showed stronger effect when compared to PFR stimulation (see introduction).

As there is an imbalance between neuronal inhibition and excitation in epilepsy, a change in ectodomain shedding was assumed as a measure of epileptic activity. Thus, it was tested whether this change can be monitored in human CSF by Western blot analyses. I used the previous sample set as described in paragraph 3.8.2 was included and comparative analysis of 17 epilepsy patients and 19 control subjects was performed. As shown in the same paragraph, the sample set from the age-associated study and compared a set of four samples from epilepsy patients and the age-matched individuals. I determined the calsyntenin-1 ectodomain levels by seperating 30 µl CSF on 4-12% NuPAGE gels followed by Western blot analyses using antibody R131 3rd boost.

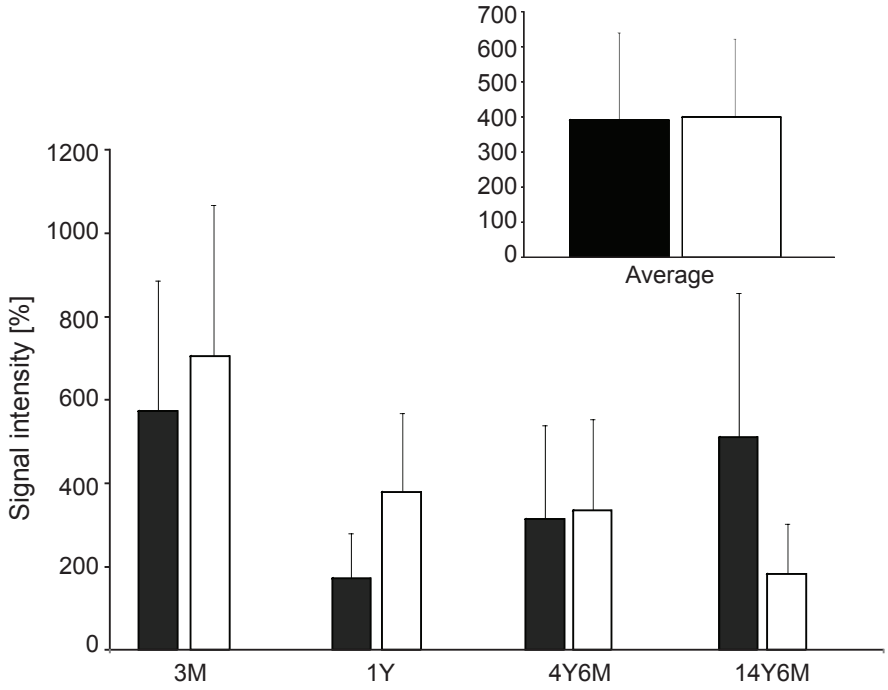

Figure: 3-35. Quantitative analysis of calsyntenin-1 ectodomain in human CSF from epilepsy patients (black bars) compared to samples from the age-dependent study (open bars) at corresponding age. Samples were separated with 4-12% NuPAGE gels and Western blots were performed from each sample in triplicates. Error bars show STDEV. The insert shows the average of all four samples for each group.

The results from the experiments showed no clear differences in calsyntenin-1 ectodomain levels between epilepsy patients and healthy control subjects. Additionally, analyses with age-matched sample pairs (Figure 3-35) confirm that there is no tendency whether calsyntenin-1 ectodomain is increased or decreased in epilepsy.

4 Discussion

The quantification of differences in protein amounts in the physiological states of a biological system is among the most important tasks to unravel novel and pathological pathways. In addition to the classical quantification methods, analyzing proteins by SDS PAGE gel or immunoblot staining, mass-spectrometry-based quantification methods have gained increasing popularity.

The neuronal serine protease neurotrypsin is predominantly expressed in the nervous system and has been located in non-neuronal tissues as well (Wolfer et al, 2001). Neurotrypsin cleaves agrin *in vitro* (Reif et al, 2007). This proteolytic processing was observed at the NMJ *in vivo* (Bolliger et al, 2010). To further analyze whether agrin is a substrate of neurotrypsin *in vivo* and to quantify the proteolytic activity of neurotrypsin in non-neuronal tissue as well as in the central nervous system (CNS), mass spectrometric measures and quantitative Western blot analyses of murine serum and human cerebrospinal fluid (CSF) were performed. I further analyzed the potential functional effects of the neurotrypsin-agrin interaction *in vivo* using human CSF samples in relation to age and in the context of neurological disorders such as Alzheimer`s disease and epilepsy. The catalytic activity of neurotrypsin on agrin in murine serum was increased in neurotrypsin-overexpressing mice and completely diminished in neurotrypsin-deficient mice. In the CNS as well as in non-neuronal tissues, neurotrypsin certainly recognizes the proteoglycan agrin and proteolytically cleaves it at two positions termed α- and β-sites. The proteolytic activity on the β-site can be screened in human CSF samples, as this cleavage step leads to the release of the C-terminal 22 kDa fragment (agrin-22) into body fluids.

Furthermore, I identified and quantified the transmembrane protein calsyntenin-1. Calsyntenin-1 and APP undergo a similar coordinated proteolytic processing. After ectodomain shedding (ξ-cleavage) by ADAM10 and ADAM17, cleavage by γ-secretase regulates intramembrane proteolysis (Araki et al, 2003). The transmembrane stump is internalized and accumulated in the spine apparatus of the synapse. Thus, proteolysis-dependent translocation is suggested to illustrate an independent downstream event in protease-mediated synaptic plasticity. Furthermore, the metabolism of calsyntenin-1 and APP may be related to neuronal disorders like AD and it was recently shown that calsyntenin-1 ectodomain-shedding is increased by induction of synapse activity (unpublished results). To evaluate ectodomain shedding of calsyntenin-1, mass spectrometric identification of cleavage products in human CSF was performed. I further analyzed the potential functional effects of ectodomain shedding *in vivo* by quantitative Western blot using human CSF samples in association to age and in the relation to neurological disorders such as Alzheimer`s disease and epilepsy. Proteolytic ectodomain shedding of calsyntenin-1 can be screened in human CSF samples. The cleavage of calsyntenin-1 leads to the accumulation of calsyntenin-1 in the surrounding CSF.

4.1 Neurotrypsin-dependent agrin fragments are accumulated in body fluids

The spatio-temporal expression pattern of neurotrypsin has been verified on the mRNA level and showed a peak at the postnatal day 10 (P10) in murine brain and in non-neuronal tissues (Wolfer et al, 2001). Neurotrypsin`s substrate agrin is either expressed in neurons, mainly as type II transmembrane protein, or as a secreted isoform in the whole brain and peripheral tissues such as kidney and lung. The distribution of agrin`s z-transcripts in tissue can be differentiated as well. The z0 transcript is the predominant isoform in non-neuronal tissues whereas all isoforms (z0, 8, 11, and 19) have been detected in the CNS (O`Connor et al, 1994). Recently, the developmental course of neurotrypsin-dependent agrin cleavage in murine brain tissue of wild-type mice from embryonic age E16 until postnatal day P730 was documented by Western blot using anti-agrin and anti-neurotrypsin antibodies (Reif et al, 2007). The distinct cleavage at the α-site and thus the release of the intermediate 90 kDa cleavage product (agrin-90) was shown to be persistent throughout life, whereas agrin-22 was detectable only until P60. It was therefore assumed that agrin-22 is more diffusible compared to agrin-90 and thus may pass the non-synaptic tissue into the cerebrospinal fluid (CSF). From what is known in our group, neither agrin nor neurotrypsin could be isolated and identified by mass spectrometry from synaptosomal preparations in neurotrypsin-overexpressing mice (Walther, 2007). There is no clear explanation for this finding. Possibly, the traceable amounts of neurotrypsin even from overexpressing mice were already lost during sample preparation, since neurotrypsin is known to be an extremely sticky protein (unpublished observation). Taken together, it was argued that it might be possible to monitor neurotrypsin`s proteolytic activity in the CNS and non-neuronal tissues by quantifying the level of cleavage products of its unique substrate agrin, particularly of its 22 kDa variant, in body fluids such as serum and CSF.

This study is the first analysis of proteolytic cleavage products of agrin in these body fluids. To test this concept, agrin was isolated by immuno-affinity chromatography from murine serum and rat CSF using affinity-purified antibody R139 which is raised against the C-terminal agrin-22 fragment. The elution fractions were analyzed by Western blot and mass spectrometric analysis to identify the enriched agrin components. The results confirmed that targeting of the neurotrypsin-dependent fragment agrin-22 was possible in both body fluids. Therefore, we compelling evidence can be provided that agrin-22 is present in traceable amounts. Four tryptic peptides matching the amino acid sequences of mouse and rat agrin-22 have been identified by mass spectrometric analysis for each body fluid. The mass spectrometric data further indicated that the full-length form of agrin as well as the agrin-90 fragment is absent in serum and CSF. In respect of CSF, this strengthens the finding that mainly transmembrane agrin, which is predominantly expressed in neurons, is locally cleaved at the synapse, releasing the agrin-90 and agrin-22 fragments into the synaptic cleft (Stephan et al, 2008). It is hypothesized that the transmembrane N-terminal part of agrin is internalized after α- and β-cleavage. Both cleavage fragments might interact with respective receptors which are possibly not accessible for full-length agrin. However, specific proteotypic tryptic peptides of the agrin-22 splice variants z0, 8, 11, and 19 have not been identified. This could either show that for these specific peptides in-gel digestion and elution from the gel is hindered or that the sensitivity of the mass spectrometric methods used during these experiments is not sufficient.

4.2 Neurotrypsin`s cleavage activity is age- and genotype-specific

Endogenous neurotrypsin as well as agrin show a particularly high expression during late embryonic development and the first postnatal week in the brain, peripheral nervous system, and non-neuronal tissues (Wolfer et al, 2001; Stephan et al, 2008). Semi-quantitative analyses during prenatal development in non-neuronal tissues revealed a strong expression of neurotrypsin at mesenchymal boundaries and indicated that it may have additional roles in tissue and organ morphogenesis. Neurotrypsin cleaves agrin at two distinct sites and an intermediate agrin-90 molecule and the C-terminal agrin-22 fragment are released (Reif et al, 2007). The agrin-90 cleavage product was detected in brain, kidney, and lung of wild-type mice but was absent in neurotrypsin-deficient animals. Similar results were obtained for agrin-22 except for lung.

In this work, the first quantitative profiling of agrin-22 in murine serum samples is presented. In order to confirm the neurotrypsin-dependent cleavage of agrin in non-neuronal tissues, I performed quantitative profiling by Western blot of murine sera from neurotrypsin-overexpressing, neurotrypsin-deficient as well as wild-type animals. With serum samples from neurotrypsin-deficient mice I wanted to test whether agrin is proteolytically processed by other proteases than neurotrypsin.

First, I took a comparative view on sera at P4 and P10, where the agrin-22 signal is present in well detectable amounts. Sera were diluted (1:10) and analyzed by Western blot in triplicates using antibody R139 against the agrin-22 fragment. Consequently, analyzes were performed volume-adjusted in order to identify intermediate changes related to the different subjects. Interestingly, significantly higher agrin-22 amounts were observed for the neurotrypsin-overexpressing mice at P4 compared to wild-type mice. This result clearly indicated a higher proteolytic activity due to the enhanced expression of neurotrypsin in transgenic mice. In fact, agrin-22 levels were much higher at P4 in neurotrypsin-overexpressing mice and in their wild-type littermates compared to the levels at P10. The difference in the amount of agrin-22 between both mouse groups as shown for P4 could not be observed at P10. The signal for agrin-22 was clearly absent in sera of homozygous neurotrypsin-deficient animals at both ages, P4 and P10. Enhanced proteolytic cleavage can be monitored in neurotrypsin-overexpressing mice at early stages of development, whereas no cleavage was observed in mice lacking neurotrypsin. The combined data indicates that agrin is exclusively processed by neurotrypsin in peripheral body tissues. The antibody used in this study is raised against the C-terminal domain of agrin enabling the detection of full-length agrin. Since no other proteolytic products in addition to agrin-22 have been detected, neurotrypsin`s cleavage of agrin at both sites ($\alpha$- and $\beta$-) is suggested to be highly specific. Thus, the level of agrin-22 can serve as a direct reporter for neurotrypsin`s proteolytic activity *in vivo*.

In transgenic mice, the activity of the Thy-1.2 promoter cassette declines to baseline after postnatal day 15 (P15). Therefore, quantitative profiling by Western blot of murine serum from P1 to P30 mice was undertaken in order to identify long-term activity changes of neurotrypsin`s proteolysis in transgenic, neurotrypsin-deficient as well as wild-type animals. I wanted to shed light on the changes that are temporally related to neurotrypsin`s activity during development in non-neuronal tissues. The amount of agrin-22 in murine serum of transgenic neurotrypsin-overexpressing mice and their wild-type littermates showed both a decrease following a similar age-dependent course. The highest agrin-22 level was detected at P1 and consistently declines until P30, where a faint band is still visible. In addition, I compared

signal intensities of agrin-22 between homo- and heterozygous neurotrypsin-deficient mice as well as their wild-type littermates at different ages. The signal for agrin-22 was clearly absent in all sera of homozygous animals, whereas in sera of their heterozygous and wild-type littermates signals for agrin-22 could be observed. The amount of cleavage product followed the same age-dependent pattern as already shown for the transgenic mouse line and their wild-type littermates. Together, the results are in perfect accordance with previously published data for mRNA expression and endogenous protein analyses for both, neurotrypsin and agrin, in non-neuronal tissues. In fact, it reinforces the concept that agrin-22 is more diffusible compared to agrin-90 and may pass tissues more easily to be accumulated in surrounding body fluids. In conclusion, the data supports the hypothesis that neurotrypsin and agrin may play an important role in the morphogenesis of connective tissues during development.

4.3 Quantification of agrin-22 z-transcripts by LC-MS/MS analysis – drawbacks and opportunities

Agrin-22 can serve as a marker for neurotrypsin`s proteolytic activity *in vivo* as shown in the previous section. The previously discussed, Western blot analyses were performed with 4-12% NuPAGE Bis-Tris gradient gels. Nonetheless, the four isoforms of agrin-22 appeared as one band at the molecular level of 22 kDa. Thus, differentiation of the four splice variants (z0, 8, 11, and 19) was not possible by Western blot. In addition, the antibody R139 used for immunoblot is raised against a common epitope in the C-terminal part of agrin-22 and thus cannot discriminate betwen the distinct splice variants.

Agrin-22 z+ transcripts are implemented in the accumulation of acetylcholine receptors (AChRs) at the neuromuscular junction, whereas the agrin z0 transcript did not show any activity (Ferns et al, 1992). Furthermore, the mRNA pattern of the four isoforms showed a regionally specific expression in the CNS. While neurons predominantly express various combinations of all transcripts, non-neuronal cells exclusively contain agrin z0 (O`Connor et al, 1994). The agrin z0 transcript comprises the highest percentage (> 40%) in the adult rat CNS followed by agrin z8 and 19 with 60%. Agrin z11 constitutes the lowest percentage (< 7%) of these transcripts. Differences in the expression in matters of brain region and amount of transcript, indicate a physiologically significant regulation of agrin`s activity. In contrast to the activity at the NMJ, all z-splice variants showed similar effects in rescuing the filopodial response in hippocampal neurons of neurotrypsin-deficient animals (Matsumoto-Miyai et al, 2009). Since there is no data available on the protein expression level of these isoforms, information which would be available after quantitative proteomics, could shed light on agrin`s role in the CNS. The identification of such low expressed proteins is still a challenge (Zhang, 2007) and this fact is even potentiated when it comes to quantification. Nonetheless, such low-abundant proteins are thought to be diagnostic markers. Hence, it was speculate that agrin-22 isoforms could serve as reporter for neurotrypsin-dependent proteolytic changes at synapses in the CNS.

4.3.1 Depletion and in-solution digestion are essential in sample preparation

Developing quantitative LC-MS methods is a complex task and involves many technical considerations: development time, number of samples, sample preparation, matrix composition, required sensitivity and accuracy, robustness and instrumentation. One way to enhance the availability and detection of the low-abundant agrin-22 isoforms is the creation of a depleted fraction before mass spectrometric analysis. On this purpose, I used techniques based on individual physico-chemical properties such as immuno-affinity, cation-exchange, ion-exchange and size-exclusion, trying to fractionate and deplete serum proteins and thereby enriching low-abundant proteins. Four commercialized depletion kits have been tested by applying either murine serum samples or recombinant agrin-22 according to the capacity of the column material. All depletion experiments were carried out at room temperature according to manufacturer`s instructions. The agrin-22 recovery was in all cases tested by SDS-PAGE and Western blot with antibody R139. However, it appeared that endogenous agrin-22 failed to elute in depleted serum fractions using four commercially available depletion kits. Agrin-22 was predominantly present in the eluates containing the high-abundant proteins, which suggested non-specific binding to either the column resin or the depleted bound proteins on the resin. For instance, it is likely that agrin-22 is accumulated by albumin. The biological force underlying this phenomenon could simply be the transport function that albumin exhibits in serum. By adding recombinant agrin-22, an inhibiting effect on the non-specific interaction of the endogenous cleavage product with the column material or high abundant serum proteins like albumin was observed. Further, three fractionation methods e.g. Microcon centrifugal filter devices (MWCO 30 kDa and 50 kDa), precipitation with ammonium sulfate, and gel filtration have been evaluated. Promising results were achieved by precipitation and size exclusion chromatography while the centrifugal filter devices displayed non-specific binding of agrin-22 to either the filter or proteins in the high-molecular weight fraction. Taken together, the test of seven different depletion methods suggested gel filtration as the most efficient technique to remove albumin as well as other high-molecular weight proteins from serum. In addition, the protein separation of murine serum by size exclusion chromatography enabled the isolation of agrin-22 in one of the low-molecular weight fractions. This was not possible with any other depletion techniques which were tested in this study. By removing high-abundant proteins, total protein load for further analysis can be increased, improving the likelihood of detecting and identifying low-abundant agrin-22.

The CSF has a low protein concentration (150–450 mg/ml) and a high salt concentration (4150 mmol/l). However, the concentration of albumin (60% of the total CSF protein) and immunoglobulin is extremely high in the CSF (Hammack et al, 2003). The preparation of human CSF samples required a different protocol. The test of the depletion methods from the previously described sample preparation of murine serum was not applicable because of the low sample volume (50-100 µl) provided by the clinics. Additionally, the high salt concentration in CSF requires an additional desalting step. Results from a study of Zhang suggested dialysis in order to assure optimal protein recovery (Zhang, 2007). Depletion was achieved by fractionation with graduated addition of acetonitrile (ACN). In order to test whether this protocol would be an appropriate method for serum, I similarly performed the preparation for both sample systems. The obtained pellets (P1 and P2) and the supernatant (S2) were analyzed by Western blot analysis. As expected, higher protein amounts were detected in murine serum samples compared to the human CSF. In human CSF, agrin-22 was isolated in the low-molecular weight fraction e.g. the second supernatant (S2). In contrast, agrin-22 was isolated in murine serum samples in the first pellet (P1) which represents the fraction of high-molecular weight proteins. Taken together, the result clearly indicates the strong influence on the isolation of the

protein of interest which is induced by the different protein composition in these two sample systems. Serum and CSF samples had to be differently prepared in order to deplete the protein composition and isolate agrin-22.

In mass spectrometry-based quantification, the protein amount is usually not directly measured, but is rather inferred from the experimentally determined amount of peptides rendered by in-solution or in-gel digestion of the target protein (Havlis & Shevchenko, 2004). Since chemical and physical properties of proteins are diverse, the recovery of peptides might vary considerably. It is documented that significantly more proteins can be identified in samples separated by SDS-PAGE (ten fractions) than those separated by organic precipitation (three fractions) (Xu et al, 2006). Nonetheless, digestion of proteins embedded into a polyacrylamide matrix affects the recovery of peptides, and therefore, the results may strongly depend on which peptides were selected as a reference for the quantification. The efficiency of an in-gel digestion is protein-dependent and comprises strong variations for different peptides that originate from the same protein. It is concluded that using in-gel digestion strongly affects the accuracy of the absolute quantification, and priority should be given to technologies that enable direct quantification in complex in-solution protein mixtures (Peng & Gygi, 2001). Particularly as digestion of proteins in-solution enabled their robust quantification. The reduction in sample processing however could interfere with the detection of low-abundant proteins such agrin-22 in some way that suppresses its signal intensity. However, intensive, multi-step sample preparation is problematic concerning the reproducibility of the analyses. As it was aimed at quantifying agrin-22 z-transcript levels, the most reproducible sample processing was preferred. Therefore, in-solution digestion was chosen, as it is an adequate tool for sample preparation in a quantization assay. The risk of high variations in peptide recovery is limited.

4.3.2 Targeted mass spectrometry - evaluating optimized parameters

Mass spectrometry-based targeted protein quantification provides a powerful tool to systematically assess quantitative differences in protein amounts of individual samples. The recent advance in biomedical and clinical research is highlighted by an emerging number of reports on proteomics in trauma patients, diagnosis of ovarian cancer, biomarkers in psychiatry, proteomics in cardiovascular surgery, and biomarker discovery in the CSF for neurodegenerative diseases (Alpantaki et al, 2007; Ardenaki et al, 2002; Hunnerkopf et al, 2007; Matt et al, 2007; Zhang et al, 2005). After comparison of the proteome of a diseased sample versus normal, novel protein candidates have been associated with the pathogenesis of a disease. Further characterization and validation of these putative biomarkers is extremely sophisticated due to the huge complexity of biological systems and the heterogeneity of human samples (Pan et al, 2009). This is reflected by the remarkably small number of validated biomarkers (Aebersold et al, 2005; Anderson & Anderson, 2002). The major method used for targeted protein quantification has been the enzyme-linked immunosorbent assay (ELISA). Nonetheless, the ELISA approach is limited by the lack of antibodies with high specificity for most novel biomarker candidates. The development and implementation of mass spectrometry-based targeted proteomics for clinical applications offers an alternative to circumvent these limitations. A robust and highly sensitive assay using mass spectrometry is provided by moving from full scan spectrum monitoring to single ion monitoring (SIM) or selected reaction monitoring (SRM). To gain maximum sensitivity, SRM allows for the selection of a single mass ion to quantify and further filter via a distinct fragment ion to discriminate it from other components that share the initial mass ion. It is particularly suited to the analysis of complex

matrices. Therefore, the confirmation of a protein in human CSF using an SRM approach should overcome the huge dynamic range of CSF. The SRM approach offers higher sensitivity when compared to normal proteomics profiling experiments.

I was using in-solution digestion mixtures of the four recombinant agrin-22 z-transcripts and four synthetic specific tryptic peptides (proteotypic peptides, PTPs) to develop optimized parameter settings. Synthetic PTPs are of high need in SRM quantification assays when the PTPs are fixed like in this particular case to distinguish between splice variants of a single protein of interest. If these PTPs do not show up under standard conditions, which are automatically defined by the software, additional experiments with synthetic PTPs are indispensable in order to set up all parameters for satisfying performance and spectra. The performance is linked to reproducible spectra as well as to correct quantification values for targeted PTPs. After the first measurements with the in-solution digestion mixtures of the four recombinant agrin-22 isoforms, a dramatic difference in the relative abundance between the PTPs was recognized. The following sections describe the systematic study which was performed to unravel the set of problems.

The unit resolution setting enhances PTP detection

Each mass analyzer has some variation in its capabilities because of the individual design. The performance of a mass analyzer can be defined by the characteristics accuracy, resolution and mass range and scan speed. The ability of a mass analyzer to accurately measure m/z values is a direct funtion of the resoltuion of the instrument. The reoslution (also termed resolving power) is the ability of the mass analyzer to distinguish between two m/z falues and can be determined by the measurement of m/z and the full with at half maixmum (FWHM). Higher resolution offers the separation of individual isotopes of an ion. Additionally, enhanced resolution is leading to more narrow peaks, thus allows a more accurate determination of the elution time. These factors directly influence the spetrum quality in the SRM approach. I wanted to test the performance of the instrument in relation to the resolution of the measurement. The impact of the resolution settings for the first quadrupole (Q1) was especially critical for the agrin-22 z19 variant. The detection failed for two fragment ions in the enhanced resolution mode (Q1 = 0.1) whereas unit resolution (Q1 = 0.7) enabled detection of all four fragment ions. Therefore, I preferred a lower setting for the resolution and accepted the loss in sensitivity which is associated therewith.

The in-solution digestion is sufficient for recombinant agrin-22 z-transcripts

I evaluated the efficiency of the in-solution trypsin digestion of the recombinant agrin-22 isoforms and the ionization of the PTPs by SIM on the triple quadrupole instrument. The spectra were recorded manually during direct injection of the digestion mixtures. As ionization devices and experimental conditions influence the charge state, I chose a direct infusion method with 50% acetonitrile (ACN) for sample introduction to mimic the amount of eluent needed for C18 elution of the PTPs when using the LC-MS approach. Furthermore, all SIM experiments were performed on the triple quadrupole instrument where the SRM was carried out as well. This secures that no additional effect caused by a different ionization source influences the dominant charge state of the precursor. All PTPs could be detected with the same relative abundance, indicating that the digestion was sufficient. Main differences between the PTPs were observed

in the charge state. The charge distribution is based on the amino acid sequence and showed the expected pattern. The SIM spectra provided clear evidence that all PTPs are present in similar concentrations and ionize with comparable sufficiency. Therefore, the differences in relative abundance have to originate from other parameters in the workflow.

The poor fragmentation of agrin-22 z19 leads to signal loss

A limitation of current proteomics quantification approaches for SRM analyses is the theoretically selected precursor and product ions and corresponding collision energy (CE) used for the fragmentation. This process is fully automated by the software which is used for setting up the list of transitions. It leads to a theoretically ideal selection of transitions. In the case of the current study, this selection lead to false annotations of precursor ion charge states as only doubly charged ions are selected as usual species. Besides, the chosen CE used for the fragmentation process showed not to produce the amount of fragmentation required for satisfactory precursor ion spectrums. Targeting the dominant precursor charge state is essential for satisfying product ion spectra. Furthermore, the efficiency of fragmentation is linked to the quality of the observed product ion spectra. Therefore, I evaluated whether it is possible to assign any differences between the agrin isoforms. Fragmentation of agrin-22 z0, 8, and 11 was sufficient, but agrin-22 z19 showed a dramatic loss in the ability of fragmentation. I manually defined the ideal collision energy to optimize fragmentation, but the fragmentation pattern was still inadequate. This is one major reason for the pronounced decrease of relative abundance for the product ions of agrin-22 z19. Furthermore, one single peptide MS/MS measurement is used for protein quantification in the SRM approach, therefore this problem is exacerbated. As the ability of breaking peptide bonds is a matter of the amino acid composition, there is no possibility to compensate this effect.

Higher amount of acetonitrile enhance the elution of all PTPs

Flow injection experiments at different ACN concentrations (5, 20, and 50%) confirmed a high non-specific affinity of the z+ transcripts to tubings and fittings in the chromatographic system. While the non-specific interaction existed at 5 and 20% ACN, the interaction was conspicuously inhibited using a high ACN concentration of 50%. Additionally, the *in silico* calculated retention time index for all agrin-22 splice variants indicated that high ACN concentration is a precondition for the z+ transcripts. In addition, the Bull Breese index was *in silico* calculated for all four splice variants with the prospector program and suggests medium hydrophobicity due to the surface tension of the amino acid sequence.

I wanted to implement these findings in order to optimize the analytical conditions for the C18 separation of the PTPs. There are two major possibilities to enhance polar/ionic interaction on RP-phases to enhance the peptide recovery: optimization of the gradient and the column temperature. Recently, it was suggested by several reports that elevated temperature is indispensable especially for hydrophobic proteins and peptides (Martosella et al, 2006; Blackler et al, 2008). I was using four individual gradients to evaluate the possibility of decreasing the retardation of the agrin-22 PTPs on the reversed-phase C18 resin and to prevent non-specific binding to the surface in the chromatographic system. Therefore, starting conditions of the gradient were increased from 5 to 10, 20 and 40% ACN, respectively. The recovery of all agrin-22 z-transcripts was clearly enhanced by the application of higher ACN

concentrations directly at the beginning of the gradient. The four transitions of the PTP for the agrin-22 transcript z0 showed improved detection using the 10% gradient compared to their relative abundance at the 5% gradient and only a slight enhancement was detected applying the 20% gradient. Therefore, recovery of agrin-22 z0 is suggested to be sufficient even at lower ACN concentrations. The transitions for the agrin-22 z8 transcript showed strong enhancement in their recovery only on the 20 % gradient and the same was true for the agrin-22 z11 transcript. In contrast, the transitions of the agrin-22 z19 transcript were not detectable at any gradient below 20%. Two transitions were detected applying the 20 % gradient. Their relative abundance showed strong improvement at the 40% gradient. However, the analysis of the agrin-22 z19 transitions was not reproducible in three replicates. In parallel, application of the 40% gradient was leading to the loss of retardation for all other agrin-22 transcripts as they eluted with the solvent directly after the gradient developed. Therefore, the 20% gradient is suggested as ideal condition for the optimized elution of all PTPs. The results indicated that the selection of a higher ACN proportion at the beginning of the gradient was essential for the detection of the agrin-22 PTPs. In parallel, sample carry over between the measurements was inhibited by an 10% isopropanol wash step of the column between all samples.

Elevated column temperature has no effect on PTP elution

Elevated temperature can be used to reduce the viscosity as it enhances solute diffusion which leads to highly narrow and symmetrical peaks (Boyes et al, 1993). I measured the effect on the retention time and peptide recovery using the standard gradient and heating the micro C18 column to 40, 50, and 60°C, respectively. The measurements for a fetuin digest, which I chose as representative standard sample system, displayed irreducible retention times for 40 and 50°C, but no specific signal of any tryptic peptide of fetuin could be observed at 60°C. Furthermore, the synthetic PTPs of agrin-22 have been detected exclusively at 40°C. For both sample systems, a high number of unspecific signals with a high relative abundance were observed applying 60°C. The appearance of unspecific signals were ascribed either to the instability of the electrospray performance or to the column material. Poor spray performance was especially observed at 50°C and with much higher impact at 60°C. As the flow rate was kept constant throughout all runs, a decrease in back pressure with increasing temperature was observed. I wanted to compare the retention times between the runs and therefore accepted the poor electrospray performance. All unspecific signals during the whole measurement could be assigned to one [M+H]+ species with a m/z-value of 512 which is by definition not a tryptic peptide. It could be possibly an indication for the degradation of the C18 column resin.

The complex protein composition increases retention

Matrix effects cause a strong variation in the response from the analyte. In particular, ion suppression from interfering compounds and various cross talk effects can have a dramatic effect on the precision of the method. Hence, I wanted to elucidate the effect on the recovery of the agrin-22 PTPs based on the complex protein matrix in human CSF. The comparison of SRM spectra of the agrin-22 z0 PTP which was spiked into two differentially diluted CSF samples revealed a strong difference in the retention time between both solutions. The retention time of agrin-22 z0 transitions in the 1:10 diluted CSF sample was increased by about ten minutes compared to the retention in the 1:100 diluted CSF. Hence, it was claimed that there is indeed a strong matrix effect in human CSF samples. A sample dilution of 1:100 would possibly decrease

the detection of agrin-22 z-isoforms. On the purpose to indentify the minimal dilution needed to get rid of the matrix effect, I analyzed 1:10. 1:20. 1:30, and 1:40 dilutions of CSF. In addition, I included the detection of the highly abundant tryptic peptide TEATQGLVLWSGK which is located in agrin-22 and could provide quantitative information about the overall agrin-22 level. Based on the quantitative data from agrin-22 z0 and the TEATQGLVLWSGK peptide, it would be possible to calculate the amount of the less accessible agrin-22 z+ isoforms. Additionally, the analyses offered the alternative to evaluate the matrix effect for a standard tryptic peptide which showed a standard elution profile between 10-30% ACN on a reversed-phase C18 material in previous experiments. Measurements for both tryptic peptides clearly indicated the strong influence of the CSF matrix on retention and relative abundance. In the case of agrin-22 z0, the CSF dilution of 1:40 showed a shift back to the same retention time as observed for the pure digestion mixture of recombinant agrin-22 z0. Furthermore, I measured the 1:30 diluted human CSF sample with LC-ICR-FT-MS and analyzed the resulting spectra with the Mascot database search algorithm. The identification of agrin-22 z0 as well as the highly abundant tryptic peptide TEATQGLVLWSGK was found to be impossible.

Assuming that the method had all the analytical power which was needed, it was still not possible to run analyses with reproducible results. The absence of agrin-22 z0, 8, 11, and 19 was found to be due to several parameters influencing the SRM efficiency: (i) non-specific binding of all PTPs to the chromatographic system and the reversed-phase C18 resin which increases referring to the molecular weight, (ii) poor fragmentation of agrin-22 z19, (iii) strong matrix effect from protein composition of human CSF. Taken together, the quantitative analyses of agrin-22 as well as of the z-transcripts have been found to be impossible with the established mass spectrometric method.

4.4 Neurotrypsin`s activity can be monitored in human CSF

The emerging interest in extracellular proteolysis in the nervous system was originated by a huge number of reports implementing this process into the regulation of neurogenesis, cell migration, axonal growth, and synapse elimination. Hence, it is described to be important for adaptive changes in signal transmission. The expression pattern of neurotrypsin in the adult murine brain is claimed to be highly intriguing in a distinct subset of neurons (Gschwend et al, 1997). *In situ* hybridization showed elevated labeling in the cerebral cortex, the hippocampus, and the amygdala, indicating that neurotrypsin may have a role in learning and memory processes during crucial stages of nervous system development. Agrin, the so far unique substrate for neurotrypsin, is expressed in neuronal tissues especially during development and throughout adulthood. Recent findings showed that the activity-dependent formation of dendritic filopodia was abolished in hippocampal neurons of neurotrypsin-deficient mice (Matsumoto-Miyai et al, 2009). The filopodial response could be fully rescued by exogenous application of agrin-22. It implicates the neurotrypsin-dependent cleavage of agrin as crucial step in activity-dependent reorganization of synaptic circuits in the brain. Physiologically, the

amount of agrin-22 in human CSF samples can provide insights into neurotrypsin`s activity and agrin`s role in the developing brain. I performed quantitative Western blots for agrin-22 using antibody R139 for three independent subject groups. To obtain inter-subject differences, all analyses were performed volume-adjusted.

4.4.1 Neurotrypsin`s activity is modulated throughout development

First, I evaluated age-dependent changes of neurotrypsin`s proteolytic activity in a large sample set of 84 independent subjects at the age of 2 months until 35 years. As the CSF flow is initiated earliest in the first days after birth and accumulation of proteins is therefore not reliable, I excluded samples from subjects younger than 2 months from the study. Information about a possible status of disease was not provided by the clinic, thus the obtained amounts of the cleavage product agrin-22 were defined as age-associated. The results suggested high evidence that agrin-22 can be separated and quantified precisely by the applied method. The agrin-22 level was clearly elevated in samples from 2 months old subjects. The signal intensity follows a conspicuously decrease at the age of 6 months and therefore highly correlates with the neurotrypsin-dependent cleavage pattern in murine brain tissue during early development (Reif et al, 2007). The study demonstrates that agrin-22 levels decline with aging and ongoing development of the CNS. However, it is most likely that neurotrypsin`s proteolytic activity persists at a basal level throughout adulthood. The difference between samples from 10 year-old until 35 year-old subjects was slight. In addition, the presence of several cases can be demostrated where agrin-22 gains high levels independent of the subject's age. It is most likely that these specific cases represent the upregulation of either neurotrypsin`s activity or of the expression of both proteins due to individual changes in the nervous system. Whether these changes are caused upon physiological- or diseased-based processes is currently not understood.

4.4.2 Neurotrypsin`s activity is moderately increased in Epilepsy

Short-term memory is defined as a process in which information is evaluated after a few seconds, whereas in long-term memory processes, the information is stored for more than a few minutes and can be exactly retrieved after the process of consolidation (Squire et al, 1984). Furthermore, it is thought that this process is dependent on reorganizations at the neural systems level which last for weeks, months or even years (Squire and Alvarez, 1995). The standard memory tests are mainly based on information retention after a delay of 30 minutes. Thus, little is known about long-term memory (Butler and Zeman, 2008). Patients with epilepsy report very often on memory dysfunctions, especially subjects with adult-onset temporal lobe epilepsy (TLE) where memory-related brain structures such as the hippocampus are affected by seizure activity (Hermann et al, 1997). It is documented that epileptic activity in temporal lobe and hippocampus is likely to disrupt simultaneous activity in neocortical cell assemblies (Blake et al, 2000). The process of consolidation in long-term memory is especially impaired in patients with TLE (Martin et al, 1991). These patients had problems to recall verbal memory after a delay of 24 hours. No differences could be observed after 30 minutes when compared to controls. Blake and colleagues could show that there is additional evidence of accelerated long-term forgetting in case of verbal material in patients with TLE after very long-term retention intervals of 8 weeks (Blake et al, 2000). The short-term and episodic memory performance was indistinguishable from the same group of patients and controls after 30

minutes delay. These findings indicate defects in selective memory in subjects with TLE. Butler and Zeman hypothesize several contributory mechanisms to accelerated long-term forgetting (ALF) in some patients with epilepsy: (i) clinical or subclinical seizure activity, (ii) structural or other underlying brain pathology, (iii) an adverse effect of anticonvulsant medication, or (iv) psychological mechanisms and showed that (i) as well as (ii) are the most likely cases (Butler and Zeman, 2008). The expression of agrin and neurotrypsin is high in the CA1 region of the hippocampus and the interaction of both molecules is hypothesized to play an important role in the process of learning and memory.

Recently it was shown in cultured hippocampal neurons that the release of neurotrypsin into the extracellular synaptic space is activity-dependent (Frischknecht et al, 2008). I speculated about following situation: elevated agrin-22 concentrations in the CSF of epilepsy patients may result during high neuronal activity and reflect one significant symptom of this disease. Another reason for selecting this neuronal disorder was due to reports confirming impairment of memory in epilepsy patients. To address these questions, I performed a comparative study of human CSF samples including 17 epilepsy patients, 19 healthy controls as well as an age-associated correlation with the sample set from the previous study on age-dependent agrin-22 regulation. Latter samples were particularly included since the provided healthy control samples were grouped towards higher age in comparison to the epilepsy cases. Concerning the age-dependent regulation of neurotrypsin's activity, the correlation of signal intensities between the first two groups caused deceptive high levels of agrin-22 in subjects with epilepsy. However, the agrin-22 amount was slightly increased in an enhanced number of epilepsy patients compared to the age-matched samples. It was possible to directly compare a set of four independent epilepsy and age-related samples of exactly the same age. Statistical significancy could not be assessed due to the low number of samples matching the same age. However, preliminary results assume a tendency for enhanced neurotrypsin activity in subjects with epilepsy but do not allow for a significant distinction between the three groups in this study. A larger number of samples for detailed future analysis will therefore be needed. In addition, detailed information about the type of epilepsy and the onset of the disease will be an important means to obtain meaningful insights into neurotrypsin`s activity in the brain of epilepsy patients.

4.4.3 The agrin-22 amount is slightly decreased in Alzheimer`s disease

It was reported that heparan sulfate proteoglycans (HSPG) levels are increased in brains from Alzheimer's disease (AD) patients (Snow & Wight, 1989). Highest agrin expression has been detected in severely affected brain regions such as hippocampus and amygdala (Boew & Fallon, 1995; Braak& Braak, 1991). Furthermore, it was shown that agrin binds β-amyloid peptide Aβ (1-40) in its fibrillar state via a mechanism involving the heparan sulfate glycosaminoglycan chains of agrin (Cotman et al, 2000). It is suggested that agrin is able to accelerate Aβ fibril formation and to protect Aβ(1-40) from proteolysis *in vitro*. Therefore, it was concluded that agrin may be an important factor in the progression of Aβ peptide aggregation and in Aβ persistence in the brain of AD patients. Additionally, there are emerging speculations about the idea that dementia may be a cause of epilepsy as seizures and dementia describe a concurrently manner (Abou-Khalil, 2010). Recently, it has been shown in a small number of patients with a progressive form of memory dysfunction that there is not necessarily a loss in brain volume which is typically provoked by AD (Hogh et al, 2002). Those patients recovered to normal memory performance after anti-epileptic medication. Several cases of memory impairment

occurred in patients with epilepsy and encourage the hypothesis of an epilepsy-derived form of AD (Ito et al, 2009).

I performed quantitative Western blot analyses of CSF from 10 AD patients versus 10 healthy control subjects. A slight decrease of the agrin-22 level was shown in the AD parents compared to the healthy controls. This may reflect a lower proteolytic activity of neurotrypsin which could be a result of the perturbed neuronal activity in AD. In parallel, it may be a possible effect of the suggested aggregation of agrin with the Aβ peptide. Therefore, agrin`s accessibility to be cleaved by neurotrypsin might be hindered. Statistical analysis could not confirm a significant difference between AD patients and healthy controls for agrin-22 levels. Taken together, the result render it difficult to conclude whether neurotrypsin`s activity is reduced in AD. In addition, the low number of samples and the missing information about the type of AD and the age of the patients does not allow for a clear statement. Hence, it will be a necessary requirement for detailed future analysis to obtain a larger number of grouped samples to obtain meaningful insights into neurotrypsin`s activity in the brain of AD patients.

4.5 Monitoring of calsyntenin-1 ectodomain shedding in human CSF

The N-terminus of calsyntenin-1 is released into the extracellular space after ξ-cleavage by ADAM10 and ADAM17 (Hata et al, 2010). Thus it exhibits strikingly similar features as the prominent transmembrane, amyloid precursor protein (APP), whose misregulation in proteolytic processing is thought to contribute to Alzheimer`s disease. Calsyntenin-1 is mainly expressed in all CNS neurons, whereas expression levels of Calsyntenin-2 and -3 vary between neuronal subpopulations (Hintsch et al, 2002). The pyramidal neurons in the hippocampal CA1 region reveal high expression of only Calsyntenin-1. In contrast, part of the Purkinje cells in the cerebellum express calsyntenin-2 and -3, but lack in calsyntenin-1. The distinct pattern for each of the members suggests specific functions in distinct neuronal areas.

4.5.1 The ectodomain of calsyntenin-1 is accumulated in human CSF

I wanted to shed light into the proteolytic processing of the calsyntenin family and identify the proteolytic fragments present in the human CSF. Therefore, I performed data-dependent FT-ICR analysis for all tryptic peptides of calsyntenin-1, -2, and -3 covering the m/z range 300 – 1.600 and Mascot database search. Data analysis revealed highly reliable protein identification for calsyntenin-1. The identified eleven tryptic peptides are restricted to the proteolytically released N-terminal part of calsyntenin-1 and could be identified in three independent human CSF samples. The impossibility to identify calsyntenin-2 and -3 with FT-ICR was assumedly to their remarkably low expression level in the brain. Hence, the sensitivity of the mass spectrometric method used in this measure is not sufficient for their detection. The presence of calsyntenin-1 in human CSF was further confirmed by targeted mass spectrometry. For

this, a selected reaction monitoring (SRM) experiment was designed using the highly abundant proteotypic peptides and their respective fragments identified by Mascot data. I chose the PTPs IPDGVVSVSPK (549 m/z) and EGLDLQVLEDSGRGVQIQ (715 m/z) both representing the N-terminal ectodomain of calsyntenin-1. It was possible to detect all four transitions in four independent human CSF samples with considerable response. Concerning the significant result of the SRM measure, it is suggested that calsyntenin-1 is the predominant member present in human CSF.

4.5.2 Proteolytic processing of calsyntenin-1 is consistent throughout aging

Furthermore, I wanted to firstly investigate whether there is an age-dependent regulation of the proteolytic processing of calsyntenin-1. Secondly, I wanted to evaluate whether it is possible to monitor the ectodomain shedding in human CSF by quantitative Western blot.

The distribution of calsyntenin-1 underlies a basal level. Comparing the protein abundance between the ages of 2 months until 35 years, the differences are very subtle. Interestingly, there are several CSF samples which show a strong accumulation of calsyntenin-1 irrespective of the age. This finding is giving evidence of the possibility to monitor a potential misregulation of calsyntenin-1 processing, which is most likely a consequence of pathological changes in the nervous system in human CSF.

4.5.3 Unaltered ectodomain shedding of calsyntenin-1 in Alzheimer`s disease

Calsyntenins and APP undergo a similar coordinated proteolytic processing (Araki et al, 2003). APP and the cytoplasmic X11L/Mint2 protein form a tripartite complex with calsyntenin-1. Therefore it was suggested that formation of this complex stabilizes intracellular APP metabolism and mediates suppression of the Aβ generation. Cleavage of calsyntenin-1 and APP at their primary cleavage sites (ξ and α or β, respectively) is enabled when X11L dissociates from the tripartite complex. Subsequent secondary intramembranous γ-secretase-mediated cleavage at the γ/ε-site results in the formation of intracellular fragments of APP (AICD) and calsyntenin-1 (CICD). The cytosolic AICD cleavage product is thought to bind the nucleo-cytoplasmic shuttling protein Fe65 and the histone acetyltransferase Tip60 and forms a transcriptionally active complex (Araki et al, 2004). Similarly, the intracellular fragment CICD can associate with Fe65, and it was suggested that this process suppresses the Fe65-dependent gene transactivation activity of APP, probably because CICD competes with the AICD for binding to Fe65. In addition, deficiencies in the X11L-mediated interaction and imbalance in the metabolism of calsyntenin-1 and APP may be related to neuronal disorders like AD.

Quantitative Western blots of human CSF samples from 10 AD versus 10 healthy control subjects (HCS) were performed. The average value of ectodomain shedding of calsyntenin-1 in AD patients was marginally increased compared to the HCS. Statistical analyses revealed no significant changes between both groups. Because of the low number of samples available for this study, it is not possible to give a definite conclusion on whether calsyntenin-1 processing in AD is diverging from HCS. The requirement for detailed future analysis is to obtain a larger number of grouped samples which would provide closer insights into calsyntenin-1 ectodomain shedding of AD patients.

4.5.4 Calsyntenin-1 ectodomain shedding is stable in Epilepsy patients

Recently, it was shown in our group that proteolytic processing of calsyntenin-1 and APP is dependent on neuronal activity (unpublished results). The chemical LTP stimulation was performed in whole hippocampi of young mice. Both potassium-based TEA and non-potassium-based PFR chemical LTP stimulation protocols increase ectodomain shedding of the two molecules, whereas TEA elicits a stronger LTP-inducing effect than PFR. It might well be, that there is a connection of neuronal activity and proteolytic processing which could contribute to a better understanding of pathological mechanisms leading to neuronal disorders.

CSF samples from 17 epilepsy patients and 19 healthy control subjects were analyzed by quantitative Western blot. In addition, I included age-associated samples from the previously described study. Ectodomain shedding was not changed by a conspicuous amount in epilepsy patients, neither compared to healthy control subjects nor to age-associated controls. The small-scale quantitative data obtained in this study gives useful information about tendencies of proteolytic product accumulation in the CSF as a cause of neuronal disorders. But it appears difficult to decisively answer the question whether neurotrypsin`s activity or calsyntenin-1 ectodomain shedding are considerably involved into or a cause of the processes of AD and epilepsy. A large sample set would be required for future analyses to monitor the accumulation of these proteolytic fragments. In addition, detailed information about the type of epilepsy and the onset of the disease will be an important means to shed light on the proteolytic processing of calsyntenin-1.

5 Materials and Methods

5.1 Cell biology

5.1.1 HEK Ebna cell cultivation

Optimal growth of HEK Ebna cells was achieved with a cell density between 2x 10^5 – 3x 10^6 cells/ml in Ex-cell 293 medium. Usually, cells were splitted to a concentration of 2x 10^5 cells/ml twice a week by diluting the cells with fresh media (dilution ~1:10). Cells were cultivated in Erlenmeyer flasks (optimal flask size ~5x of culture volume) and counted to determine accurate dilution.

5.1.2 Transient DNA transfection with polyethylenimin

The production of the recombinant proteins (agrin-22 z0, 8, 11, and 19) was performed using transient DNA transfection with non-viral gene delivery agent polyethylenimin (PEI) as DNA carrier (Baldi, 2005). PEI stock solution was prepared at 1 mg/ml, its pH adjusted to 7 with HCl and stored at -80°C. Cells were grown to a density of 1 x 10^6 – 3.5 x 10^6 cells/ml at the day of transfection, sedimented at 500xg for 30 min and adjusted to 1x 10^6 cells/ml in 500 ml RPMI buffered with 25 mM HEPES. Transfection mixture was prepared 10 minutes prior to transfection by mixing solutions A and B (A: 1.25 mg DNA in 25 ml 150 mM NaCl; B: 3.75 ml PEI stock solution in 25 ml 150 mM NaCl). Cells were diluted 1:1 with Ex-cell 293 medium 5 h after transfection, and incubated for three days at 37°C and 10% CO_2 at a constant spinning rate of 75 rpm.

5.1.3 Protein Purification

HEK Ebna cell supernatant (2l) was dialyzed 12 hours at 4°C with 20 mM Tris-HCl (pH 8.5) containing 400 mM NaCl. The buffer was exchanged three times to allow for complete replacement. The dialyzed supernatant was clarified and concentrated to a volume of 200 ml using a tangential flow filtration device using a Pellicon XL membrane (MWCO 10 kDa, Filtration area 50 cm^2; Millipore, Switzerland)

5.1.4 Immobilized metal-ion affinity chromatography

The concentrated cell supernatant (200 ml) with recombinant histidine-tagged protein was affinity-purified by HIS-Select HF nickel-affinity gel (Sigma), which enables the purification of histidine-tagged proteins due to hydrophilic nickel chelate-linkage. After wash, histidine-tagged proteins were eluted elution buffer (Tris buffered saline: 20 mM Tris-HCl, pH 8 containing 400 mM NaCl, 250 mM imidazole) by a gradient from 8% to 100% in 10 column volumes. The presence of the protein was confirmed by silver-stained SDS PAGE and Western blot with antibody R139. Elution fractions were concentrated to 1 ml by centrifugal filter devices (Amicon Ultra-15, MWCO 5.000; Millipore, Switzerland) by centrifugation at 3.500 rpm for 30 minutes. The concentrate was further desalted with a NAP-5 column (GE Healthcare, Zurich, Switzerland) by elution with 500 ml buffer (20 mM MOPS, 100 mM NaCl, pH 7.5).

5.2 Generation of neurotrypsin-specific mouse lines

In this study, we were using a neurotrypsin transgenic mouse line overexpressing neurotrypsin (Muslik 533). Expression of neurotrypsin in this line is controlled by the brain-specific Thy-1.2 expression cassette. It drives strong constitutive expression of the transgene specifically in neurons (Caroni, 1997). Transgenic expression starts around postnatal day 6 (P6) to P10, at a time when it can influence activity-dependent rearrangements of synaptic connections and neuron-glia interactions during the late phase of nervous system development. The Thy-1.2 activity peaks at P12 and remains relatively low throughout adulthood (Radrizzani et al., 1995). Furthermore, neurotrypsin knock-out (NT-KO) mice were used to demonstrate that proteolysis of agrin and thus the generation of its fragments is dependent on neurotrypsin. The animals were tested for the presence of the transgene or the deficiency of neurotrypsin by PCR genotyping using specific primers.

5.2.1 Polymerase Chain Reaction (PCR) - PCR genotyping

Genomic DNA was extracted with alkaline lysis from tail biopsies of offspring from hNT overexpressing mice crossed with wild-type Black/6 mice. 300 µl alkaline lysis reagent (25 mM NaOH; 0.2 mM EDTA, pH 12.0) were added to tail biopsies and lysed for 45 min at 96°C. To stop the reaction, 300 µl neutralizing reagent (400 mM Tris-HCl, pH 5.0) were added. 1 µl of cleared extraction mixture was used for 20 µl reaction mix. For all PCR reactions, the following reaction mix was prepared: 1x Buffer, 0.25 mM dNTPs, 1.5 mM $MgCl_2$ and 0.1 µl Taq-Polymerase (5 U/µl; Applied Biosystems), 0.5 µM forward primer and 0.5 µM reverse primer. The primer sequences and the PCR program for each mouse line are indicated below (for all but NTKO TAG was used as a positive control for PCR amplification, PCR products of NTKOF01 and NTKOR02 indicated NTKO and of NTKOF01 and NTKOR03 indicated wild-type alleles):

Muslik 533

hNTSIIfor 5’-GCAATGTGCCAGATTCAGCAG-3’

Thy1back 5’-CCCATGTTCTGAGATATTGGAAG-3’

TAG83for 5’-GGAGGAGAGAGACCCCGTGAAA-3’

TAG82back 5’-ACACGAAGTGACGCCCAATCCGT-3’

PCR program: 1x (3’, 95°C), 40x (45’’, 95°C; 45’’ 63°C; 60’’, 72°C), 1x (5’ 72°C)

NT-KO

NTKOF01 5’-CAGAGCTCCTGGCGCTCATC-3’

NTKOR02 5’-GGAAGACAATAGCAGGCATGCTG-3’

NTKOR03 5’-CTCGCAGCTCAGCCCAACTG-3’

PCR program: 1x (3’, 95°C), 40x (45’’, 95°C; 45’’ 61°C; 60’’, 72°C), 1x (5’ 72°C)

5.3 Body fluids for biomarker discovery

5.3.1 Murine serum

Blood samples were taken from transgenic neurotrypsin-deficient (NT-KO), neurotrypsin-overexpressing mice (Muslik 533) and their wild-type littermates at different age from postnatal day 1 (P1) to P30. The reference sample for quantification was pooled from eight to twelve NMRI wild-type mice at embryonic day 18 (E18). All blood samples were transformed into micro-collection tubes (Microtainer, Becton Dickinson AG, Allschwil, Switzerland) with serum separator additive, left for 30 minutes at room temperature until coagulation was completed and centrifuged at 12.000x g for 15 minutes. The obtained serum includes all proteins not used in blood clotting, electrolytes, antibodies, antigens, hormones, and any exogenous substances (e.g., drugs and microorganisms). All serum samples were aliquoted and stored in Eppendorf tubes at –20°C until analysis, diluted 1:10 in PBS buffer and analyzed volume-adjusted. For the quantification by Western Blot analysis, always 1 µl serum was diluted 1:10 in PBS buffer. To determine the proteolytic neurotrypsin activity, the b-cleavage fragment agrin-22 was quantified in serum. Signal intensity for agrin-22 was observed to be strongest at the age E18, therefore the pooled serum serves as a reproducible and reliable reference.

5.3.2 Human CSF

For the screening of agrin-22 as a reporter for neurotrypsin activity *in vivo*, we obtained human cerebrospinal fluid (CSF) samples from several hospitals in Zürich, Switzerland. All CSF samples were isolated by lumbar puncture according to a standard procedure, transferred into low-binding Eppendorf tubes and stored at –80°C until analysis. All samples were loaded volume-adjusted (30 µl) onto a 4-12% SDS PAGE gel. The quantification by Western blot analysis was achieved by antibody R139 (4^{th} boost) against agrin-22 and antibody R131 (3^{rd} boost) against calsyntenin-1.

Age-related samples

81 CSF samples at different age from 2 months (2M) to 35 years (35Y) without further information about the status of any disease were obtained from the children's hospital Zürich.

Alzheimer`s disease samples

We received 10 CSF samples from Alzheimer`s disease (AD) patients and 10 CSF samples from healthy control subjects (HCS). The HCS subjects were negatively tested for AD according to the standard clinical procedure. The samples were provided by the clinic of geriatric psychiatry Zürich.

Epilepsy samples

The children`s hospital Zürich provided 17 CSF samples from epilepsy patients at a defined age and CSF from control patients without clinical symptoms for epilepsy.

5.4 Serum Depletion

Depletion of high-abundant proteins from complex sample systems is essential for the analysis of low-abundant molecules by mass spectrometry. The expression of agrin and neurotrypsin in mouse tissues was shown to peak in the first postnatal days and declines to a low level in adulthood. Therefore, we wanted to enable the detection of neurotrypsin-dependent agrin-22 splice variants by separating murine serum to obtain a sample system with less protein complexity. Seven different depletion techniques based on various physico-chemical characteristics were tested in this study. All depletion experiments were carried out at room temperature according to manufacturer`s instructions. The agrin-22 recovery was always verified by SDS-PAGE and Western blot with antibody R139.

5.4.1 ProteomeLab IgY-12 Kit

The ProteomeLab IgY-12 kit (Beckman Coulter Intl. SA, Nyon, Switzerland) allows the removal of twelve highly abundant proteins from biological fluids: albumin, IgG, a1-antitrypsin, IgA, IgM, transferrin, haptoglobin, a1-acid glycoprotein, a2-macroglobulin, HDL and fibrinogen in one single step. The kit is based on affinity columns using antigen affinity-purified polyclonal avian antibody (IgY)-antigen interactions. It has a capacity of 10 µl human serum per spin column cycle. On the purpose of depletion, 10 µl murine serum (wild-type, E18) were diluted 1:50 in dilution buffer (Tris buffered saline: 100 mM Tris-HCl, pH 7.4, 1.5 M NaCl). The sample is incubated with the column material for 15 minutes on an end-to-end rotator at room temperature, centrifuged for 30 seconds at 400 x g and the flow-through sample is collected for further analysis. To remove non-specifically bound proteins, three wash steps with dilution buffer were applied. The bound proteins were eluted using stripping buffer (1 M Glycine-HCl, pH 2.5) a total of 2 times. Therefore, the beads were incubated at room temperature for 3 minutes and centrifuged for 30 seconds at 400 x g to collect the eluant. All fractions were TCA-precipitated and loaded on a 12.5% SDS-PAGE for silver staining and 4-12% NuPAGE gel for Ponceau-red staining and Western blot analysis with antibody R139.

5.4.2 ProteoPrep Immunoaffinity Albumin and IgG Depletion Kit

The ProteoPrep Immunoaffinity Albumin and IgG Depletion Kit (Sigma-Aldrich, Buchs, Switzerland) has been designed to specifically remove albumin and IgG from human and murine serum (25-50 µl). The ProteoPrep Immunoaffinity medium in the pre-packed spin columns is based on a mixture of two beaded media containing recombinant expressed, small single-chain antibody ligands. We were using 25 µl murine serum (wild-type, E18) and another 25 µl from the same serum sample with addition of recombinant agrin-22 z19 (275 ng). The serum samples were both diluted to 100 µl with equilibration buffer, added on the column, incubated at room temperature for 10 minutes and centrifuged for 60 seconds at 8.000 x g. The eluat is reapplied on the column and incubated for 10 minutes at room temperature to ensure optimal depletion. The spin column is centrifuged for 60 seconds and the twice depleted serum is obtained. A wash step is applied to elute remaining unbound proteins from the spin column by adding 125 µl equilibration buffer and centrifuge for 60 seconds. The bound proteins are extracted two times by adding 150 µl of the Protein Extraction Reagent Type 4. All fractions were Wessel-Flügge precipitated, separated using 4-12% NuPAGE gels and analyzed by Western Blot with antibody R139.

5.4.3 ProteoSpin Abundant Serum Protein Depletion Kit

The ProteoSpin Abundant Serum Protein Depletion Kit (Norgen, BioCat GmbH, Heidelberg, Germany) provides a fast and simple procedure for the effective depletion of major serum proteins including albumin, a-antitrypsin, transferrin and haptoglobin from serum samples. It is based on an ion-exchange mechanism. The complexity of the sample is reduced, allowing for the detection of less abundant proteins. The eluted samples are ready for use in downstream applications including LC-MS. In a first step, the column is activated by adding 500 µl column activation buffer and wash buffer. Serum sample (10 µl, wild-type, P5) is diluted 1:50 in the same buffer, applied on the column and centrifuged for one minute at 6.700 x g. The flow-through is kept for analysis of assessing albumin and high abundance protein depletion. After

a column wash with 500 µl of column activation and wash buffer, the depleted serum is eluted by applying two times 100 µl of elution buffer, centrifugation of one minute at 6.700 x g and addition of 5 µl neutralizer to the eluat. Depletion efficiency was analyzed by silver gel and Western blot with antibody R139.

5.4.4 ProteoExtract Albumin/IgG Removal Kit

The ProteoExtract Albumin/IgG Removal Kit (Calbiochem) provides a fast, reproducible and highly specific method to simultaneously remove serum albumin and IgG from various body fluids like serum and CSF. It uses gravity-flow columns pre-packed with a novel albumin affinity resin and a unique immobilized protein A polymeric resin. For samples with high albumin content a volume of 20 µl serum is recommended. We were using 15 µl murine serum (wild-type, P5) which was diluted to a volume of 350 µl with the provided binding buffer. The column is equilibrated with 850 µl binding buffer; the diluted sample is applied and passes through the column by gravity-flow. To wash the column, 600 µl binding buffer is applied two times. All fractions are pooled and consequently contain the depleted serum samples. The bound proteins (albumin and IgG) remain trapped on the column. The depleted serum was analyzed by silver gel and Western blot using antibody R139.

5.4.5 Microcon YM-30 and YM-50

On the purpose to separate serum by molecular weight, Microcon centrifugal filter devices (Millipore) were used according to manufacturer's instructions. We wanted to test the efficiency of depletion by concentrating the high molecular weight fraction in serum in the supernatant and the separation of the low-molecular weight proteins in the flow-through. The experiments were performed with 30 mg/ml recombinant agrin-22 z19 and 200 µl rat CSF. The protein concentrations of the load, flow-through and supernatant were measured by UV-spectroscopy on a nano-Drop spectrophotometer (Thermo Scientific; Wohlen, Switzerland). Recovery of agrin-22 z19 was further confirmed by Western blot using antibody R139.

5.4.6 Gel filtration

The chromatographically method is based on size-exclusion and molecules are mainly separated according to their molecular weight. Gel filtration was performed using a Superose12 (10/30) column, 100 µl murine serum (wild-type, P10) and 2x PBS as elution buffer. For chromatography, a flow rate of 0.3 ml/min for 1.5 column volumes was chosen and elution fractions of 300 ml were sampled in a 96-well plate. All fractions were analyzed volume-adjusted (20 µl) by separation on 4-12% NuPAGE Bis-Tris gels, silver-staining and Western blot analysis with R139 antibody.

5.4.7 Ammonium sulfate precipitation

We precipitated and fractionated serum proteins with regard to their solubility in a solvent. The solubility is defined by the interaction of the charged functional groups of the protein with the molecules of the solvent. A 4M stock solution of ammonium sulfate and 5 ml murine

serum (wild-type, E18) diluted 1:2 in PBS buffer were used. The ammonium sulfate solution was added stepwise to the serum starting at 10% (v/v) and increasing the amount in steps of 10% until 100% (v/v). In order to avoid high local concentrations of ammonium sulfate, addition of the stock solution was performed by continuous shaking. The precipitate and the supernatant were analyzed in parallel with 4-12% NuPAGE Bis-Tris gels, Ponceau-red staining of the membrane and Western blot using antibody R139.

5.5 SDS PAGE

Murine serum samples and human cerebrospinal fluid (CSF) with equal volumes were boiled in NuPAGE LDS sample buffer following manufacturer's instructions and electrophoretically separated on 4-12% NuPAGE Bis-Tris gels (Invitrogen, Basel, Switzerland) using MOPS buffer and constant current of 30 mA per gel. These pre-cast gels were mainly used for optimized agrin-22 detection in murine serum samples and human CSF. Alternatively, samples with equal volumes were resolved by SDS-PAGE on conventional, discontinuous 12.5 % gels (Laemmli, 1970).

5.6 Immunoblotting

In order to detect agrin-22 isoforms, proteins separated via SDS PAGE were transferred onto Immobilon-P polyvinylidene difluoride (PVDF) membrane (45 mm, Millipore, Switzerland) in a semi-dry blotter Trans-Blot SD Transfer Cell (Bio Rad Laboryties, Inc., Hercules, CA, USA) using 1 x blotting buffer (25 mM Tris, 192 mM glycine, 20 % methanol) at 24 Volts for 1 hour at room temperature. On the purpose to detect calsyntenin-1 ecto-domain, proteins were wet blotted in a Criterion blotter (Bio Rad Laboryties, Inc., Hercules, CA, USA) using 0.5x blotting buffer (12.5 mM Tris, 96 mM glycine, 10% methanol) at 60 Volts for 3 hours at 4°C. Membranes were washed in methanol and air-dried for 30 minutes. The membranes were stained with Ponceau red solution (2 % Ponceau-S, 30 % trichloric acid, 30 % sulfosalicylic acid) and destained in distilled water. Primary antibodies were diluted in PBS buffer containing 0.1% (v/v) Tween-20 (PBS-T) and 5% (v/v) skim milk powder (Migros, Switzerland) and membranes were incubated overnight at 4°C. After wash with PBS-T, incubation with the peroxidase-conjugated secondary antibodies was performed for 1 hour at room temperature in PBS-T containing 5% skim milk powder. Immunoreactive bands were developed using chemiluminescent substrate ChemiGlow (Alpha Innotech GmbH, Kasendorf, Germany) and analyzed on a Fujifilm LAS-3000 Imager (Raytest AG, Wetzikon, Switzerland) with AIDA software (Raytest GmbH, Straubenhardt, Germany).

5.6.1 Antibodies

Polyclonal antibodies

Polyclonal rabbit antiserum R132 and goat antiserum G91 were raised against the C-terminal 90-kDa fragment of agrin (agrin-90). Goat antiserum G92 and rabbit antiserum R139 were raised against the C-terminal 22-kDa fragment of agrin (agrin-22; Reif et al., 2007). *Western blotting:* To verify the presence of full-length agrin as well as neurotrypsin-dependent agrin fragments in murine serum and human CSF, both antibodies against agrin-90 and agrin-22 were used. The antibodies anti-agrin-90 and anti-agrin-22 are able to detect both full-length agrin (data not shown). Co-expression of agrin and neurotrypsin in HeLa cells resulted in the release of agrin-22, agrin-90, and agrin-110 that originated from partial cleavage at the α-site (Reif et al., 2007). This pattern demonstrates that neurotrypsin-dependent cleavage at the β-site is not necessary for cleavage at the α-site. It is suggested that either agrin cleavage at the α-site precedes cleavage at the β-site, or that cleavage occurs at both sites in parallel. As analyses of murine serum and human CSF showed only the presence of agrin-22, Western blotting was performed with anti-agrin-22 antibodies to monitor neurotrypsin`s activity *in vivo*. The antibody R139 showed less background signals in the complex protein samples compared to G92 and was therefore used for quantification.

The polyclonal antibody R131 (3rd boost) was generated against murine calsyntenin-1 ectodomain.

Purchased antibodies

Purchased antibodies were from Chemicon (Lucerne, Switzerland; APP N-term [MAB348; clone 22C11; m; WB 1:3.000]), Santa Cruz Biotechnology (Nunningen, Switzerland; anti-myc [Sc-78]), Sigma Aldrich (Buchs, Switzerland; b-actin [A5316; m; WB 1:5.000]), Roche (Basel, Switzerland; anti-GFP [1814460; m; WB 1:2.000]), and Invitrogen (Basel, Switzerland; human IgG l-chain [HP6054; h; WB 1:2.000]).

Horseradish peroxidase (HRP)-conjugated secondary antibodies (WB 1:20.000) were from Kirkegaard & Perry Laboratories (Gaithersburg, MD, USA) and Chemicon (Lucerne, Switzerland).

Affinity-purified antibodies

Polyclonal rabbit antibody R139 was generated against murine agrin-22. For the isolation of IgGs, rabbit serum (5ml, R139 3rd boost) was diluted 1:10 in coupling buffer (10 mM Na_2HPO_4 x $2H_2O$, 10 mM NaCl, pH 7) and loaded onto a protein A column (GE, Healthcare, Zurich, Switzerland). Elution was performed with 100 mM Glycin-HCl (pH 2.7) and neutralized with 2M Tris-HCl (pH 11). The specific IgGs were isolated via CN-Br-Sepharose column (GE Helathcare, Zurich, Switzerland) with agrin-22 z19 as ligand, eluted using 100 mM Glycine, 0.05% Tween-20, 10% glycerol (pH 2.7) and neutralized with 2 M Tris-buffer (pH 11).

Antibody dilutions

Name/antigen	Type	Dilution for Western blotting
G91 (agrin-90)	serum	1:10.000
R132 (agrin-90)	serum (2nd boost)	1:3.000
G92 (agrin-22)	serum	1:10.000
R139 (agrin-22)	serum (4th boost)	1:1.000
R139 (agrin-22)	affinity-purified	1 µg/ml
R131 (calsyntenin-1)	IgG fraction (3rd boost)	1:2.000
anti-APP N-term		1:3.000
anti-GFP		1:2.000
IgGl chain		1:2.000
anti-ß-actin	ascites fluid	1:10.000
HRP-conjugated anti-rabbit	IgG	1:20.000
HRP-conjugated anti-mouse	IgG	1:20.000
HRP-conjugated anti-goat	IgG	1:30.000

5.6.2 Quantification and statistical analysis

Densitometric analyses of the protein bands were performed using AIDA software. Signals of two independent blots per genotype were quantified and used for statistical analyses. For analyses of agrin-22 in murine serum and human CSF, agrin-22 signals were normalized to the reference signal from murine serum of wild type E18. For the analyses of calsyntenin-1 ectodomain, signals were normalized to the reference signal for calsyntenin-1 ectodomain in a CSF sample pool. Then, adjusted values obtained from transgenic or neurotrypsin-deficient samples of each experiment were compared to the corresponding adjusted signals from the samples of wild-type littermates, whereby the control signal of the reference (wild type, E18) was set to 100 percent. Data are presented as mean ± S.E.M. Statistical analyses were performed using unpaired Student's *t*-test (Sigmaplot, Systat Software, Inc., San Jose, CA, USA).

5.7 Sample preparation for Mass spectrometry

All mass spectrometric measurements were performed at the Functional Genomics Center Zurich (FGCZ), either in the service (Protein Analysis Group) or in the User Lab.

On the purpose to analyze agrin-22 isoforms by mass spectrometry (MS), several sample preparation protocols were tested. As a high non-specific binding of agrin-22 isoforms to all kind of surfaces was suggested and approved by MS, it was essential to reduce sample manipulation as much as possible. In addition, particular care has to be taken in the selection of tubes for sample preparation. We were using low-binding tubes and washed them three times with methanol prior usage to remove sanitizers which were leading to signal suppression during MS analyses. They showed no/low non-specific binding of agrin-22 which was confirmed by MS analysis with synthetic agrin-22 peptides (data not shown). When handling larger sample volumes of several ml, glass test tubes were used to avoid non-specific binding.

5.7.1 In-gel digestion

Proteins were separated by 4-12% NuPAGE Bis-Tris gels and visualized by Coomassie Brilliant Blue (Invitrogen) staining. Protein bands at the molecular weight of interest were excised, cut into 1 mm3 cubes and put into low-binding tubes. The bands were destained with 50% acetonitrile and dehydrated in a vacuum centrifuge for 20 minutes until gel pieces show an opaque color. Destained, washed, and dehydrated gel pieces were rehydrated in digestion buffer (25mM NH_4HCO_3, pH 8) containing 50 ng trypsin for 5 minutes on ice and then covered with digestion buffer. The digestion mixture was incubated over night at 37°C and stopped by the addition of 10% formic acid. To extract the proteolytic peptides from the gel matrix, gel pieces were incubated three times with extraction solution (50% acetonitrile / 5% TFA). The recovered extracts were pooled together and dried down in a vacuum centrifuge. The dried extracts were stored at -20°C until mass spectrometric analysis. For the analysis, peptides were redissolved in equilibration buffer (5% acetonitrile / 1% TFA) used as starting condition for LC-separation.

5.7.2 In-solution digestion

Digest (1)

After acetonitrile fractionation and evaporation of the liquid phase, proteins were dissolved in digestion buffer (25mM NH_4HCO_3 pH 8) containing 10% acetonitrile (v/v). Protein concentration was measured using the Q-Bit system to evaluate the required amount of trypsin (2%, w/w). To increase the solubility of the proteins and therefore the efficiency of digestion, 10% RapiGest (v/v) was used as detergent. The digestion mixture was incubated over night at 37°C followed by evaporation of the solvent in a speed-vac. The samples were stored at -20°C until mass spectrometric analysis. For the analysis, peptides were resuspended in equilibration buffer (5% acetonitrile / 1% TFA) used as starting condition for LC-separation.

Digest (2)

Proteins were dissolved in digestion buffer (25mM NH_4HCO_3 pH 8) containing 50% methanol (v/v). Protein concentration was measured using the Q-Bit system, to evaluate the amount of trypsin (2%, w/w) needed. To increase the solubility of the proteins and therefore the efficiency of digestion, 10% RapiGest (v/v) was used as detergent. The digestion mixture was incubated three hours at room temperature followed by evaporation of the solvent in a speed-vac. The samples were stored at -20°C until mass spectrometric analysis. For the analysis, peptides were resuspended in equilibration buffer (5% acetonitrile / 1% TFA) used as starting condition for LC-separation.

5.8 Protein identification with nano-LC-ESI-MS/MS

5.8.1 Protein Analysis Group

Murine serum samples were pooled and agrin-22 was isolated by immunoaffinity chromatography using immobilized affinity-purified R129 antibody. As column material NHS-activated sepharose was used to covalently link affinity-purified polyclonal rabbit antibody (R139). Column material was prepared following manufacturer's instructions. The appearance of agrin-22 in the elution fractions was confirmed with Western blot and corresponding elution fractions were pooled. Samples were separated on 4-12% NuPAGE gels as previously described. Separated proteins were visualized using the Colloidal Coomassie blue staining kit (Invitrogen AG, Basel, Switzerland). Bands in the 25-20 kDa region corresponding to the 22kDa fragment of agrin were cut out, trypsin-digested and analyzed via nanoflow-LC-ESI-MS/MS using a nanoAquity UPLC/Q-TOF Ultima API (Waters, Baden, Switzerland). Peptides were separated on a BEH C18 column (75 µm x 15 cm) at a flow rate of 350 nl/min using a gradient formed between solvent A (0.1% formic acid) and B (0.1% fromic acid in actetonitrile). Protein identification was carried out with Mascot.

5.8.2 User Lab

In-house columns

The production of the fused silica capillary columns (75 µm x 8 cm) was performed with a LASER puller. Reversed phase material (Magic C18 AQ beads 5 µm, 100 Å (Michrom)) was added in a minimal amount to a glass micro-vial with a small magnetic stirring rod and 1ml of methanol to make a slurry. A high-pressure vessel was used for packing the column. Packing was performed on a magnetic stir plate using a Helium pressure of up to 30 bars and stopped when the bed volume reached 8 cm. The capillary was washed with methanol for 30 minutes and two chromatographic separations with a standard peptide (e.g. 50 fmol/ml Glufib) were performed to evaluate and optimize the LC-MS system and to block active sites in the column material. On the purpose to wash and equilibrate the in-house fused silica capillary columns used for LC-MS analysis, we injected 20% ACN using the gradient which was chosen for the sample analysis. After the equilibration, the C18 resin was additionally primed for the analysis by injection of the standard Glufib. This step was performed three to five times until the retention time and

peptide recovery was reproducible which was calculated by integrated peak area of Glufib in an extracted ion chromatogram. The gradient used for this measure is listed in the section LC-gradients as Standard gradient.

Data-dependent mass spectrometry

RP-nano-LC-ESI-MS was performed on an Agilent 1100 LC-System (Agilent Technologies AG, Basel, Switzerland) coupled to an LTQ-TOF mass spectrometer (Waters, Baden, Switzerland), operating in split flow to reduce the flow rate. Samples were automatically injected into a 10-µl loop and loaded onto an analytical column (75 µm x 8 cm column packed in-house) prior to ionization. Peptide mixtures were delivered to the analytical column at a flow rate of 300 nl/min using various gradients formed between solvent A (various % ACN, 0.2% formic acid) and solvent B (0.2% formic acid), in 80% ACN). The gradients used for analysis are listed below in the section LC-gradients.

Alternatively, nano-LC MS/MS was performed on a nano-LC Eksigent system (Eksigent, Axel Semrau, Sprockhövel, Germany) in-line to a 7-Tesla LTQ-FT mass spectrometer (Thermo Fisher Scientific AG, Reinach, Switzerland). With a flow rate of 150 nl/min, peptides were transferred to the analytical column (75 µm x 8 cm column packed in-house) and eluted with various gradients fromed between solvent A (0.1% fromic acid) and solvent B (0.1% formic acid in 80% ACN, see section LC-gradients). Survey scans were recorded in the ICR cell with a target value of 10^6 and a resolution of 100.000 at 400 m/z. MS/MS spectra were recorded in a data-dependent manner using an inclusion list of tryptic peptides for either agrin-22 or the calsyntenin members at the ion trap from the three most intense signals. Charge state screening was enabled and singly, quadruply and not-assigned charge states were rejected. Precursor masses already selected for MS/MS were excluded for further selection for 60 seconds and the exclusion window was set to 20 parts per million (ppm). The size of the exclusion list was set to maximum (500 entries).

Targeted mass spectrometry

Targeted nanoflow-LC MS/MS was performed on a nano-LC (Eksigent, Axel Semrau, Sprockhövel, Germany) in-line to the triple quadrupole mass spectrometer (TSQ Vantage and TSQ Quantum; Thermo Fisher Scientific AG, Reinach, Switzerland). The flow rate for peptide elution was of 150 nl/min and peptides were transferred to the analytical column (75 µm x 8 cm column packed in-house) and eluted in a gradient of acetonitrile in 0.1 M acetic acid. The different gradients used for the measure are listed below in the section LC-gradients. The mass peak width for Q1 full width half maximum (FWHM) was set to Q1 = 0.7 Th for unit resolution and to 0.1 Th for enhanced resolution. The Q3 FWHM was in all cases set to 0.7 Th, scan width to 0.002 m/z and scan time to 0.05 sec (16 transitions = 0.8 sec/cycle). The selected reaction monitoring (SRM) MS spectra were acquired in targeted mode using a transition list of proteotypic peptides for either agrin-22 or the calsyntenin-1 ectodomain. The list of agrin-22 PTPs for each z-transcript, their product ions and the collision energy for fragmentation is described in Table 5.2. To avoid sample carry-over, wash cycles with 10% isopropanol were applied after each run.

Description	Proteotypic peptide	m/z	Fragment	CE [V]
Agrin-22 z0	TFVEYLNAVTESEK	815.4044	492.229	31
			593.277	
			692.346	
			763.383	
			877.426	
			990.510	
			1153.573	
			1282.616	
Agrin-22 z8	TFVEYLNAVTESELANEIPVEK	1248.131	427.276	45
			585.360	
			714.403	
			899.483	
			1141.609	
			1357.648	
			1458.732	
			1628.837	
Agrin-22 z11	TFVEYLNAVTESPETLDSGALHSEK	913.112	943.447	43
			1383.675	
			1470.707	
			1599.749	
			1201.596	
			1383.675	56
			1597.796	
			1821.922	
			1935.965	
Agrin-22 z19	TFVEYLNAVTESELANEIPVPETLDSGALHSEK	1369.164	943.447	50
			1383.675	
			1470.707	
			1599.749	
			1801.891	
			1383.675	65
			1579.796	
			1821.922	
			1935.965	

Table 5-2. Agrin-22 PTPs for each z-transcript , fragment ions and CE for the first test of targeted mass spectrometry.

Instrument maintenance on the TSQ Vantage and Quantum

The TSQ Vantage and Quantum were calibrated monthly with polytyrosine-1,3,6 (Thermo Electron) that comprised Tyr, $(Tyr)_3$, and $(Tyr)_6$, by following the instructions of the instrument manual.

To test the instrument performance before analyzing the samples, we measured a dilution series of the standard peptide Glu-1 fibrinopeptide (Glufib) from 800 amol, 8 fmol to 80 fmol using the Standard gradient for LC-MS (see section LC-Gradients). We calculated the regression coefficient of a calibration curve based on the integrated peak areas of the tryptic peptide EGVNDNEEGFFSAR with the m/z 785.842.

For optimized, reproducible MS analyses, the calibration and inter-day mass axis stability of the instruments was regularly tested and monitored after a set of five samples. Therefore we performed selected reaction monitoring of the standard peptide Glufib. We chose the highly abundant proteotypic peptide (PTP) EGVNDNEEGFFSAR with the m/z 785.842 and the retention time of 29.4 minutes (standard gradient). For SRM analysis, the fragments with m/z 627,324; 684,346; 813,388, and 887,377 were selected to monitor the transitions.

LC-Gradients

Standard Gradient 1: start at 5% ACN, in 1 minute to 10%, in 7 minutes to 35%, in 4 minutes to 80% (for 12 minutes).

Gradient 2: start at 20%, in 25 minutes to 60%, in 12 minutes to 80% (for 10 minutes).

Gradient 3: start at 40%, in 25 minutes to 60%, in 12 minutes to 80% (for 10 minutes).

MALDI

The digestion solutions were spotted on the MALDI target plate using recrystallized α-cyano-4-hydroxycinnamic acid matrix solution with a 1:1 ratio. The spotted samples were analyzed by a MALDI-TOF/TOF mass spectrometer (ABI 4700 Proteomics Analyzer, Applied Biosystems, Rotkreuz, Switzerland).

5.8.3 Database search and protein identification

The raw files from the mass spectrometer were converted into Mascot generic files (mgf) with Mascot Distiller and searched against a Swissprot-d database using Mascot Server (version 2.2; Matrix Science, London, UK) (Perkins et al., 1999). The parameters for precursor tolerance and fragment ion tolerance were set to ±5 ppm and ±0.8 Da, respectively.

6 References

Adam, B.L., Qu, Y., Davis, J.W., Ward, M.D., Clements, M.A., Cazares, L.H., Semmes, O.J., Schellhammer, P.F., Yasui, Y., Feng, Z., et al. (2002). Serum protein fingerprinting coupled with a pattern-matching algorithm distinguishes prostate cancer from benign prostate hyperplasia and healthy men. Cancer Res 62, 3609-3614.

Aebersold, R., and Mann, M. (2003). Mass spectrometry-based proteomics. Nature 422, 198-207.

Aebersold, R, Anderson, L., Caprioli, R., Druker, B., Hartwell, L., Smith, R. (2005). Perspective: a program to improve protein biomarker discovery for cancer. J Proteome Res. 4, 1104-1109.

Alpantaki, K., Tsiridis, E., Pape, H.C., Giannoudis, P.V. (2007). Application of clinical proteomics in diagnosis and management of trauma patients. Injury 38, 263–271.

Anderson, N.L., and Anderson, N.G. (2002). The human plasma proteome: history, character, and diagnostic prospects. Mol Cell Proteomics 1, 845-867.

Anderson, N.L., Anderson, N.G., Haines, L.R., Hardie, D.B., Olafson, R.W., and Pearson, T.W. (2004). Mass spectrometric quantitation of peptides and proteins using Stable Isotope Standards and Capture by Anti-Peptide Antibodies (SISCAPA). J Proteome Res 3, 235-244.

Annies, M., Bittcher, G., Ramseger, R., Loschinger, J., Woll, S., Porten, E., Abraham, C., Ruegg, M. A., and Kroger, S. (2006). Clustering transmembrane-agrin induces filopodia-like processes on axons and dendrites. Mol. Cell Neurosci. 31. 515–524.

Anspach, J.A., Maloney, T.D., Colon, L.A. (2007). Ultrahigh-pressure liquid chromatography using a 1-mm id column packed with 1.5-microm porous particles. J. Sep. Sci. 3,:1207–13.

Ardekani, A.M., Liotta, L.A., Petricoin, E.F. III (2002). Clinical potential of proteomics in the diagnosis of ovarian cancer. Expert Rev Mol Diagn. 2, 312–320.

Armstead, W.M., Riley, J., Kiessling, J.W., Cines, D.B., and Higazi, A.A. (2010). Novel plasminogen activator inhibitor-1-derived peptide protects against impairment of cerebrovasodilation after photothrombosis through inhibition of JNK MAPK. Am J Physiol Regul Integr Comp Physiol 299, R480-485.

Baldi, L., Muller, N., Picasso, S., Jacquet, R., Girard, P., Thanh, H. P., Derow, E., and Wurm, F. M. (2005). Transient gene expression in suspension HEK-293 cells: application to largescale protein production. Biotechnol. Prog. 21, 148–153.

Baranes, D., Lederfein, D., Huang, Y.Y., Chen, M., Bailey, C.H., and Kandel, E.R. (1998). Tissue plasminogen activator contributes to the late phase of LTP and to synaptic growth in the hippocampal mossy fiber pathway. Neuron 21, 813-825.

Barrett, A.J., Rawlings, ND., Woessner, J.F. (2003). The Handbook of Proteolytic Enzymes, 2nd ed. Academic Press.

Barros, C., Crosby, J.A., and Moreno, R.D. (1996). Early steps of sperm-egg interactions during mammalian fertilization. Cell Biol Int 20, 33-39.

Baumann, S., Ceglarek, U., Fiedler, G.M., Lembcke, J., Leichtle, A., and Thiery, J. (2005). Standardized approach to proteome profiling of human serum based on magnetic bead separation and matrix-assisted laser desorption/ionization time-of-flight mass spectrometry. Clin Chem 51, 973-980.

Benchenane, K., Lopez-Atalaya, J.P., Fernandez-Monreal, M., Touzani, O., and Vivien, D. (2004). Equivocal roles of tissue-type plasminogen activator in stroke-induced injury. Trends Neurosci 27, 155-160.

Bezakova G., Ruegg, M.A. (2003). New insights into the role of agrin. Molecular Cell Biology 4, 295-308.

Bishop, M.L., Duben-Engelkirk, J.L., Fody, E.P. (2000). Clinical Chemistry: Priciples, Procedures, Correlations, 4th ed, Lippincott Williams Wilkins, 378-386.

Blackler, A.R., Speers, A.E., Ladinsky, M.S., and Wu, C.C. (2008). A shotgun proteomic method for the identification of membrane-embedded proteins and peptides. J Proteome Res 7, 3028-3034.

Blackler, A.R., Speers, A.E., and Wu, C.C. (2008). Chromatographic benefits of elevated temperature for the proteomic analysis of membrane proteins. Proteomics 8, 3956-3964.

Blake, R.V., Wroe, S.J., Breen, E.K., and McCarthy, R.A. (2000). Accelerated forgetting in patients with epilepsy: evidence for an impairment in memory consolidation. Brain 123 Pt 3, 472-483.

Bondarenko, P.V., Chelius, D., and Shaler, T.A. (2002). Identification and relative quantitation of protein mixtures by enzymatic digestion followed by capillary reversed-phase liquid chromatography-tandem mass spectrometry. Anal Chem 74, 4741-4749.

Bondarenko, P.V., Chelius, D., and Shaler, T.A. (2002). Identification and relative quantitation of protein mixtures by enzymatic digestion followed by capillary reversed-phase liquid chromatography-tandem mass spectrometry. Anal Chem 74, 4741-4749.

Bose, C.M., Qiu, D., Bergamaschi, A., Gravante, B., Bossi, M., Villa, A., Rupp, F., and Malgaroli, A. (2000). Agrin controls synaptic differentiation in hippocampal neurons. J Neurosci 20, 9086-9095.

Bowe, M.A., and Fallon, J.R. (1995). The role of agrin in synapse formation. Annu Rev Neurosci 18, 443-462.

Boyes, B. E., Kirkland, J. J. (1993). Rapid, high-resolution HPLC separation of peptides using small particles at elevated temperatures. Pept. Res. 6, 249–258.

Braak, H., and Braak, E. (1991). Neuropathological stageing of Alzheimer-related changes. Acta Neuropathol 82, 239-259.

Browers, G.N.Jr., Fassett, J.D., White, E. (1993). Isotope dilution mass spectrometry and the national reference system. Anal. Chem. 65, 475R-479R.

Brown,e C.A., Bennett, H.P.J., Solomon, S. (1982). The isolation of peptides by high-performance liquid chromatography using predicted elution positions. Anal. Biochem. 124: 201-208.
Bishop M.L., Duben-Engelkirk J.L., Fody E.P. (Eds.) (2000) Clinical Chemistry: Principles, Procedures, Correlations, 4th ed, Lippincott Williams & Wilkins. 378-386.

Bull, H.B., Breese, K. (1974). Surface tension of amino acid solutions: a hydrophobicity scale of the amino acid residues. Arch. Biophys. 161, 665-670.

Burgess, R.W., Nguyen, Q.T., Son, Y. J., Lichtman, J.W., Sanes, J.R. (1999). Alternative spliced isoforms of nerve- and muscle-derived agrin: their roles at the neuromuscular junction. Neuron 23, 33-44.

Butler, C.R., and Zeman, A.Z. (2008). Recent insights into the impairment of memory in epilepsy: transient epileptic amnesia, accelerated long-term forgetting and remote memory impairment. Brain 131, 2243-2263.

Callesen, A.K., Mohammed, S., Bunkenborg, J., Kruse, T.A., Cold, S., Mogensen, O., Christensen, R., Vach, W.,

Jorgensen, P.E., and Jensen, O.N. (2005). Serum protein profiling by miniaturized solid-phase extraction and matrix-assisted laser desorption/ionization mass spectrometry. Rapid Commun Mass Spectrom 19, 1578-1586.

Carroll, P.M., Tsirka, S.E., Richards, W.G., Frohman, M.A., and Strickland, S. (1994). The mouse tissue plasminogen activator gene 5' flanking region directs appropriate expression in development and a seizure-enhanced response in the CNS. Development 120, 3173-3183.

Chelius, D., and Bondarenko, P.V. (2002). Quantitative profiling of proteins in complex mixtures using liquid chromatography and mass spectrometry. J Proteome Res 1, 317-323.

Chen, Z.L., and Strickland, S. (1997). Neuronal death in the hippocampus is promoted by plasmin-catalyzed degradation of laminin. Cell 91, 917-925.

Cheusova, T., Khan, M.A., Schubert, S.W., Gavin, A.C., Buchou, T., Jacob, G., Sticht, H., Allende, J., Boldyreff, B., Brenner, H.R., Hashemolhosseini, S. (2006). Casein kinase 2-dependent serine phosphorylation of MuSK regulates acetylcholine receptor aggregation at the neuromuscular junction. Genes Dev. 20, 1800–1816.

Colantonio D.A., Dunkinson C., Bovenkamp D.E., Van Eyk J.E. (2005) Effectice removal of albumin from serum. Proteomics 5: 3831-3835.

Cohen, N.A., Kaufmann, W.E., Worley, P.F., and Rupp, F. (1997). Expression of agrin in the developing and adult rat brain. Neuroscience 76, 581-596.

Coombes, K.R., Tsavachidis, S., Morris, J.S., Baggerly, K.A., Hung, M.C., and Kuerer, H.M. (2005). Improved peak detection and quantification of mass spectrometry data acquired from surface-enhanced laser desorption and ionization by denoising spectra with the undecimated discrete wavelet transform. Proteomics 5, 4107-4117.

Cornish, T., Chi, J., Johnson, S., Lu, Y., Campanelli, J.T. (1999). Globular domains of agrin are functional units that collaborate to induce acetylcholine receptor clustering. J. Cell Sci. 112, 1213-1223.

Cotman, S.L., Halfter, W., and Cole, G.J. (2000). Agrin binds to beta-amyloid (Abeta), accelerates abeta fibril formation, and is localized to Abeta deposits in Alzheimer›s disease brain. Mol Cell Neurosci 15, 183-198.

Coughlin, S.R. (2000). Thrombin signalling and protease-activated receptors. Nature 407, 258-264.

Davies, C.A., Mann, D.M., Sumpter, P.Q., and Yates, P.O. (1987). A quantitative morphometric analysis of the neuronal and synaptic content of the frontal and temporal cortex in patients with Alzheimer›s disease. J Neurol Sci 78, 151-164.

DeChiara, T.M., Bowen, D.C., Valenzuela, D.M., Simmons, M.V., Poueymirou, W.T., Thomas, S., Kinetz, E., Compton, D.L., Rojas, E., Park, J.S., et al. (1996). The receptor tyrosine kinase MuSK is required for neuromuscular junction formation in vivo. Cell 85, 501-512.

Diamandis, E.P. (2003). Point: Proteomic patterns in biological fluids: do they represent the future of cancer diagnostics? Clin Chem 49, 1272-1275.

Diamandis, E.P. (2004). Mass spectrometry as a diagnostic and a cancer biomarker discovery tool: opportunities and potential limitations. Mol Cell Proteomics 3, 367-378.

Dodson, G., and Wlodawer, A. (1998). Catalytic triads and their relatives. Trends Biochem Sci 23, 347-352.

Domon, B.. & Aebersold, R. (2010). Options and considerations when selecting a quantitative proteomics strategy. Nature Biotechnology. 2,: 710-721.

Donahue, J.E., Berzin, T.M., Rafii, M.S., Glass, D.J., Yancopoulos, G.D., Fallon, J.R., and Stopa, E.G. (1999). Agrin in Alzheimer›s disease: altered solubility and abnormal distribution within microvasculature and

brain parenchyma. Proc Natl Acad Sci U S A 96, 6468-6472.

Echan, L.A., Tang, H.Y., Ali-Khan, N., Lee, K., and Speicher, D.W. (2005). Depletion of multiple high-abundance proteins improves protein profiling capacities of human serum and plasma. Proteomics 5, 3292-3303.

Emmett, M.R., Caprioli, R.M. (1994).Micro-electrospray mass spectrometry: ultra-high-sensitivity analysis of peptides and proteins. J. Am. Soc. Mass Spectrom. 5, 605–13.

Feng, Z., Prentice, R., and Srivastava, S. (2004). Research issues and strategies for genomic and proteomic biomarker discovery and validation: a statistical perspective. Pharmacogenomics 5, 709-719.

Fenn, J.B., Mann, M., Meng, C.K., Wong, S.F., and Whitehouse, C.M. (1989). Electrospray ionization for mass spectrometry of large biomolecules. Science 246, 64-71.

Ferreira, A. (1999). Abnormal synapse formation in agrin-depleted hippocampal neurons. J Cell Sci 112 (Pt 24), 4729-4738.

Fountoulakis, M. (2001.) Proteomics: current technologies and applications in neurological disorders and toxicology. Amino Acids 21, 19-41.

Frischknecht, R., Fejtova, A., Viesti, M., Stephan, A., and Sonderegger, P. (2008). Activity-induced synaptic capture and exocytosis of the neuronal serine protease neurotrypsin. J Neurosci 28, 1568-1579.

Fukuchi, K., Hart, M., and Li, L. (1998). Alzheimer›s disease and heparan sulfate proteoglycan. Front Biosci 3, d327-337.

Galliciotti, G., and Sonderegger, P. (2006). Neuroserpin. Front Biosci 11, 33-45.

Gautam, M., Noakes, P.G., Moscoso, L., Rupp, F., Scheller, R.H., Merlie, J.P., and Sanes, J.R. (1996). Defective neuromuscular synaptogenesis in agrin-deficient mutant mice. Cell 85, 525-535.

Gesemann, M. et al (1996). Alternative splicing of agrin alters its binding to heparin, dystroglycan, and the putative agrin receptor. Neuron 16, 755-767.

Gesemann, M., Denzer, A.J., Ruegg, M.A. (1995). Acetylcholine receptor-aggregating activity of agrin isoforms and mapping of the active site. J. Cell Biol. 128, 625-636.

Gillette, M.A., Mani, D.R., and Carr, S.A. (2005). Place of pattern in proteomic biomarker discovery. J Proteome Res 4, 1143-1154.

Glass, D.J., Bowen, D.C., Stitt, T.N., Radziejewski, C., Bruno, J., Ryan, T.E., Gies, D.R., Shah, S., Mattsson, K., Burden, S.J., et al. (1996). Agrin acts via a MuSK receptor complex. Cell 85, 513-523.

Godfrey, E.W., Nitkin, R.M., Wallace, B.G., Rubin, L.L., and McMahan, U.J. (1984). Components of Torpedo electric organ and muscle that cause aggregation of acetylcholine receptors on cultured muscle cells. J Cell Biol 99, 615-627.

Granger, J., Siddiqui, J., Copeland, S., and Remick, D. (2005). Albumin depletion of human plasma also removes low abundance proteins including the cytokines. Proteomics 5, 4713-4718.

Griffin, P.R., Coffman, J.A., Hood, L.E., Yates, J.R. (1991). Structural analysis of proteins by capillary HPLC electrospray tandem mass spectrometry. Int. J. Mass Spectrom. Ion Process. 111, 131–49.

Grossmann J., Roschitzki B., Panse C., Fortes C., Barkow-Oesterreicher S., Rutishauser D., Schlapbach R. (2010) Implementation and evaluation of relative and absolute quantification in shotgun proteomics with label-free methods. Journal of Proteomics. 73, 1740-1746.

Gschwend, T.P., Krueger, S.R., Kozlov, S.V., Wolfer, D.P., and Sonderegger, P. (1997). Neurotrypsin, a novel multidomain serine protease expressed in the nervous system. Mol Cell Neurosci 9, 207-219.

Gygi, S. P., Rist, B., Gerber, S. A., Turecek, F. et al (1999). Quantitative analysis of complex protein mixtures using isotope-coded affinity tags. Nat. Biotechnol. 17, 994–999.

Gygi, S.P., Corthals, G.L., Zhang, Y., Rochon, Y., and Aebersold, R. (2000). Evaluation of two-dimensional gel electrophoresis-based proteome analysis technology. Proc Natl Acad Sci U S A 97, 9390-9395.

Haab, B.B., Paulovich, A.G., Anderson, N.L., Clark, A.M., Downing, G.J., Hermjakob, H., Labaer, J., and Uhlen, M. (2006). A reagent resource to identify proteins and peptides of interest for the cancer community: a workshop report. Mol Cell Proteomics 5, 1996-2007.

Hammack, B.N., Owens, G.P., Burgoon, M.P., and Gilden, D.H. (2003). Improved resolution of human cerebrospinal fluid proteins on two-dimensional gels. Mult Scler 9, 472-475.

Hamos, J.E., DeGennaro, L.J., and Drachman, D.A. (1989). Synaptic loss in Alzheimer›s disease and other dementias. Neurology 39, 355-361.

Hancock,W. S., Chloupek, R. C., Kirkland, J. J., Snyder, L. R. (1994). Temperature as a variable in reversed-phase high-performance liquid chromatographic separations of peptide and protein samples. I. Optimizing the separation of a growth hormone tryptic digest. J. Chromatogr. A 686, 31–43.

Hata, S., Fujishige, S., Araki, Y., Kato, N., Araseki, M., Nishimura, M., Hartmann, D., Saftig, P., Fahrenholz, F., Taniguchi, M., Urakami, K., Akatsu, H., Martins, R.N., Yamamoto, K., Masahiro Maeda, M., Yamamoto, T., Nakaya, T., Gandy, S., Suzuki, T., (2009). Alcadein cleavages by APP α- and γ-secretases generate small peptides p3-Alcs indicating Alzheimer disease-related γ-secretase dysfunction. J. Biol. Chem. 25, 36024-36033.

Havlis, J., Shevchenko, A. (2004). Absolute quantification of proteins in solutions and in polyacrylamide gels by mass spectrometry. Anal Chem. 76, 3029-3036.

Hedstrom, L. (2002). Serine protease mechanism and specificity. Chem Rev 102, 4501-4524.

Hermann, B.P., Seidenberg, M., Schoenfeld, J., and Davies, K. (1997). Neuropsychological characteristics of the syndrome of mesial temporal lobe epilepsy. Arch Neurol 54, 369-376.

Hesse, C., Rosengren, L., Andreasen, N., Davidsson, P., Vanderstichele, H., Vanmechelen, E., and Blennow, K. (2001). Transient increase in total tau but not phospho-tau in human cerebrospinal fluid after acute stroke. Neurosci Lett 297, 187-190.

Hilario, M., Kalousis, A., Pellegrini, C., and Muller, M. (2006). Processing and classification of protein mass spectra. Mass Spectrom Rev 25, 409-449.

Hilgenberg, L.G., Hoover, C.L., and Smith, M.A. (1999). Evidence of an agrin receptor in cortical neurons. J Neurosci 19, 7384-7393.

Hilgenberg, L.G., and Smith, M.A. (2004). Agrin signaling in cortical neurons is mediated by a tyrosine kinase-dependent increase in intracellular Ca2+ that engages both CaMKII and MAPK signal pathways. J Neurobiol 61, 289-300.

Hilgenberg, L.G., Su, H., Gu, H., O›Dowd, D.K., and Smith, M.A. (2006). Alpha3Na+/K+-ATPase is a neuronal receptor for agrin. Cell 125, 359-369.

Hintsch,G., Zurlinden, A., Meskenaite, V., Steuble, M., Fink-Widmer, K., Kinter, J., Sonderegger P. (2002). The Calsyntenins—A Family of Postsynaptic Membrane Proteins with Distinct Neuronal Expression Patterns. Molecular and Cellular Neuroscience 21, 393-409.

Hogh, P., Smith, S.J., Scahill, R.I., Chan, D., Harvey R.J., Fox, N.C., Rossor, M.N. (2002). Epilepsy presenting as AD: neuroimaging, electroclinical features, and response to treatment. Neurology 58, 298-301.

Hoover, C.L., Hilgenberg, L.G., and Smith, M.A. (2003). The COOH-terminal domain of agrin signals via a synaptic receptor in central nervous system neurons. J Cell Biol 161, 923-932.

Hopf, C. & Hoch W. (1996). Agrin binding to a-dystroglycans - domains of agrin necessary to induce acetylcholine receptor clustering are overlapping but not identical to the a-dystroglycan-binding region. J. Biol. Chem. 271, 5231-5236.

Huang, L., Harvie, G., Feitelson, J.S., Gramatikoff, K., Herold, D.A., Allen, D.L., Amunngama, R., Hagler, R.A., Pisano, M.R., Zhang, W.W., et al. (2005). Immunoaffinity separation of plasma proteins by IgY microbeads: meeting the needs of proteomic sample preparation and analysis. Proteomics 5, 3314-3328.

Huang, Y.Y., Bach, M.E., Lipp, H.P., Zhuo, M., Wolfer, D.P., Hawkins, R.D., Schoonjans, L., Kandel, E.R., Godfraind, J.M., Mulligan, R., et al. (1996). Mice lacking the gene encoding tissue-type plasminogen activator show a selective interference with late-phase long-term potentiation in both Schaffer collateral and mossy fiber pathways. Proc Natl Acad Sci U S A 93, 8699-8704.

Hunnerkopf, R., Grassl, J., Thome, J. (2007). Proteomics: biomarker research in psychiatry. Fortschr Neurol Psychiatr. 75, 579–586.

Ishikawa, K., Nishimura, T., Koga, Y., Niwa, Y. (1994). Role of Coulomb energy in promoting collisionally activated dissociation of multiply charged peptides formed by electrospray ionization. Rapid Commun. Mass Spectrom. 8, 933-938.

Ito, M., Echizenya, N., Nemoto, D., Kase, M. (2009). Case Series of Epilepsy-derived Memory Impairment Resembling Alzheimer Disease. Alzheimer Disease & Associated Disorders. 23, 406-409.

Janecki, D.J., Bemis, K.G., Tegeler, T.J., Sanghani, P.C., Zhai, L., Hurley, T.D., Bosron, W.F., and Wang, M. (2007). A multiple reaction monitoring method for absolute quantification of the human liver alcohol dehydrogenase ADH1C1 isoenzyme. Anal Biochem 369, 18-26.

Johnson, D.E. (2000). Noncaspase proteases in apoptosis. Leukemia 14, 1695-1703.

Joseph, K., Ghebrehiwet, B., and Kaplan, A.P. (2001). Activation of the kinin-forming cascade on the surface of endothelial cells. Biol Chem 382, 71-75.

Karas, M., and Hillenkamp, F. (1988). Laser desorption ionization of proteins with molecular masses exceeding 10,000 daltons. Anal Chem 60, 2299-2301.

Kim, N., Stiegler, A.L., Cameron, T.O., Hallock, P.T., Gomez, A.M., Huang, J.H., Hubbard, S.R., Dustin, M.L., and Burden, S.J. (2008). Lrp4 is a receptor for Agrin and forms a complex with MuSK. Cell 135, 334-342.

Kirkpatrick, D.S., Gerber, S.A., and Gygi, S.P. (2005). The absolute quantification strategy: a general procedure for the quantification of proteins and post-translational modifications. Methods 35, 265-273.

Koomen, J.M., Shih, L.N., Coombes, K.R., Li, D., Xiao, L.C., Fidler, I.J., Abbruzzese, J.L., and Kobayashi, R. (2005). Plasma protein profiling for diagnosis of pancreatic cancer reveals the presence of host response proteins. Clin Cancer Res 11, 1110-1118.

Kvajo, M., Albrecht, H., Meins, M., Hengst, U., Troncoso, E., Lefort, S., Kiss, J.Z., Petersen, C.C., and Monard, D. (2004). Regulation of brain proteolytic activity is necessary for the in vivo function of NMDA receptors. J Neurosci 24, 9734-9743.

Li, J., Zhang, Z., Rosenzweig, J., Wang, Y.Y., and Chan, D.W. (2002). Proteomics and bioinformatics approaches for identification of serum biomarkers to detect breast cancer. Clin Chem 48, 1296-1304.

Li, X.J., Yi, E.C., Kemp, C.J., Zhang, H., and Aebersold, R. (2005). A software suite for the generation and comparison of peptide arrays from sets of data collected by liquid chromatography-mass spectrometry. Mol Cell Proteomics 4, 1328-1340.

Lindner, J.R., Kahn, M.L., Coughlin, S.R., Sambrano, G.R., Schauble, E., Bernstein, D., Foy, D., Hafezi-Moghadam, A., and Ley, K. (2000). Delayed onset of inflammation in protease-activated receptor-2-deficient mice. J Immunol 165, 6504-6510.

Liot, G., Benchenane, K., Leveille, F., Lopez-Atalaya, J.P., Fernandez-Monreal, M., Ruocco, A., Mackenzie, E.T., Buisson, A., Ali, C., and Vivien, D. (2004). 2,7-Bis-(4-amidinobenzylidene)-cycloheptan-1-one dihydrochloride, tPA stop, prevents tPA-enhanced excitotoxicity both in vitro and in vivo. J Cereb Blood Flow Metab 24, 1153-1159.

Lu, P., Vogel, C., Wang, R., Yao, X., and Marcotte, E.M. (2007). Absolute protein expression profiling estimates the relative contributions of transcriptional and translational regulation. Nat Biotechnol 25, 117-124.

Madani, R., Hulo, S., Toni, N., Madani, H., Steimer, T., Muller, D., and Vassalli, J.D. (1999). Enhanced hippocampal long-term potentiation and learning by increased neuronal expression of tissue-type plasminogen activator in transgenic mice. EMBO J 18, 3007-3012.

Magill-Solc, C., and McMahan, U.J. (1990). Agrin-like molecules in motor neurons. J Physiol (Paris) 84, 78-81.

Mann, S., and Kroger, S. (1996). Agrin is synthesized by retinal cells and colocalizes with gephyrin [corrected]. Mol Cell Neurosci 8, 1-13.

Marcello, E., Gardoni, F., Mauceri, D., Romorini, S., Jeromin, A., Epis, R., Borroni, B., Cattabeni, F., Sala, C., Padovani, A., Di Luca, M. (2007). Synapse-associated protein-97 mediates alpha-secretase ADAM10 trafficking and promotes its activity. J Neurosci. 27, 1682-91.

Martin, L.J., Pardo, C.A., Cork, L.C., and Price, D.L. (1994). Synaptic pathology and glial responses to neuronal injury precede the formation of senile plaques and amyloid deposits in the aging cerebral cortex. Am J Pathol 145, 1358-1381.

Martin, R.C., Meador, K.J., and Loring, D.W. (1991). Differential effects of unilateral temporal lobectomy on visuospatial memory and attention. J Clin Exp Neuropsychol 13, 965-971.

Martosella, J., Zolotarjova, N., Liu, H., Moyer, S.C., Perkins, P.D., and Boyes, B.E. (2006). High recovery HPLC separation of lipid rafts for membrane proteome analysis. J Proteome Res 5, 1301-1312.

Matt, P., Carrel, T., White, M., Lefkovits, I., Van Eyk, J. (2007). Proteomics in cardiovascular surgery. J Thorac Cardiovasc Surg. 133, 210–214.

McCroskery, S., Chaudhry, A., Lin, L., and Daniels, M. P. (2006). Transmembrane agrin regulates filopodia in rat hippocampal neurons in culture. Mol. Cell Neurosci. 33, 15–28.

McMahan, U.J. (1990). The agrin hypothesis. Cold Spring Harb Symp Quant Biol 55, 407-418.

Medina, M.G., Ledesma, M.D., Dominguez, J.E., Medina, M., Zafra, D., Alameda, F., Dotti, C.G., and Navarro, P. (2005). Tissue plasminogen activator mediates amyloid-induced neurotoxicity via Erk1/2 activation. EMBO J 24, 1706-1716.

Mitchell, B.L., Yasui, Y., Lampe, J.W., Gafken, P.R., and Lampe, P.D. (2005). Evaluation of matrix-assisted laser desorption/ionization-time of flight mass spectrometry proteomic profiling: identification of alpha 2-HS glycoprotein B-chain as a biomarker of diet. Proteomics 5, 2238-2246.

Moritz, R.L., Clippingdale, A.B., Kapp, E.A., Eddes, J.S., Ji, H., Gilbert, S., Connolly, L.M., and Simpson, R.J. (2005). Application of 2-D free-flow electrophoresis/RP-HPLC for proteomic analysis of human plasma depleted of multi high-abundance proteins. Proteomics 5, 3402-3413.

Mueller, L.N., Brusniak, M.Y., Mani, D.R., and Aebersold, R. (2008). An assessment of software solutions for the analysis of mass spectrometry based quantitative proteomics data. J Proteome Res 7, 51-61.

Neurath, H. (1994). Proteolytic enzymes past and present: the second golden era. Recollections, special section in honor of Max Perutz. Protein Sci 3, 1734-1739.

Nicole, O., Docagne, F., Ali, C., Margaill, I., Carmeliet, P., MacKenzie, E.T., Vivien, D., and Buisson, A. (2001).

The proteolytic activity of tissue-plasminogen activator enhances NMDA receptor-mediated signaling. Nat Med 7, 59-64.

Nitkin, R.M., Smith, M.A., Magill, C., Fallon, J.R., Yao, Y.M., Wallace, B.G., and McMahan, U.J. (1987). Identification of agrin, a synaptic organizing protein from Torpedo electric organ. J Cell Biol 105, 2471-2478.

O'Connor, L.T., Lauterborn, J.C., Gall, C.M., and Smith, M.A. (1994). Localization and alternative splicing of agrin mRNA in adult rat brain: transcripts encoding isoforms that aggregate acetylcholine receptors are not restricted to cholinergic regions. J Neurosci 14, 1141-1152.

Olson, T.R., & Pawlina W. (2008). A.D.A.M. Student atlas of anatomy, 2nd Edition. Cambridge University Press.

Omenn, G.S., States, D.J., Adamski, M., Blackwell, T.W., Menon, R., Hermjakob, H., Apweiler, R., Haab, B.B., Simpson, R.J., Eddes, J.S., et al. (2005). Overview of the HUPO Plasma Proteome Project: results from the pilot phase with 35 collaborating laboratories and multiple analytical groups, generating a core dataset of 3020 proteins and a publicly-available database. Proteomics 5, 3226-3245.

Ong, S.E., Blagoev, B., Kratchmarova, I., Kristensen, D.B., Steen, H., Pandey, A., and Mann, M. (2002). Stable isotope labeling by amino acids in cell culture, SILAC, as a simple and accurate approach to expression proteomics. Mol Cell Proteomics 1, 376-386.

Pan, S., Aebersold, R., Chen, R., Rush, J., Goodlett, D.R., McIntosh, M.W., Zhang, J., and Brentnall, T.A. (2009). Mass spectrometry based targeted protein quantification: methods and applications. J Proteome Res 8, 787-797.

Pawlak, R., Rao, B.S., Melchor, J.P., Chattarji, S., McEwen, B., and Strickland, S. (2005). Tissue plasminogen activator and plasminogen mediate stress-induced decline of neuronal and cognitive functions in the mouse hippocampus. Proc Natl Acad Sci U S A 102, 18201-18206.

Peng, J. M., Gygi, S. P. J. (2001). Proteomics: the move to mixtures. Mass Spectrom. 36, 1083-1091.

Qian, Z., Gilbert, M.E., Colicos, M.A., Kandel, E.R., and Kuhl, D. (1993). Tissue-plasminogen activator is induced as an immediate-early gene during seizure, kindling and long-term potentiation. Nature 361, 453-457.

Qu, Y., Adam, B.L., Yasui, Y., Ward, M.D., Cazares, L.H., Schellhammer, P.F., Feng, Z., Semmes, O.J., and Wright, G.L., Jr. (2002). Boosted decision tree analysis of surface-enhanced laser desorption/ionization mass spectral serum profiles discriminates prostate cancer from noncancer patients. Clin Chem 48, 1835-1843.

Rawlings, N.D., Barrett, A.J., and Bateman, A. (2010). MEROPS: the peptidase database. Nucleic Acids Res 38, D227-233.

Reif, R., Sales, S., Dreier, B., Luscher, D., Wolfel, J., Gisler, C., Baici, A., Kunz, B., and Sonderegger, P. (2008). Purification and enzymological characterization of murine neurotrypsin. Protein Expr Purif 61, 13-21.

Reif, R., Sales, S., Hettwer, S., Dreier, B., Gisler, C., Wolfel, J., Luscher, D., Zurlinden, A., Stephan, A., Ahmed, S., et al. (2007). Specific cleavage of agrin by neurotrypsin, a synaptic protease linked to mental retardation. FASEB J 21, 3468-3478.

Rezaee, F., Casetta, B., Levels, J.H., Speijer, D., and Meijers, J.C. (2006). Proteomic analysis of high-density lipoprotein. Proteomics 6, 721-730.

Roepstorff, P., Fohlman, J. (19984). Proposal for a common nomenclature for sequence ions in mass spectra of peptides. Biomed Mass Spectrom. 11, 601.

Roses, A.D. (1996). The Alzheimer diseases. Curr Opin Neurobiol 6, 644-650.

Ross, P.L. et al (2004). Multiplexed protein quantification in Saccharomyces cerevisiae using amine-reactive isobaric tagging reagents. Mol. Cell. Proteomics 3, 1154-1169.

Ruegg, M.A. (2001). Molecules involved in the formation of synaptic connections in muscle and brain. Matrix Biol 20, 3-12.

Samson, A.L., and Medcalf, R.L. (2006). Tissue-type plasminogen activator: a multifaceted modulator of neurotransmission and synaptic plasticity. Neuron 50, 673-678.

Sanes, J.R., and Lichtman, J.W. (2001). Induction, assembly, maturation and maintenance of a postsynaptic apparatus. Nat Rev Neurosci 2, 791-805.

Sappino, A.P., Madani, R., Huarte, J., Belin, D., Kiss, J.Z., Wohlwend, A., and Vassalli, J.D. (1993). Extracellular proteolysis in the adult murine brain. J Clin Invest 92, 679-685.

Scarmeas, N., Honig, L.S., Choi, H., Cantero, J., Brandt, J., Blacker, D., Albert, M., Amatniek, J.C., Marder, K., Bell, K., Hauser, W.A., Stern, Y. (2009). Seizures in Alzheimers Disease: Who, When, and How Common? Arch Neurol 66, 992-997.

Schechter, I., and Berger, A. (1967). On the size of the active site in proteases. I. Papain. Biochem. Biophys. Res. Commun. 27, 157–162.

Schiess, R., Wollscheid, B., and Aebersold, R. (2009). Targeted proteomic strategy for clinical biomarker discovery. Mol Oncol 3, 33-44.

Seeds, N.W., Williams, B.L., and Bickford, P.C. (1995). Tissue plasminogen activator induction in Purkinje neurons after cerebellar motor learning. Science 270, 1992-1994.

Shen, Y., Zhao, R., Berger, S.J., Anderson, G.A., Rodriguez, N., Smith, R.D. (2002). High-efficiency nanoscale liquid chromatography coupled on-line with mass spectrometry using nanoelectrospray ionization for proteomics. Anal. Chem. 74, 4235–49.

Shen, Y., Smith, R.D. (2002). Proteomics based on high-efficiency capillary separations. Electrophoresis 23, 3106–24.

Shen, Y., Moore, R.J., Zhao, R., Blonder, J., Auberry, D.L., et al. (2003). High-efficiency on-line solid-phase extraction coupling to 15–150-microm-i.d. column liquid chromatography for proteomic analysis. Anal. Chem. 75, 3596–605.

Shen, Y., Zhang, R., Moore, R.J., Kim, J., Metz, T.O., et al (2005). Automated 20 kpsi RPLC-MS and MS/MS with chromatographic peak capacities of 1000–1500 and capabilities in proteomics and metabolomics. Anal. Chem. 77, 3090–100.

Shen, Y., Kim, J., Strittmatter, E.F., Jacobs, J.M., Camp, D.G., 2nd, Fang, R., Tolie, N., Moore, R.J., and Smith, R.D. (2005). Characterization of the human blood plasma proteome. Proteomics 5, 4034-4045.

Siao, C.J., Fernandez, S.R., and Tsirka, S.E. (2003). Cell type-specific roles for tissue plasminogen activator released by neurons or microglia after excitotoxic injury. J Neurosci 23, 3234-3242.

Silva, J.C., Gorenstein, M.V., Li, G.Z., Vissers, J.P., Geromanos, S.J.(2006). Mol Cell Proteomics 5,144–56.

Simpkins, F., Czechowicz, J.A., Liotta, L., and Kohn, E.C. (2005). SELDI-TOF mass spectrometry for cancer biomarker discovery and serum proteomic diagnostics. Pharmacogenomics 6, 647-653.

Small, D.H., Nurcombe, V., Reed, G., Clarris, H., Moir, R., Beyreuther, K., and Masters, C.L. (1994). A heparin-binding domain in the amyloid protein precursor of Alzheimer›s disease is involved in the regulation of neurite outgrowth. J Neurosci 14, 2117-2127.

Small, D.H., Williamson, T., Reed, G., Clarris, H., Beyreuther, K., Masters, C.L., and Nurcombe, V. (1996). The role of heparan sulfate proteoglycans in the pathogenesis of Alzheimer›s disease. Ann N Y Acad Sci 777, 316-321.

Snow, A.D., Mar, H., Nochlin, D., Kimata, K., Kato, M., Suzuki, S., Hassell, J., and Wight, T.N. (1988). The presence of heparan sulfate proteoglycans in the neuritic plaques and congophilic angiopathy in Alzheimer›s disease. Am J Pathol 133, 456-463.

Snow, A.D., and Wight, T.N. (1989). Proteoglycans in the pathogenesis of Alzheimer›s disease and other amyloidoses. Neurobiol Aging 10, 481-497.

Squire, L.R., and Alvarez, P. (1995). Retrograde amnesia and memory consolidation: a neurobiological perspective. Curr Opin Neurobiol 5, 169-177.

Squire, L.R., and Spanis, C.W. (1984). Long gradient of retrograde amnesia in mice: continuity with the findings in humans. Behav Neurosci 98, 345-348.

Stephan, A., Mateos, J.M., Kozlov, S.V., Cinelli, P., Kistler, A.D., Hettwer, S., Rulicke, T., Streit, P., Kunz, B., and Sonderegger, P. (2008). Neurotrypsin cleaves agrin locally at the synapse. FASEB J 22, 1861-1873.

Steuble, M. (2008). Proteomic Analysis of Calsyntenin-1 Organelles and their Functional and Structural Characterization. Dissertation, Universität Zürich.

The National Institute of Neurological Disorders and Stroke rt-PA Stroke Study Group (1995). Tissue plasminogen activator for acute ischemic stroke. N. Engl. J. Med. 33, 1581–1587.

Tsirka, S.E., Gualandris, A., Amaral, D.G., and Strickland, S. (1995). Excitotoxin-induced neuronal degeneration and seizure are mediated by tissue plasminogen activator. Nature 377, 340-344.

Pan, S., Aebersold R., Chen, R., Rusch J., Goodlet,t D.R., Mc Intosh, M.W., Zhang, J., Brentnall, T.A. (2009). Mass spectrometry based targeted protein quantification: methods and applications. J. Proteome Res. 8, 787-797.

Perkins, D.N., Pappin, D.J., Creasy, D.M., and Cottrell, J.S. (1999.) Probability-based protein identification by searching sequence databases using mass spectrometry data. Electrophoresi. 20, 3551-3567.

Van Horssen, J., Wesseling, P., van den Heuvel, L.P.W.J., de Waal, R.M.W., Verbeek, M.M. (2003). Heparan sulphate proteoglycans in Alzheimer's disease and amyloid-related disorders. Lancet Neurology 2,482–492.

Villanueva, J., Philip, J., Entenberg, D., Chaparro, C.A., Tanwar, M.K., Holland, E.C., and Tempst, P. (2004). Serum peptide profiling by magnetic particle-assisted, automated sample processing and MALDI-TOF mass spectrometry. Anal Chem 76, 1560-1570.

Villanueva, J., Shaffer, D.R., Philip, J., Chaparro, C.A., Erdjument-Bromage, H., Olshen, A.B., Fleisher, M., Lilja, H., Brogi, E., Boyd, J., et al. (2006). Differential exoprotease activities confer tumor-specific serum peptidome patterns. J Clin Invest 116, 271-284.

Vogt, L., Schrimpf, S.P., Meskenaiten, V., Frischknecht, R., Kinter, J., Leone, D.P., Ziegler, U., Sonderegger, P. (2001). Calsyntenin-1, a Proteolytically Processed Postsynaptic Membrane Protein with a Cytoplasmic Calcium-Binding Domain. Molecular and Cellular Neuroscience 17, 151–166.

Wagner, M., Naik, D.N., Pothen, A., Kasukurti, S., Devineni, R.R., Adam, B.L., Semmes, O.J., and Wright, G.L., Jr. (2004). Computational protein biomarker prediction: a case study for prostate cancer. BMC Bioinformatics 5, 26.

Washburn, M. P., Wolters, D., and Yates III, J. R. (2001) Large-scale analysis of the yeast proteome by multidimensional protein identification technology. Nature Biotechnology 19, 242–247.

Wang, G., Wu, W.W., Zeng, W., Chou, C.L., and Shen, R.F. (2006). Label-free protein quantification using LC-coupled ion trap or FT mass spectrometry: Reproducibility, linearity, and application with complex proteomes. J Proteome Res 5, 1214-1223.

Wang, X., Lee, S.R., Arai, K., Tsuji, K., Rebeck, G.W., and Lo, E.H. (2003). Lipoprotein receptor-mediated

induction of matrix metalloproteinase by tissue plasminogen activator. Nat Med 9, 1313-1317.

Wessel, D., & Flügge, U.I. (1984). A method for the quantitative recovery of protein un dilute solution in the presence of detergents and lipids. Anal. Biochem. 138, 141-143.

Wolfer, D.P., Lang, R., Cinelli, P., Madani, R., and Sonderegger, P. (2001). Multiple roles of neurotrypsin in tissue morphogenesis and nervous system development suggested by the mRNA expression pattern. Mol Cell Neurosci 18, 407-433.

Yang, J.F., Cao, G., Koirala, S., Reddy, L.V., Ko, C.P. (2001). Schwann cells express active agrin and enhance aggregation of acetylcholine receptors on muscle fibers. J. Neurosci. 21, 9527-9584.

Yates, J.R., Ruse, C.I., and Nakorchevsky, A. (2009). Proteomics by mass spectrometry: approaches, advances, and applications. Annu Rev Biomed Eng 11, 49-79.

Yepes, M., and Lawrence, D.A. (2004). New functions for an old enzyme: nonhemostatic roles for tissue-type plasminogen activator in the central nervous system. Exp Biol Med (Maywood) 229, 1097-1104.

Yepes, M., Roussel, B.D., Ali, C., and Vivien, D. (2009). Tissue-type plasminogen activator in the ischemic brain: more than a thrombolytic. Trends Neurosci 32, 48-55.

Yepes, M., Sandkvist, M., Coleman, T.A., Moore, E., Wu, J.Y., Mitola, D., Bugge, T.H., and Lawrence, D.A. (2002). Regulation of seizure spreading by neuroserpin and tissue-type plasminogen activator is plasminogen-independent. J Clin Invest 109, 1571-1578.

Yepes, M., Sandkvist, M., Wong, M.K., Coleman, T.A., Smith, E., Cohan, S.L., and Lawrence, D.A. (2000). Neuroserpin reduces cerebral infarct volume and protects neurons from ischemia-induced apoptosis. Blood 96, 569-576.

Zhang, J., Goodlett, D.R., Montine, T.J. (2005). Proteomic biomarker discovery in cerebrospinal fluid for neurodegenerative diseases. J Alzheimers Dis. 8, 377-386.

Zhang, B., Luo, S., Wang, Q., Suzuki, T., Xiong, W.C., and Mei, L. (2008). LRP4 serves as a coreceptor of agrin. Neuron 60, 285-297.

Zhu, C., Goodall, D., Wren, S. (2004). Elevated temperature HPLC: Principles and applications to small molecules and biomolecules. LC-GC Eur. 17, 530–540.

Zhang, J. (2007). Proteomics of human cerebrospinal fluid – the good, the bad, and the ugly. Proteomics Clin. Appl. 1, 805–819.

Zhu, W., Smith, J.W., and Huang, C.M. (2010). Mass spectrometry-based label-free quantitative proteomics. J Biomed Biotechnol 2010, 840518.

Zolotarjova, N., Martosella, J., Nicol, G., Bailey, J., Boyes, B.E., and Barrett, W.C. (2005). Differences among techniques for high-abundant protein depletion. Proteomics 5, 3304-3313.

Zybailov, B., Mosley, A.L., Sardiu, M.E., Coleman, M.K., Florens, L., and Washburn, M.P. (2006). Statistical analysis of membrane proteome expression changes in Saccharomyces cerevisiae. J Proteome Res 5, 2339-2347.

Curriculum vitae

Name	KLINGLER
Vorname	Diana
Geburtsdatum	14.02.1978
Heimatort	Aalen, Deutschland
Nationalität	Deutsch

Ausbildung

Gymnasium	Justus-von-Liebig-Schule, Aalen, Deutschland; 1990-1997 Abschluss 1997, Abitur
Diplomstudium	Universität Ulm, Deutschland; 1998-2004 Diplomfach Analytische und Umweltchemie Diplomarbeit in der Gruppe von Prof. Dr. K.-H. Ballschmiter Thema: "Bestimmung des log Kow-Wertes über die normierte gaschromatographische Retention unter Verwendung eines PCB Standards" Abschluss als Diplom Chemikerin 08/2004
Wissenschaftliche Mitarbeiterin	Universität Ulm, Deutschland; 08/2004-05/2005 Wissenschaftliche Mitarbeiterin in der Gruppe von Prof. Dr. K.-H. Ballschmiter Thema: "Qualitative Identifikation Polybromierter Diphenylether (PBDE) als Flammschutzmittel in elektronischen Bauteilen mit Gaschromatographie"
Promotionsstudium	Universität Konstanz, Deutschland; 06/2005-11/2006 Promotionsstudium in der Gruppe von Prof. Dr. Dr. M. Przybylski Thema: "Development of new methods for high resolution mass spectrometry in Proteomics" Universität Zürich, Schweiz; seit Dezember 2006 Promotionsstudium in der Gruppe von Prof. Dr. P. Sonderegger Thema: "Biomarker for the Proteolytic Aktivity of Neurotrypsin *in vivo*"

Publikationen und Präsentationen

Teile der Dissertation

Klingler, D., Sonderegger, P., Laczko, E. (2009). Targeting and quantifying the hydrophobic peptidome fraction by high resolution multiple selected reaction monitoring (H-mSRM). *Annual Meeting of the Swiss Proteomics Society, Zurich, Switzerland. Meeting Abstract.*

Klingler, D., Sonderegger, P., Laczko, E. (2009). Targeting and quantifying the hydrophobic peptidome fraction by high resolution multiple selected reaction monitoring (H-mSRM). *Annual Conference of the American society of mass spectrometry 2009, Philadelphia, USA. Meeting abstract.*

Weitere Projekte

Klingler, D., Marquardt, A., Paraschiv, G., Amstalden van Hove, E., Manea, M., Przybylski, M. (2006). Application of Affinity Proteomics and High Resolution FTICR Mass Spectrometry for Elucidation of Antibody-Paratope Peptides (PAREXPROT). *17th International Mass Spectrometry Conference, Prag, Czech Republic. Meeting Abstract.*

Klingler, D., Marquardt, A., Paraschiv, G., Amstalden, E., Manea, M., Przybylski, M. (2006) Application of Affinity Proteomics and High Resolution FTICR Mass Spectrometry for Elucidation of Antibody-Paratope Peptides (PAREXPROT). *39th Annual meeting of the German society of mass spectrometry, Mainz, Germany. Meeting Abstract.*

Teile der Diplomarbeit

Ballschmiter, K., Klingler, D., Ellinger, S., Hackenberg, R. (2005). High resolution gas chromatography retention data as a basis for the estimation of the Octanol-Water Distribution coefficient (Kow) of POPs: The influence of experimental parameters. *Analytical and Bioanalytical Chemistry*, 382 (8), 1859-1870.

Acknowledgments

First of all I am pleased to thank Prof. Dr. Peter Sonderegger for giving me the opportunity to accomplish my doctoral thesis in his group, for his supervision and his constant advice and great support of my work and my scientific education.

I am very grateful to my PhD committee member Dr. Peter Hunziker for taking the time to answer all my questions, all his positive inputs and his continuous and great support.

In addition, I would like to thank Prof. Dr. Heinz Gehring for joining my PhD committee and his kind support during the last period of my PhD studies.

I would like to thank Prof. Dr. Ralph Schlappbach for giving me the opportunity to work with the state-of-the-art instrumentation at the Functional Genomics Center Zurich and for co-examining my thesis.

Furthermore, I want to thank the members of the Functional Genomics Center Zurich Doro Rutishauser, Claudia Fortes, Peter Gehring and Jonas Grossmann for all their advice and help in mass spectrometry and bioinformatics. Bernd Roschitzki and Endre Laczko deserve special merits for sharing their knowledge with me which was of significant importance for my scientific education. Without your competence and support we would never have managed to conduct this wok.

Many thanks go to all the past and present members of Peter Sonderegger`s group for their constructive discussion, assistance, and advice and for spreading an excellent and really friendly working atmosphere.

I would like to thank Beat Kunz for his effort on the organization of the lab instrumentation and the animal facility.

I am grateful to Tu-My Diep, Ewa Sokolowska, Andrea Galeano and Sonja Müller-Späth for the girls-nights during which I had the pleasure to enjoy your fantastic cuisine. Thanks also to Philipp Schätzle for your long-lasting IT-support. I will always remember the entertaining discussions we had. Stefan Hettwer, thanks for guiding me during my first year and for introducing me into the world of biology. Jens Wölfel, thanks for introducing me into the secrets of protein purification and enzyme kinetics and for taking me out of the lab. Alexander Ludwig, thanks for sharing your experience with science and showing me the nice places in Zurich to relax. Martin Steuble, thanks for coaching me during my PhD inside and outside the lab. You were always there to meet and talk about my ideas, to proofread and mark up my chapters, and to ask me good questions to help me think through my problems.

My parents, Gabi and Reiner, deserve special thanks for their endless love and their continuous support of my education, and their thoroughly believe in my scientific career.

I am deeply indebted to Dominik Gauss for his endless love and support during the past years. I am grateful to you for sharing with me this special time of our life, for being my best friend, for listening to my complaints and frustrations, and for always believing in me.

Special thanks go to my beloved flat mates Karin Nadig and Anja Gundlfinger, who helped me turning our flat into our home. Besides being true and special friends, you gave me never-ending support during the highs and lows of my PhD.

Last but by no means least, I want to thank my family and friends outside the lab. I am grateful to Kathrin Schneider. You were always there to meet and to support me during the last year of my PhD, and so many things would have been different without you. Thanks to Evi Hämmerer, Claudia Apic, Yvonne Denkwitz, and Stefan Woidich. You have been in my life ever since I started my scientific journey. I hope we will be able to stay in touch despite the long distances between us.